UNIVERSITÀ DEGLI STUDI DI PADOVA

UNIVERSITA' DEGLI STUDI DI PADOVA

Dipartimento di Ingegneria Industriale DII

Corso di Laurea Magistrale in Ingegneria Energetica

Integration of Salt Cavern Hydrogen Storage in a 100% Renewable Energy Supply Scenario

Relatore: Prof.ssa Anna Stoppato

Co-supervisore: Ali Akbar Eftekhari

Piovesan Francesco Matricola 2018744

Anno Accademico 2022/2023

To my family,
to my old and new friends
and to all the special people who supported me in this journey

Abstract

The fast development of electrolysis technology and renewable power capacity has increased interest in the conversion of surplus electricity to hydrogen for large-scale storage. Artificial subsurface salt caverns, created by the controlled circulation of freshwater and dissolution of deep salt layers through a well, offer a safe storage solution. Taking Denmark as a successful case of wind power development, we estimate the amount of hydrogen that can be produced and stored in 2050 based on the surplus electricity forecast and then calculate the required salt caverns volume. We assign the total storage volume to multiple salt caverns of different sizes such that their charge/discharge response time matches the fluctuating supply of renewable sources and the dynamic behaviour of hydrogen production and conversion processes with a minimum energy loss. We finally compare the optimum output energy of the above storage system with the estimated energy demand of Denmark and suggest several improvements that bring the stored supply closer to the demand.

Sommario

Il rapido sviluppo della tecnologia dell'elettrolisi e l'aumento della produzione di energia elettrica da fonti rinnovabili ha aumentato l'interesse nella conversione del surplus di elettricità in idrogeno per lo stoccaggio in grande scala. Le caverne saline sotterranee, create da una circolazione controllata di acqua dolce e dalla dissoluzione degli strati salini profondi attraverso una perforazione, offre una soluzione di stoccaggio sicura. Prendendo la Danimarca come caso di successo per lo sviluppo della produzione eolica, viene stimata la quantità di idrogeno che deve essere prodotta e stoccata nel 2050 basata sulla previsione di surplus di elettricità e successivamente calcolato il volume di caverne saline richiesto. Viene assegnato il volume totale di stoccaggio a diverse caverne saline di differenti dimensioni cosicché il loro tempo di carica/scarica possa combaciare con la produzione variabile delle risorse rinnovabili e il comportamento dinamico della produzione e conversione dell'idrogeno con perdite energetiche minime. Infine, viene comparato l'ottimo output energetico del suddetto sistema di stoccaggio con la domanda danese stimata di energia e vengono considerati diversi miglioramenti che portino la fornitura di energia accumulata più vicina alla domanda.

Contents

List of Figures

List of Tables

List of Code Snippets

List of Acronyms

VRFB Vanadium Redox Flow Batteries

PSB Polysulphide bromine batteries

TES Thermal energy storage

MSTES Molten Salt thermal energy storage

PCM Latent-phase change material

TCS Thermochemical storage

FC Fuel Cell

El Electrolyzer

HV High Voltage

HVAC High Voltage Alternate Current

HVDC High Voltage Direct Current

CS Conversion Station

LCC Lince Commutated Converter

VSC Voltage Source Converter

1

Introduction

The unprecedented consequences of climate change (see Figure 1.1) caused by greenhouse gases emissions and the geopolitical circumstances have driven important investments on renewable energy production (see Figure 1.2) to limit the environmental impact while maintaining the energy security.

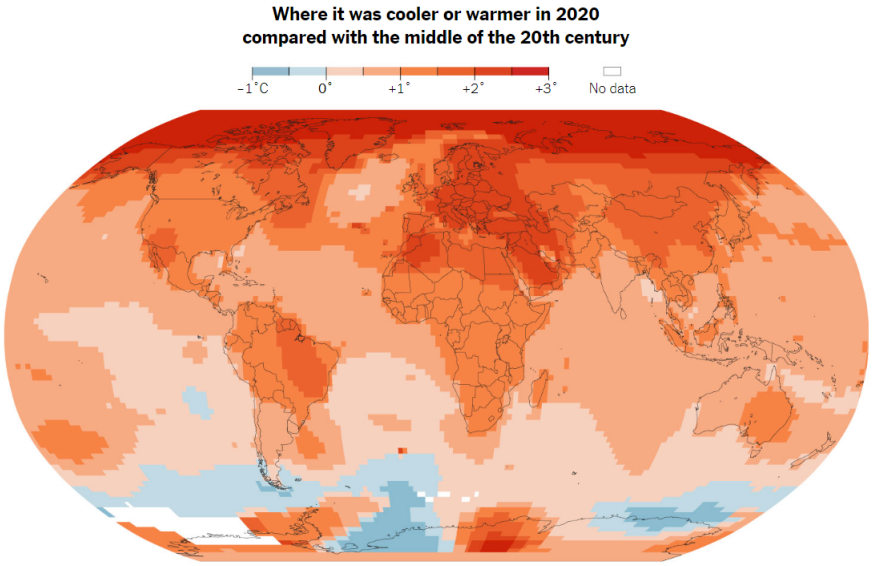

Figure 1.1: *Temperatures in 2020 compared to mid-20th century ones in the same areas [27]*

The increasing penetration of renewable energy sources in the energy production mix stresses the necessity of finding storage solutions to cope with the intrinsic intermittency and unpredictability of renewable energy sources such as wind and solar. In a fully renewable scenario, it is necessary to evaluate

which are the most convenient and relevant solutions for storage. Different solutions for energy storage exist (Figure 1.3), with different storage capacity and power rating (i.e. energy charge and discharge per unit time). Many of these technologies are already available commercially, while some others are in lower Technology Readiness Level (TRL).

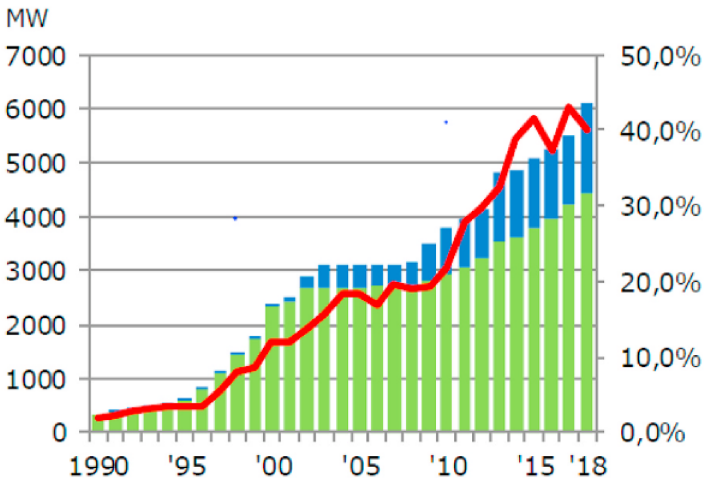

Figure 1.2: *Wind Power Capacity and Wind Power Ratio of Domestic Electricity Consumption in Denmark [12]*

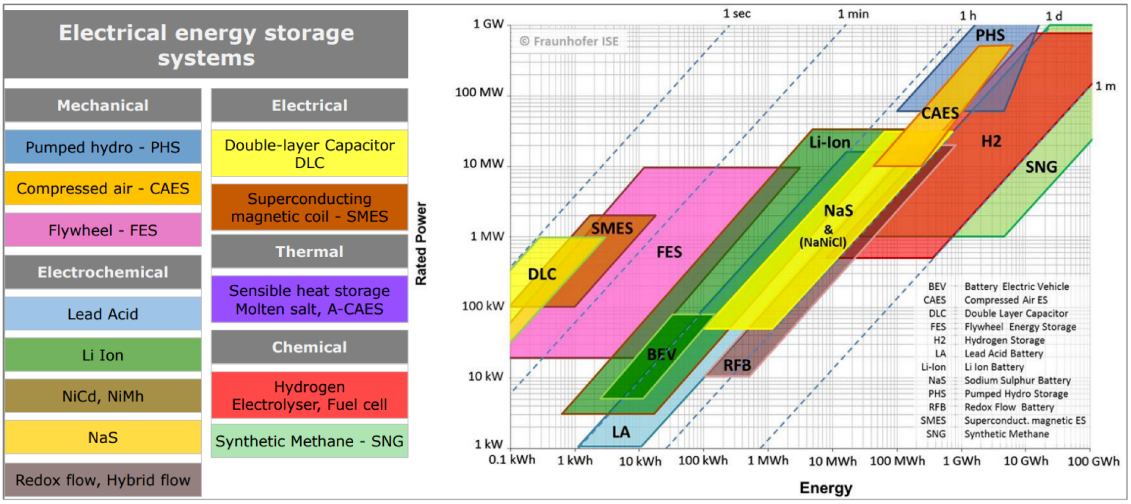

Figure 1.3: *Classification of electrical energy storage systems according to energy form (a); Comparison of rated power, energy content and discharge time of different EES technologies (b), own representation based on (International Eletrotechnical Commission (IEC), 2011).*

Some types of technologies can deliver high power but cannot store large quantities of energy as it is necessary for peak shaving and seasonal storage.

Here, some of the aforementioned technologies are briefly presented with the goal of explaining the importance and the role of the hydrogen storage technology.

1.1 Electrochemical storage technologies

Electrochemical technologies cover the majority (over 85% as 2016 new installation data) of the new energy storage solutions, with the Li-Ion technology being the predominant one. Research and development is focused on increasing the number of charge cycles (i.e. the number of times the battery can charge and discharge), reducing production costs and tackling the recycling problem. The range of values of the most important parameters, the main technologies available and those under development stage are presented in the following subsections. [13]

1.1.1 Sodium Sulphur (NaS) batteries

Energy Density (kWh/m3)	Energy Cost ($/kWh)	Technological Maturity	Environmental Impact	Storage Period (Short-Long Term)	Response Time (ms to hr)
150-250	300-500	Commercialized/proven	High	Long term	12min
150-250	326-543	Commercialized/proven	High	Long term	sec-min
180-280 150-280	-	Commercialized/proven	High	Long term	-

Table 1.1: *Main characteristics of NaS electrochemical energy storage technology [13]*

Sodium sulphur battery is an emerging technology with promising performance parameters (Table 1.1), in particular the energy density which can reach higher or comparable values compared to other solutions, and can be used for stationary storage. With respect to other technologies, though, it has a higher environmental impact.

1.1.2 Sodium Nickel Chloride ($NaNiCl_2$) batteries

Energy Density (kWh/m3)	Energy Cost ($/kWh)	Technological Maturity	Environmental Impact	Storage Period (Short-Long Term)	Response Time (ms to hr)
150-180	100-345	Proven/Commercializing	Medium/low	Mid-long term	<sec
100-190	100-200	Proven/Commercializing	Medium/low	Mid-long term	
181		Proven/Commercializing	Medium/low	Mid-long term	

Table 1.2: *Main characteristics of $NaNiCl_2$ electrochemical energy storage technology [13]*

As the NaS batteries (Table 1.2), also the $NaNiCl_2$ can be used for stationary storage with slight difference in terms of energy densities but more important

differences in terms of energy storage cost and the environmental impact (which results lower than the previously cited technology).

1.1.3 Lead-Acid (Pb-Acid) batteries

Energy Density (kWh/m3)	Energy Cost ($/kWh)	Technological Maturity	Environmental Impact	Storage Period (Short-Long Term)	Response Time (ms to hr)
50-80	120-150	Mature	High	Short-mid term	milli sec
25-100 50-90	54-337	Fully Commercialized	High	Short-mid term	5-10 milli sec

Table 1.3: *Main characteristics of Pb-Acid electrochemical energy storage technology [13]*

Pb-Acid batteries (Table 1.3) present average round trip efficiencies, moderately low cost in terms of cost per kWh of storage installed and high technological maturity. This technology presents a short-mid term storage period (so not suitable for long terms storage) and a high environmental impact.

1.1.4 Lithium-ion (Li-ion) batteries

Energy Density (kWh/m3)	Energy Cost ($/kWh)	Technological Maturity	Environmental Impact	Storage Period (Short-Long Term)	Response Time (ms to hr)
200-500	600-2500	Demonstration	Medium-low	Short-mid term	20 milli sec-sec
200-500	300-1300	Proven/Commercializing	Medium-low	Short-mid term	-
170-300 150-400	-	Proven/Commercializing	Medium-low	Short-mid term	-

Table 1.4: *Main characteristics of Li-ion electrochemical energy storage technology [13]*

Li-ion based batteries are the most widely electrochemical energy storage technologies used: they present high energy densities with make them suitable not only for stationary storage but also for mobile one (like electric vehicles or mobile devices). They also cause a medium-low environmental impact but present a significant cost per kWh of energy storage.

1.1.5 Nickel metal hybrid (Ni−MH) batteries

Ni−MH batteries have been used for electric vehicles in the past, now they have been substituted by Li−ion batteries since they present higher energy density and much lower self-discharge rate (that would have made this type of technology unsuitable for long time storage). [13]

1.1.6 Nickel-Cadmium (Ni−Cd) batteries

Ni−Cd batteries have been used for stationary energy storage as it's a commercialized technology but the important self discharge rate don't make them

Energy Density (kWh/m3)	Energy Cost ($/kWh)	Technological Maturity	Environmental Impact	Storage Period (Short-Long Term)	Response Time (ms to hr)
60-150	800-1500	Commercialized	High	Short-long Term	20 ms-sec
30-150 15-140	400-2400	Commercialized	High	Short-long Term	-

Table 1.5: *Main characteristics of Ni−Cd electrochemical energy storage technology [13]*

suitable for long terms storage like monthly or seasonal one.

1.1.7 Flow Batteries

Technology	Energy Density (kWh/m3)	Energy Cost ($/kWh)	Technological Maturity	Environmental Impact	Storage Period (Short-Long Term)	Response Time (ms to hr)
VRFB	16-33	190-1085	Early commercialized	Medium/Low	Long Term	10 min
	20-70 10-70	150-1000	Proven/Commercializing	Medium/Low	Long Term	Sec
PSB	20-30	150-2000	Developing	Medium	Long Term	-
	16-60	110-130	Developing	Medium	Long Term	-
Zn-Br	20-30		Demonstration	Medium	Long Term	-
	25-30		Demonstration	Medium	Long Term	-
	30-60		Demonstration	Medium	Long Term	-

Table 1.6: *Main characteristics of VRFB, PSB and Zn−Br electrochemical energy storage technology [13]*

Flow batteries are unconventional electrochemical energy storage devices based on the usage of liquid separate anolyte and catholyte pumped through a ion-selective membrane placed between two electrodes. The main technologies (Table 1.6) for this type of batteries are:

1. **VRFB**: Vanadium Redox Flow Batteries
2. **PSB**: Polysulphide bromine
3. **Zn−Br**: Zinc bromine

The characteristics of being scalable, having low self-discharge rate and fast response make them a possible good solution for stationary storage.

1.2 Thermal Energy Storage (TES) technologies

TES technologies are various but all based on the usage of thermal energy as mechanism of storing energy. Here the most important technologies are briefly reviewed [13] (see Table 1.7):

- **MSTES**: Molten Salt thermal energy storage: most used TES technology, it has good heat transfer properties and relatively low cost; drawback is the usage of corrosive salts and the necessity of mantaining a minimum temperature value to avoid the solidification of the salts

- **PCM**: Latent-phase change material: their functioning is based on the latent heat stored by latent-phase change material; as TCS this technology is still in a development stage
- **TCS**: Thermochemical storage: heat or cold is stored by means of different chemical reactants; as PCM, it is in a development stage.
- **SHS**: Sensible Heat storage: another possibility to store energy is through sensible heat storage; this storage can be done through the usage of solid materials (like sand, concrete or similar materials [11]) or liquid materials (most common used is water, fundamental in the solar thermal systems [31]).

Technology	Energy Density (kWh/m3)	Energy Cost ($/kWh)	Technological Maturity	Environmental Impact	Storage Period (Short-Long Term)	Response Time (ms to hr)
MSTES	80-120	494.35-1373.2	Mature/Commercialized	Very Low	Days-months	<4 ms-sec
PCM	150-250	200-400	Development/Mature	Low	Hours-months	10 min
TCS	80-250	10-136	Development/Mature	Low	Hours-days	10 min

Table 1.7: *Main characteristics of MSTES, PCM and TCS energy storage technology [13]*

1.3 Hydro energy storage and CAES

The most exploited large scale technologies for energy storage are based on storage of energy through gravity (for hydro) and pressure (for CAES) [11] [17]. Here are briefly presented:

- **Hydro Storage**: Energy is stored through the pumping of water to a higher geodetic level (charging process) and reconverted through the usage of turbines, converting the kinetic energy into rotational mechanical energy (and, consequently, electrical energy; this is the discharge process);
- **CAES**: CAES (Compressed Air Energy Storage) is a technology based on compression of air during production surplus periods into storage vessels; the discharge process (and, thus, the energy conversion) is based on the usage of a turbine fed by the pressurized air.

These technologies allow high long-term energy storage capacities but present major drawbacks as high investment costs (for civil constructions), high environmental impact (especially hydro), not widely available conditions for their

construction and high inertia of the system (charge-discharge process) compared to electrochemical or electrical storage technologies.

1.4 Electrical Storage

Other typologies of energy storage devices exploit electromagnetic properties of materials or polarization of materials: the first are the so called SMES (superconduction magnetic energy storage) and their functioning principle is storing energy in magnetic form through the usage of a coil opportunely cooled to minimize the losses for self discharge. The second are the so called Capacitors or Supercapacitors, based on the polarization of the dieletric material. These technologies permit to have high power densities and really fast charge/discharge times (as well as response times) but as drawbacks they have low energy density so their usage is not useful for energy storage purposes.

After this brief introduction of the energy storage technologies currently available or under development it's possible to comprehend the necessity of a storage form that permits to easily and cheaply convert high amounts of energy into a form that can be stocked. In this context hydrogen appears to be a flexible and consistent solution: in this project the storage of this element will be evaluated focusing specifically on the usage of artificial underground salt caverns.

2

Simplified Model

The base of this project is the analysis of salt caverns hydrogen storage solutions to permit the switch to a completely renewable energy-based society. In order to be able to cover the entire energy demand curve with only resources like wind or solar it is necessary to consider a storage solution that is able to cope with the intermittency and unpredictability of the renewable resource.
Considering the amount of energy that needs to be stored, hydrogen is a concrete solution to be taken into account and therefore its storage is crucial. The analysed storage solution is artificial subsurface salt caverns: the calculations have started with an estimation of the amount of hydrogen that must be produced to cover the demand. Once completed the estimation it has been possible to calculate the required salt caverns volume that had to be artificially created.
This type of static analysis has been carried out considering initially a simplified model. In this model a limited number of cities and storage locations has been considered and their positioning and connections have been manually evaluated. In order to proceed in the study it has been necessary to make few assumptions:

1. No limits on number and dimension of wind farms that can be installed in the North Sea: this hypothesis doesn't differ excessively from the actual conditions present in the North Sea

2. Analysis starts from the demand and goes backwards, considering all the efficiencies of the components of the energy system, to the necessary production to cover it

3. Electrolyzers are considered to be modular so the efficiency is evaluated as approximately independent from the size of the plant
4. It is considered possible to place caverns for storage on the entire area of the simplified map (even though some more limited regions are considered to proceed with the modelling process)
5. All industries have been able to convert their production lines and processes to the usage of hydrogen instead of methane: this hypothesis is used to pursue the simplified analysis but the conversion of the industrial lines to hydrogen could be an issue that has to be addressed
6. Injection and extraction points are considered placed in the center of the respective regions and it is supposed to have one cavern for each city of the model.

Taking into account these simplifying hypothesis, the following aspects, both in the static simplified model and the dynamic one, have been analysed:

- Electricity transport, which considers:
  - Cost of new cables
  - Energy losses in the transmission lines
  - Losses in electrolyzers and fuel cells
- Hydrogen transport, which considers:
  - Pipeline design
  - Compressor cost and design
  - Losses during large scale storage
- Onshore Cavern Storage, which considers:
  - Pipelines and compressors
  - Small-scale cavern storage
  - Small-scale fuel cells and electrolyzers
  - Energy losses in salt cavern storage.

2.0.1 Simplified map

Before defining all the scenarios it is necessary to design a simplified map for the calculations (sm stands for simplified map inside the code), which is here reported (Figure 2.1).

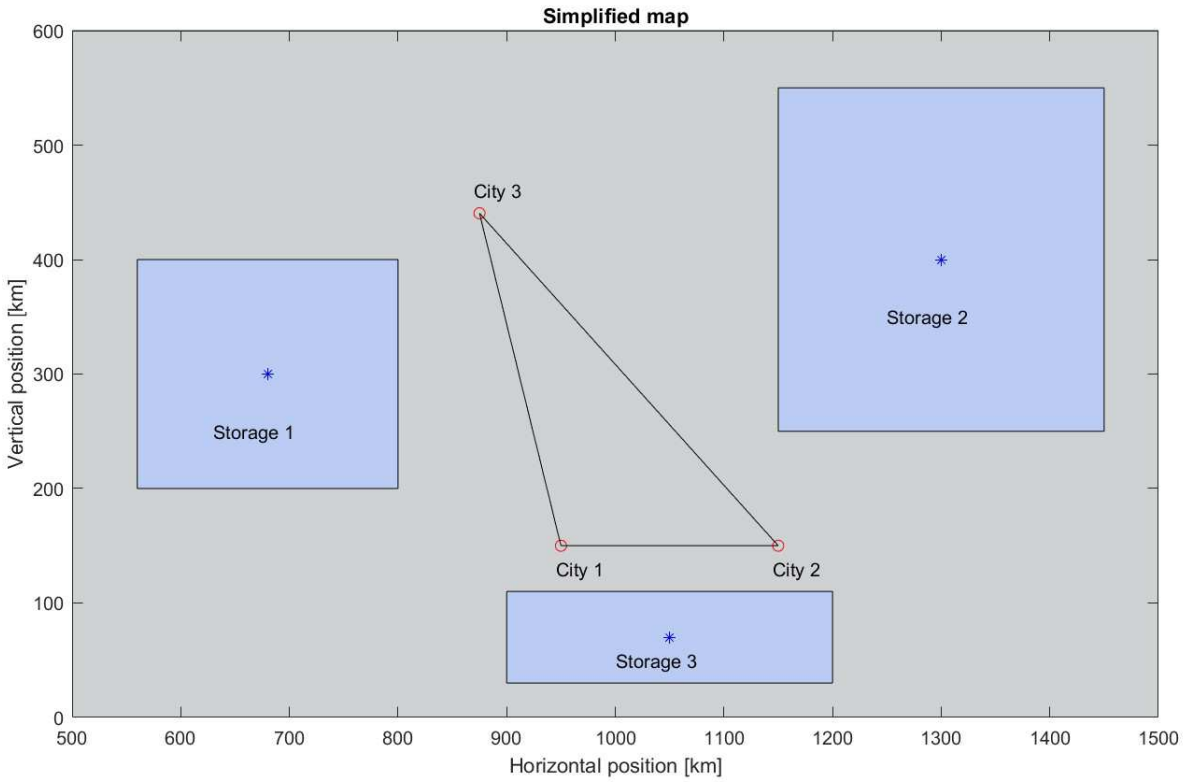

Figure 2.1: *Map for the simplified model*

In this map three cities have been reported, considering a subdivision of the peak power requested into 50%, 30% and 20% respectively for cities 2, 3 and 1. The storage sites 1, 2 and 3 are respectively dedicated to cities 3, 2 and 1. Under the hypothesis of having in 30 years four times the wind power capacity and 1.5 times the power demand by users, through the Danish data of the last 10 years the future trends of production and consumption have been evaluated for each city (Figure 2.2) and overall (Figure 2.3).

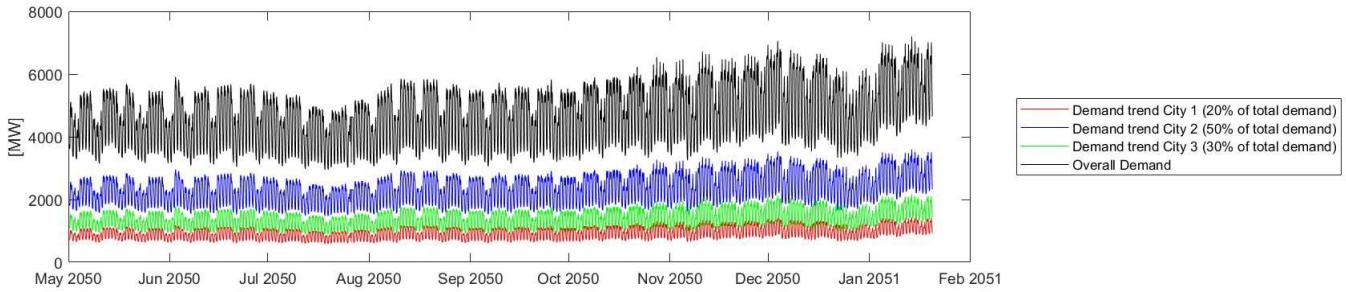

Figure 2.2: *Projection of demand trend for each city and overall in 30 years based on Danish past electricity supply and demand data*

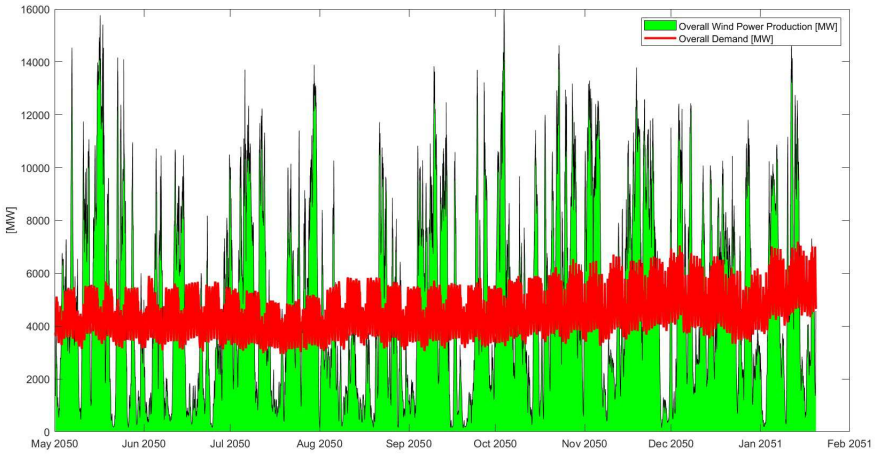

Figure 2.3: *Projection of overall demand and wind production trend in 30 years based on Denmark's supply and demand data in 2020*

Model Considered [33]	Vestas V164-10.0MW
Turbine Power	10 MW
Rotor Diameter	164 m
Horizontal Turbine Distance	1.64 km (10*Diameter)
Vertical Turbine Distance	0.82 km (5*Diameter)
Distance Wind Farm - Coast	300 km
Turbines per Row	40
Turbines per Column	20

Table 2.1: *Characteristics of the chosen reference wind turbine and of the reference wind farm*

Max Power Wind Farm	16000 MW
Average Sea Depth	0.2 km
Island Length	1.6 km
Island Height	0.995 km
Distance Wind Farm - Hydrogen Island	5 km

Table 2.2: *Characteristics of the chosen reference hydrogen island*

It has been supposed to have a defined offshore wind farm which characteristics are reported on Table 2.1. Moreover, it has been defined an hydrogen island where we have the convergence of the power produced by the wind farm, the electrical transformers and the hydrogen production and storage. It is important to notice two characteristics of this island (see Table 2.2):

- Average Sea Depth: North Sea has an average depth of 90 m with maximum depth of 700 m so it has been considered a value of 200 m for the analysis. [22]
- From the 20 GW 70% H_2 case (page 51 of [32]) I have obtained a set of reference dimensions for the artificial island.

2.0.2 Energy Shortage Calculation

It has been considered that each city has the same demand profile: with this hypothesis and the ones mentioned in Paragraph 2.0.1 it has been possible to subdivide the energy shortage (and therefore the storage necessary) for each city based on the percentages aforementioned, obtaining through integration over 9-month time period of the history of supply and demand, as described by Equation 2.1 (from Code 4.1 in Code Appendix 4):

$$average_{demand}[MW] = \frac{1}{t_2 - t_1} \int_{t_1}^{t_2} load_{total}\, dt \; = \frac{\Delta t}{t_2 - t_1} \sum d.TotalLoad \quad (2.1)$$

With Δt as resolution of the database (1 hour) and $t_2 - t_1$ the 9-months time frame considered. Once calculated the overall shortage (calculated as the difference between the overall demand and the wind farm production per each unit of time) in terms of power it is possible to integrate over time to obtain the

energy shortage (for the 9-months period) and divide per each city (see Code 4.1 in Code Appendix 4) obtaining:

- $E_{shortage,city1} = 6.97 * 10^4$ MWh
- $E_{shortage,city2} = 1.74 * 10^5$ MWh
- $E_{shortage,city3} = 1.05 * 10^5$ MWh

2.0.3 Fraction of surplus energy needed

With the efficiency ranges of fuel cells and electrolyzers (see Table 2.3 and Table 2.4) it has been possible to calculate the energy actually needed from the surplus. These quantities are considering the energy required from surplus to convert to hydrogen and reconvert to electricity and being able to cover the deficit of energy from direct production.

Technologies	Minimum Efficiency [%]	Maximum Efficiency [%]
Alkaline	51	65.3
PEM	55.5	72.4

Table 2.3: *Overview of main electrolyzers technologies efficiencies [35]*

Technologies	Electrolyte	$T_{operating,min}$[C]	$T_{operating,max}$[C]	$\eta_{electrical,min}$[%]	$\eta_{electrical,max}$[%]
AFC	Aq. KOH	60	120	60	60
DMFC	PEM	30	90	80	80
MCFC	Molten Li2CO3 and K2CO3	600	650	45	47
PAFC	Phosphoric Acid	160	200	40	40
PEMFC	PEM	60	90	53	58
SOFC	Yttrium stabilized zirconia	800	1000	35	43

Table 2.4: *Overview of main Fuel Cells technologies efficiencies [10]*

With the script reported in the Code Appendix 4 (Code 4.2) it has been possible to obtain the following results in terms of energy required and mass of hydrogen to be generated:

Technology	Minimum Efficiency [MWh]	Maximum Efficiency [MWh]	Minimum Efficiency [kg H2]	Maximum Efficiency [kg H2]
AFC	$1.16*10^5$	$1.16*10^5$	$3.49*10^6$	$3.49*10^6$
DMFC	$8.72*10^4$	$8.72*10^4$	$2.62*10^6$	$2.62*10^6$
MCFC	$1.55*10^5$	$1.48*10^5$	$4.65*10^6$	$4.46*10^6$
PAFC	$1.74*10^5$	$1.74*10^5$	$5.24*10^6$	$5.24*10^6$
PEMFC	$1.32*10^5$	$1.20*10^5$	$3.95*10^6$	$3.61*10^6$
SOFC	$1.99*10^5$	$1.62*10^5$	$5.98*10^6$	$4.87*10^6$

Table 2.5: *Energy [MWh] or Hydrogen [kg] that has to be stored to cover the shortage for city 1 considering the minimum and maximum efficiencies for each fuel cell technology*

Technology	Minimum Efficiency [MWh]	Maximum Efficiency [MWh]	Minimum Efficiency [kg H2]	Maximum Efficiency [kg H2]
AFC	$1.16*10^5$	$2.91*10^4$	$8.73*10^6$	$8.73*10^6$
DMFC	$8.72*10^4$	$2.18*10^4$	$6.55*10^6$	$6.55*10^6$
MCFC	$1.55*10^4$	$3.71*10^4$	$1.16*10^7$	$1.11*10^7$
PAFC	$1.74*10^4$	$4.36*10^4$	$1.31*10^7$	$1.31*10^7$
PEMFC	$1.32*10^4$	$3.01*10^4$	$9.88*10^6$	$9.03*10^6$
SOFC	$1.99*10^4$	$4.05*10^4$	$1.50*10^7$	$1.22*10^7$

Table 2.6: *Energy [MWh] or Hydrogen [kg] that has to be stored to cover the shortage for city 2 considering the minimum and maximum efficiencies for each fuel cell technology*

Technology	Minimum Efficiency [MWh]	Maximum Efficiency [MWh]	Minimum Efficiency [kg H2]	Maximum Efficiency [kg H2]
AFC	$1.74*10^4$	$1.74*10^4$	$5.24*10^6$	$5.24*10^6$
DMFC	$1.31*10^4$	$1.31*10^4$	$3.93*10^6$	$3.93*10^6$
MCFC	$2.32*10^4$	$2.23*10^4$	$6.98*10^6$	$6.68*10^6$
PAFC	$2.62*10^4$	$2.62*10^4$	$7.85*10^6$	$7.85*10^6$
PEMFC	$1.97*10^4$	$1.80*10^4$	$5.93*10^6$	$5.42*10^6$
SOFC	$2.99*10^4$	$2.43*10^4$	$8.98*10^6$	$7.31*10^6$

Table 2.7: *Energy [MWh] or Hydrogen [kg] that has to be stored to cover the shortage for city 3 considering the minimum and maximum efficiencies for each fuel cell technology*

From the Script 4.2 has been possible to calculate the energy that has to be stored for each city (first as energy units, then as mass of hydrogen, see Tables 2.5, 2.6 and 2.7, visually presented in bar plots of Figure 2.4) considering the efficiencies of the fuel cells (minimum and maximum [10]) for all the aforementioned technologies. These data are related to the energy that has to stored to cover the shortage of each city but don't consider the efficiency of electrolyzers. Considering these efficiencies permits to understand the amount of energy that has to be taken from the surplus to cover this shortage of electricity:

	AMC		DMFC		MCFC		PAFC		PEMFC		SOFC	
Alkaline	$1.14*10^6$	$8.90*10^4$	$8.55*10^4$	$6.68*10^4$	$1.52*10^6$	$1.13*10^6$	$1.71*10^6$	$1.34*10^6$	$1.29*10^6$	$9.21*10^4$	$1.95*10^6$	$1.24*10^6$
PEM	$1.05*10^6$	$8.03*10^4$	$7.85*10^4$	$6.02*10^4$	$1.40*10^6$	$1.03*10^6$	$1.57*10^6$	$1.20*10^6$	$1.19*10^6$	$8.30*10^4$	$1.80*10^6$	$1.12*10^6$

Table 2.8: *Energy [MWh] that has to be used from surplus to cover the shortage for all cities considering the minimum and maximum efficiencies for each fuel cell technology (columns) and electrolyzers (rows)*

	AMC		DMFC		MCFC		PAFC		PEMFC		SOFC	
Alkaline	$2.23*10^4$	$1.78*10^4$	$1.71*10^4$	$1.34*10^4$	$3.04*10^4$	$2.27*10^4$	$3.42*10^4$	$2.67*10^4$	$2.58*10^4$	$1.84*10^4$	$3.91*10^4$	$2.48*10^4$
PEM	$2.09*10^4$	$1.61*10^4$	$1.57*10^4$	$1.20*10^4$	$2.79*10^4$	$2.05*10^4$	$3.14*10^4$	$2.41*10^4$	$2.37*10^4$	$1.66*10^4$	$3.59*10^4$	$2.24*10^4$

Table 2.9: *Energy [MWh] that has to be used from surplus to cover the shortage for city 1 considering the minimum and maximum efficiencies for each fuel cell technology (columns) and electrolyzers (rows)*

	AMC		DMFC		MCFC		PAFC		PEMFC		SOFC	
Alkaline	$5.70*10^4$	$4.45*10^4$	$4.27*10^4$	$3.34*10^4$	$7.60*10^4$	$5.68*10^4$	$8.55*10^4$	$6.68*10^4$	$6.45*10^4$	$4.60*10^4$	$9.77*10^4$	$6.21*10^4$
PEM	$5.24*10^4$	$4.01*10^4$	$3.93*10^4$	$3.01*10^4$	$6.98*10^4$	$5.12*10^4$	$7.85*10^4$	$6.02*10^4$	$5.93*10^4$	$4.15*10^4$	$8.98*10^4$	$5.60*10^4$

Table 2.10: *Energy [MWh] that has to be used from surplus to cover the shortage for city 2 considering the minimum and maximum efficiencies for each fuel cell technology (columns) and electrolyzers (rows)*

	AMC		DMFC		MCFC		PAFC		PEMFC		SOFC	
Alkaline	$3.42*10^4$	$2.67*10^4$	$2.56*10^4$	$2.00*10^4$	$4.56*10^4$	$3.41*10^4$	$5.13*10^4$	$4.05*10^4$	$3.87*10^4$	$2.76*10^4$	$5.86*10^4$	$3.73*10^4$
PEM	$3.14*10^4$	$2.41*10^4$	$2.36*10^4$	$1.81*10^4$	$4.19*10^4$	$3.07*10^4$	$4.71*10^4$	$3.61*10^4$	$3.56*10^4$	$2.49*10^4$	$5.39*10^4$	$3.36*10^4$

Table 2.11: *Energy [MWh] that has to be used from surplus to cover the shortage for city 3 considering the minimum and maximum efficiencies for each fuel cell technology (columns) and electrolyzers (rows)*

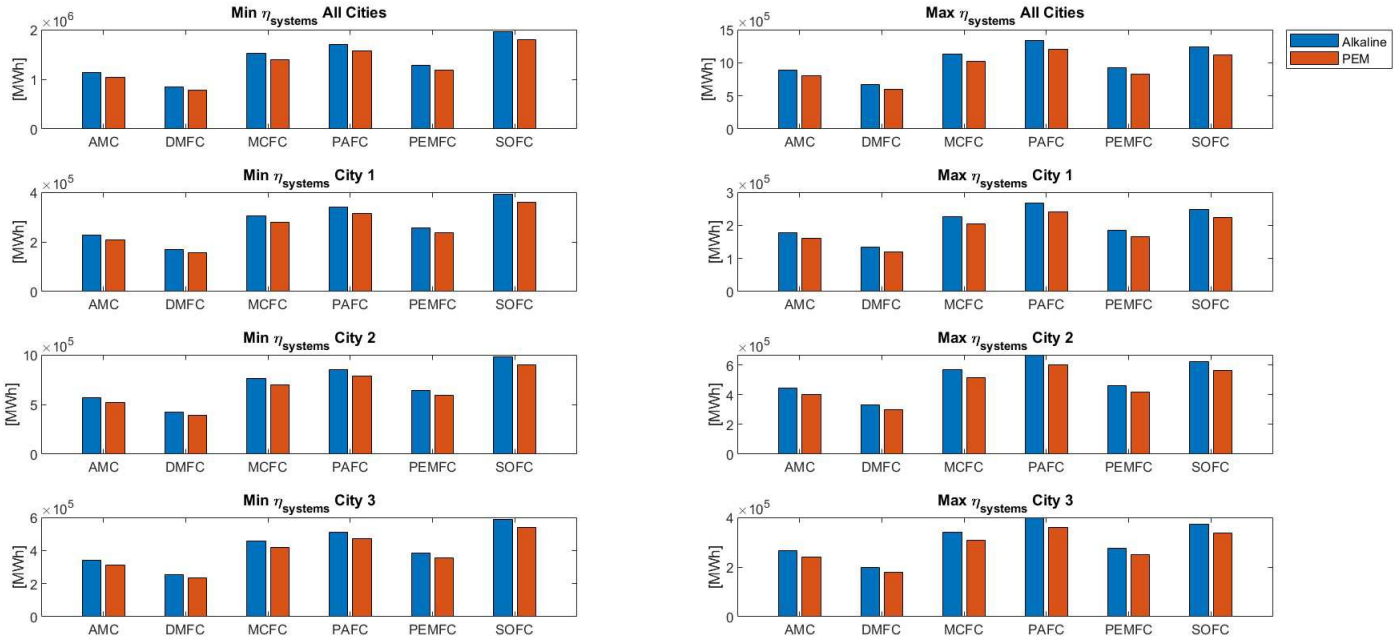

Figure 2.4: *Visual representation of energy requirements presented in Tables 2.8, 2.9, 2.10 and 2.11*

Once defined the energy that has to be stored and the fraction of energy surplus that has to used to address the energy shortage it is possible to define two scenarios. The first one is based on production of hydrogen in a dedicated offshore island and then sent to the coast to the storage sites. The second possibility is energy transmission through electrical cables, meaning that hydrogen storage and conversion is done offshore and the onshore storage is filled with

hydrogen produced only locally.

2.0.4 Scenario 1: H2 Production on Hydrogen Island and pipeline transmission to land

In this scenario it is considered that hydrogen is produced and transmitted to onshore storage sites through the usage of pipelines. In both this scenario and the following electrical one there is the presence of offshore storage site, used as first storage location. This storage site can be considered as a solution also to avoid the construction of onshore storage sites but the costs for the construction are higher offshore than onshore.
Considering the presence of an offshore wind farm at a distance of 300 km from the coast in east direction, different aspects are evaluated. It is analyzed the production and storage of hydrogen offshore, the transmission of it through pipeline and the conversion to electricity onshore through the usage of fuel cells. In paragraphs 2.0.2 and 2.0.3 the calculations of the energy shortages and the storage (energy and hydrogen) have been presented. In this paragraph it is evaluated the energy required for the compression for storage, the compression for transmission and the volume of the necessary artificial salt caverns. The production of hydrogen is carried out in a designated artificial hydrogen island which should be placed at maximum 5 km from the wind farm. Moreover, its position has to be chosen considering aspects like the positioning of salt caverns and the pipeline design.
Before evaluating the aspects previously cited, it is necessary to define the position of the pipeline shore connection, as it is presented in the map of Figure 2.5.

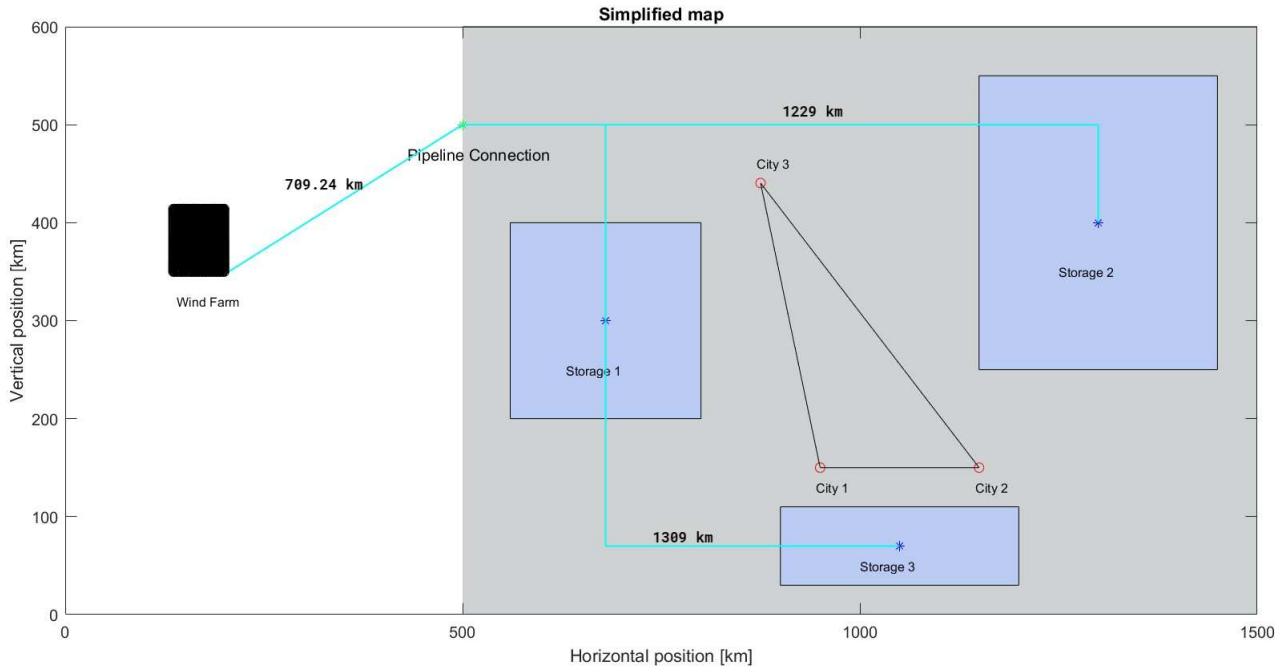

Figure 2.5: *Pipeline coast connection and design of the pipeline grid to storage sites*

The position has been considered to be at 500 km from the horizontal axis: once fixed the position it has been possible to manually define a pipeline grid connection with all the storage sites. As hypothesis, it has been considered that each storage site is supplied by a single tube of the pipeline. The results have been 3 pipelines with the following lengths:

- $L_{pipeline1} = 709.24km$ (length of pipeline from H_2 island to storage 1 for city 3)
- $L_{pipeline2} = 1229km$ (length of pipeline from H_2 island to storage 2 for city 2)
- $L_{pipeline1} = 1309km$ (length of pipeline from H_2 island to storage 3 for city 1).

With the definition of the pipeline grid design it has been possible to perform calculations concerning the energy required for the compression for storage, the energy required for the compression for transmission and the calculation of the dimentions of the artificial caverns. Each of these calculation steps are here presented.

Artificial Caverns Volume and dimensions calculation

In Tables 2.5, 2.6 and 2.7 the amounts of hydrogen that have to be stored for each city have been reported. The calculations have been carried out from these data with the scope of finding the volume of the artificial caverns and therefore also the volume of freshwater needed for their construction.
To take into account the geothermal gradient of temperature with depth an third-grade polynomial interpolation of data from Table 2.12 has been carried out:

Depth [m]	Max T [C]	Mean T [C]	Median T [C]	Min T [C]	Number of measurements	Std Deviation
50.00	11.00	8.90	8.80	7.40	94.00	0.80
75.00	11.60	9.20	9.30	6.70	132.00	0.90
100.00	13.00	9.70	9.70	7.30	103.00	1.10
150.00	15.50	10.50	10.60	7.80	43.00	1.60
200.00	17.10	11.60	11.20	8.70	32.00	2.20
250.00	17.90	13.40	13.20	9.60	20.00	2.20
300.00	19.30	14.90	14.20	12.20	13.00	2.00

Table 2.12: *Denmark Temperature distribution with statistical information [18]*

From the interpolation a function has been created for the calculation of the temperature based on the depth in meters (2.1):

```
function geotemp = dimscript_geotempcalc(p,d) % NB: depth d in m
p=double(p); d=double(d);
geotemp=polyval(p,d); % p is the vector with the polynomial
    coefficients
geotemp=geotemp+273.15;
end
```

Code 2.1: *Function for temperature calculation based on depth in meters*

Similarly, in order to be able to access in a faster way data, a mesh grid of density from pressure and temperature for interpolation has been created (2.2):

```
% Temperature (from 300 to 600 K)
Tmesh=linspace(300,600,50);          % 50 points
% Pressure (from 20 to 500 bar)
Pmesh=100000*linspace(20,500,50);          % 50 points
% Calculation of density through CoolProp
for idx13=1:length(Tmesh)                % T on columns
    for idx14=1:length(Pmesh)            % p on rows
        rhomesh(idx14,idx13)=py.CoolProp.CoolProp.PropsSI('DMASS','T'
    ,Tmesh(1,idx13),'P',Pmesh(1,idx14),'H2');
    end
```

```
end
% Mesh creation
[Tm Pm Rhom]=meshgrid(Tmesh,Pmesh,rhomesh);
% preparing data for surface fitting
[xData, yData, zData]=prepareSurfaceData(Tmesh,Pmesh,rhomesh);
cf=fit([xData,yData],zData,'poly23','Normalize','on');
```

Code 2.2: *Mesh grid of density from pressure and temperature*

With the Functions 2.1 and 2.2 it has been possible to define an iterative function (Function 2.3) that permitted to calculate the dimensions (height and diameter), average temperature and average density starting from the polynomial coefficients vector, the cavern roof depth, an initial attempt value of the cavern bottom depth, storage pressure, mass of hydrogen to be stored, interpolation coefficients of the density mesh grid and the height-diameter ratio of the cavern. The cavern roof depth and the pressure, considered to be the maximum pressure, have been taken from the set of values (cavern roof depth, maximum and minimum storage pressures) cited in [23].

```
function [H,D,T_avg,rho_avg]=dimfunction_simplified(p,d_roof,
    d_bottom_initial,pressure,m_H2,cf,H_D)
D1=double(d_roof); D2=double(d_bottom_initial); geotemp_D1=double(
    dimscript_geotempcalc(p,D1));
m_H2_calc=1000000; % [kg];
z=1;               % number of iterations
syms H

if D2>D1
    while abs(m_H2-m_H2_calc)>100
        m_H2_calc=m_H2_calc+100;
      % increase of value of m_H2_calc
        z=z+1;
        geotemp_D2=dimscript_geotempcalc(p,D2);
        rho_h2_D1=feval(cf,[geotemp_D1,pressure]);
        rho_h2_D2=feval(cf,[geotemp_D2,pressure]);
        rho_h2_avg=(rho_h2_D1+rho_h2_D2)/2;
      % avg rho
        vol_calc=m_H2_calc/rho_h2_avg;
        H=(vol_calc*400/pi)^(1/3);
        D2=H+D1;
    end
```

```
19 else
20 end
21
22 H;                                  % height   [m]
23 D=H/H_D;                            % diameter [m]
24 T_avg=(geotemp_D1+geotemp_D2)/2;    % avg temp [K]
25 rho_avg=rho_h2_avg;                 % avg rho  [kg/m3]
26
27 end
```

Code 2.3: *Iterative function for the calculation of the dimensions (height H and diameter D) of the cavern, the average temperature T_{avg} and the average density ρ_{avg}*

The iterative process that I have used it is reported in this Function 2.3. Taking into account that, due to geothermal temperature gradient, the density of hydrogen was not constant throw-out the entire cavern height I have fixed an initial value of the cavern roof and bottom position. From that, considering the average hydrogen density between the cavern top and bottom and iteratively modifying the calculated hydrogen mass value, the fluid density and the bottom position of the cavern (and, therefore, the overall dimentions) has been calculated.

This Function 2.3 has been then used inside a dedicated script that has taken into account three parameters through the usage of three linked for loops:

1. $d_{cavernroof}$ (cavern roof depth, from the set [23]; consequently also the maximum pressure has been defined from these data)
2. City considered (analysis per each city)
3. η_{FC} (efficiency of each fuel cell technology)

Which results in the following script:

```
1 % Considering max storage pressure
2 for idx12=1:length(cavern_roof_depth_m(:,1))
          % considering the possible cavern roof depth as from
    articles
3     for idx10=1:length(h2_storage_city_kg_minefficiency(1,:))
          % considering the 3 cities
4         parfor idx11=1:length(h2_storage_city_kg_minefficiency(:,1))
          % considering the efficiencies of the FC
```

```
5             [height_m_mineff(idx11,idx10,idx12),diameter_m_mineff(
    idx11,idx10,idx12),T_avg_mineff(idx11,idx10,idx12),rho_avg_mineff(
    idx11,idx10,idx12)]=dimfunction_simplified(p,cavern_roof_depth_m(
    idx12),cavern_roof_depth_m(idx12)+1,max_storage_pressure_Pa(idx12)
    ,h2_storage_city_kg_minefficiency(idx11,idx10),cf,H_D);
6             [height_m_maxeff(idx11,idx10,idx12),diameter_m_maxeff(
    idx11,idx10,idx12),T_avg_maxeff(idx11,idx10,idx12),rho_avg_maxeff(
    idx11,idx10,idx12)]=dimfunction_simplified(p,cavern_roof_depth_m(
    idx12),cavern_roof_depth_m(idx12)+1,max_storage_pressure_Pa(idx12)
    ,h2_storage_city_kg_maxefficiency(idx11,idx10),cf,H_D);
7         end
8     end
9 end
```

Code 2.4: *Salt cavern dimensions calculation script*

The results matrices are here reported: it is important to notice that these are three-dimensional matrices with first dimension (rows) is related to the fuel cells efficiencies, the second (columns) is related to the city considered and the third is related to the roof depth case considered. The results are reported considering the minimum and maximum efficiencies of the FC technologies.

From the data of Tables 2.13, 2.14 and 2.15 it is possible to notice that, for all cities, the values of cavern height and diameter, average temperature and density are similar both in minimum and maximum efficiency cases for the AFC and DMFC FC technologies since it has been considered an average efficiency value. For the other technologies it has been possible to notice how the efficiency impacts on the dimentions of the caverns in terms of height (with a ±10% tolerance) and diameter, with an effect of the diameter of ±10% on the volume. This latter aspect is crucial also in environmental terms: lower storage volumes also means that it is necessary to use, treat and dispose lower volumes of freshwater for the construction of the artificial salt caverns. The environmental aspect in terms of freshwater volumes needed are presented in the next paragraph.

Freshwater Volumes needed for cavern construction

In order to evaluate the amount of freshwater needed to build the salt cavern the construction process of the horizontal caverns HA-4 and HA-5 in Huai'an (China) has been taken as reference [6]. For these caverns the characteristics are presented in the Table 2.16.

	Height Cavern [m]											
Roof Depth [m]	457.2		609.6		762		914.4		1066.8		1219.2	
AFC	435.57	435.57	392.51	392.51	373.61	373.61	358.68	358.68	340.00	340.00	330.32	330.32
DMFC	395.31	395.31	356.30	356.30	339.19	339.19	325.68	325.68	308.78	308.78	300.04	300.04
MCFC	479.97	472.98	432.43	426.15	411.54	405.57	395.03	389.30	374.38	368.97	363.64	358.40
PAFC	499.45	499.45	449.93	449.93	428.17	428.17	410.95	410.95	389.44	389.44	378.23	378.23
PEMFC	454.19	440.58	409.25	397.01	389.51	377.89	373.92	362.78	354.42	343.88	344.30	334.08
SOFC	522.50	487.40	470.64	439.10	447.83	417.88	429.79	401.10	407.24	380.12	395.47	369.20
	Diameter [m]											
AFC	43.56	43.56	39.25	39.25	37.36	37.36	35.87	35.87	34.00	34.00	33.03	33.03
DMFC	39.53	39.53	35.63	35.63	33.92	33.92	32.57	32.57	30.88	30.88	30.00	30.00
MCFC	48.00	47.30	43.24	42.61	41.15	40.56	39.50	38.93	37.44	36.90	36.36	35.84
PAFC	49.95	49.95	44.99	44.99	42.82	42.82	41.10	41.10	38.94	38.94	37.82	37.82
PEMFC	45.42	44.06	40.92	39.70	38.95	37.79	37.39	36.28	35.44	34.39	34.43	33.41
SOFC	52.25	48.74	47.06	43.91	44.78	41.79	42.98	40.11	40.72	38.01	39.55	36.92
	Average Temperature [K]											
AFC	307.07	307.07	314.24	314.24	322.30	322.30	330.14	330.14	337.10	337.10	342.86	342.86
DMFC	305.87	305.87	313.19	313.19	321.39	321.39	329.40	329.40	336.56	336.56	342.56	342.56
MCFC	308.38	308.17	315.37	315.19	323.27	323.12	330.92	330.80	337.63	337.55	343.12	343.08
PAFC	308.95	308.95	315.86	315.86	323.68	323.68	331.24	331.24	337.85	337.85	343.22	343.22
PEMFC	307.62	307.22	314.72	314.37	322.71	322.41	330.47	330.23	337.33	337.16	342.98	342.89
SOFC	309.62	308.60	316.43	315.56	324.16	323.43	331.61	331.04	338.09	337.72	343.31	343.16
	Average Density [kg/m^3]											
AFC	5.38	5.38	7.35	7.35	8.52	8.52	9.63	9.63	11.31	11.31	12.33	12.33
DMFC	5.40	5.40	7.37	7.37	8.54	8.54	9.65	9.65	11.32	11.32	12.34	12.34
MCFC	5.36	5.36	7.33	7.33	8.50	8.51	9.61	9.62	11.29	11.30	12.32	12.32
PAFC	5.35	5.35	7.32	7.32	8.49	8.49	9.61	9.61	11.29	11.29	12.32	12.32
PEMFC	5.37	5.38	7.34	7.35	8.51	8.52	9.62	9.63	11.30	11.31	12.33	12.33
SOFC	5.34	5.36	7.31	7.32	8.48	8.50	9.60	9.61	11.28	11.29	12.32	12.32

Table 2.13: *Results for city 1 in terms of Height and Diameter of caverns, average temperature and density of hydrogen; the orange colour refers to the minimum efficiency of FC technologies, the light blue instead to the maximum*

	Height Cavern [m]											
Roof Depth [m]	457.2		609.6		762		914.4		1066.8		1219.2	
AFC	593.59	593.59	534.48	534.48	508.43	508.43	487.80	487.80	462.06	462.06	448.53	448.53
DMFC	538.56	538.56	485.07	485.07	461.53	461.53	442.91	442.91	419.65	419.65	407.48	407.48
MCFC	654.29	644.73	588.95	580.37	560.10	551.97	537.22	529.44	508.73	501.38	493.68	486.57
PAFC	680.91	680.91	612.82	612.82	582.74	582.74	558.87	558.87	529.15	529.15	513.42	513.42
PEMFC	619.04	600.44	557.32	540.63	530.10	514.26	508.53	493.38	481.64	467.33	467.48	453.63
SOFC	712.41	664.44	641.07	598.05	609.52	568.74	584.46	545.48	553.30	516.52	536.75	501.21
	Diameter [m]											
AFC	59.36	59.36	53.45	53.45	50.84	50.84	48.78	48.78	46.21	46.21	44.85	44.85
DMFC	53.86	53.86	48.51	48.51	46.15	46.15	44.29	44.29	41.96	41.96	40.75	40.75
MCFC	65.43	64.47	58.89	58.04	56.01	55.20	53.72	52.94	50.87	50.14	49.37	48.66
PAFC	68.09	68.09	61.28	61.28	58.27	58.27	55.89	55.89	52.92	52.92	51.34	51.34
PEMFC	61.90	60.04	55.73	54.06	53.01	51.43	50.85	49.34	48.16	46.73	46.75	45.36
SOFC	71.24	66.44	64.11	59.81	60.95	56.87	58.45	54.55	55.33	51.65	53.68	50.12
	Average Temperature [K]											
AFC	311.64	311.64	318.13	318.13	325.56	325.56	332.65	332.65	338.73	338.73	343.48	343.48
DMFC	310.08	310.08	316.82	316.82	324.49	324.49	331.85	331.85	338.25	338.25	343.37	343.37
MCFC	313.30	313.04	319.49	319.28	326.65	326.48	333.41	333.30	339.14	339.08	343.48	343.49
PAFC	314.00	314.00	320.07	320.07	327.09	327.09	333.71	333.71	339.27	339.27	343.43	343.43
PEMFC	312.34	311.83	318.71	318.28	326.03	325.69	332.98	332.74	338.91	338.78	343.50	343.49
SOFC	314.80	313.56	320.72	319.71	327.59	326.82	334.02	333.53	339.40	339.19	343.34	343.47
	Average Density [kg/m^3]											
AFC	5.31	5.31	7.28	7.28	8.45	8.45	9.57	9.57	11.26	11.26	12.31	12.31
DMFC	5.33	5.33	7.30	7.30	8.48	8.48	9.59	9.59	11.28	11.28	12.32	12.32
MCFC	5.29	5.29	7.25	7.26	8.43	8.43	9.56	9.56	11.25	11.25	12.31	12.31
PAFC	5.28	5.28	7.24	7.24	8.42	8.42	9.55	9.55	11.25	11.25	12.31	12.31
PEMFC	5.30	5.31	7.27	7.27	8.44	8.45	9.56	9.57	11.26	11.26	12.31	12.31
SOFC	5.27	5.29	7.23	7.25	8.41	8.43	9.54	9.55	11.25	11.25	12.32	12.31

Table 2.14: *Results for city 2 in terms of Height and Diameter of caverns, average temperature and density of hydrogen; the orange colour refers to the minimum efficiency of FC technologies, the light blue instead to the maximum*

	Height Cavern [m]											
Roof Depth [m]	457.2		609.6		762		914.4		1066.8		1219.2	
AFC	499.45	499.45	449.93	449.93	428.17	428.17	410.95	410.95	389.44	389.44	378.23	378.23
DMFC	453.23	453.23	408.39	408.39	388.69	388.69	373.14	373.14	353.68	353.68	343.57	343.57
MCFC	550.44	542.41	495.74	488.53	471.66	464.81	452.60	446.05	428.81	422.61	416.36	410.36
PAFC	572.81	572.81	515.82	515.82	490.73	490.73	470.85	470.85	446.05	446.05	433.04	433.04
PEMFC	520.83	505.20	469.14	455.10	446.40	433.07	428.42	415.65	405.95	393.88	394.22	382.53
SOFC	599.28	558.97	539.58	503.40	513.27	478.93	492.43	459.56	466.43	435.38	452.77	422.72
	Diameter [m]											
AFC	49.95	49.95	44.99	44.99	42.82	42.82	41.10	41.10	38.94	38.94	37.82	37.82
DMFC	45.32	45.32	40.84	40.84	38.87	38.87	37.31	37.31	35.37	35.37	34.36	34.36
MCFC	55.04	54.24	49.57	48.85	47.17	46.48	45.26	44.60	42.88	42.26	41.64	41.04
PAFC	57.28	57.28	51.58	51.58	49.07	49.07	47.09	47.09	44.60	44.60	43.30	43.30
PEMFC	52.08	50.52	46.91	45.51	44.64	43.31	42.84	41.57	40.60	39.39	39.42	38.25
SOFC	59.93	55.90	53.96	50.34	51.33	47.89	49.24	45.96	46.64	43.54	45.28	42.27
	Average Temperature [K]											
AFC	308.95	308.95	315.86	315.86	323.68	323.68	331.24	331.24	337.85	337.85	343.22	343.22
DMFC	307.59	307.59	314.69	314.69	322.69	322.69	330.46	330.46	337.32	337.32	342.97	342.97
MCFC	310.42	310.19	317.11	316.91	324.73	324.57	332.03	331.91	338.36	338.28	343.40	343.38
PAFC	311.06	311.06	317.64	317.64	325.16	325.16	332.36	332.36	338.56	338.56	343.45	343.45
PEMFC	309.57	309.12	316.39	316.00	324.13	323.80	331.58	331.33	338.07	337.91	343.30	343.24
SOFC	311.80	310.67	318.26	317.31	325.66	324.89	332.72	332.16	338.77	338.44	343.49	343.42
	Average Density [kg/m^3]											
AFC	5.35	5.35	7.32	7.32	8.49	8.49	9.61	9.61	11.29	11.29	12.32	12.32
DMFC	5.37	5.37	7.34	7.34	8.51	8.51	9.62	9.62	11.30	11.30	12.33	12.33
MCFC	5.33	5.33	7.30	7.30	8.47	8.47	9.59	9.59	11.27	11.28	12.32	12.32
PAFC	5.32	5.32	7.29	7.29	8.46	8.46	9.58	9.58	11.27	11.27	12.31	12.31
PEMFC	5.34	5.35	7.31	7.32	8.48	8.49	9.60	9.60	11.28	11.29	12.32	12.32
SOFC	5.31	5.33	7.27	7.29	8.45	8.47	9.57	9.58	11.26	11.27	12.31	12.31

Table 2.15: *Results for city 3 in terms of Height and Diameter of caverns, average temperature and density of hydrogen; the orange colour refers to the minimum efficiency of FC technologies, the light blue instead to the maximum*

Cavern	**HA-4**	**HA-5**
Volume Cavern [m^3]	52000	121000
Volume Freshwater Needed [m^3]	3329000	3690000
Volume Cavern/Volume Freshwater needed	64.02	30.50
Concentration Brine [kg_{salt}/m^3]	300	

Table 2.16: *HA-4 and HA-5 cavern and building process characteristics (Huai'an, China) [6]*

From the volume ratio of cavern to freshwater needed for its construction it has been evaluated the volume of freshwater needed considering the minimum and the maximum values of this ratio and the minimum and maximum efficiencies of the FC technologies. These results are presented in Tables 2.17 and 2.18.

	Min FC Efficiency											
	Min $V_{SaltCavern}/V_{Freshwater}$						**Max** $V_{SaltCavern}/V_{Freshwater}$					
	City 1 (*1.0e07) [m^3]											
Roof Depth [m]	457.24	609.6	762	914.4	1066.8	1219.2	457.24	609.6	762	914.4	1066.8	1219.2
AFC	1.9793	1.4484	1.2490	1.1052	0.9414	0.8632	4.1551	3.0406	2.6221	2.3202	1.9762	1.8122
DMFC	1.4796	1.0834	0.9346	0.8274	0.7051	0.6469	3.1061	2.2743	1.9621	1.7369	1.4802	1.3581
MCFC	2.6484	1.9368	1.6694	1.4764	1.2568	1.1517	5.5598	4.0659	3.5046	3.0994	2.6384	2.4177
PAFC	2.9841	2.1816	1.8800	1.6623	1.4147	1.2960	6.2644	4.5798	3.9467	3.4896	2.9697	2.7206
PEMFC	2.2440	1.6417	1.4155	1.2522	1.0663	0.9775	4.7109	3.4464	2.9714	2.6287	2.2385	2.0521
SOFC	3.4165	2.4969	2.1512	1.9015	1.6177	1.4814	7.1722	5.2417	4.5159	3.9917	3.3960	3.1100
	City 2 (*1e07) [m^3]											
AFC	5.0095	3.6570	3.1480	2.7800	2.3627	2.1613	10.516	7.677	6.608	5.836	4.9600	4.5372
DMFC	3.7415	2.7337	2.3547	2.0810	1.7700	1.6205	7.854	5.739	04.943	4.369	3.7158	3.4020
MCFC	6.7088	4.8928	4.2086	3.7136	3.1534	2.8818	14.084	10.271	8.835	7.796	6.6199	6.0496
PAFC	7.5615	5.5124	4.7398	4.1808	3.5488	3.2416	15.874	11.572	9.950	8.777	7.4499	6.8050
PEMFC	5.6818	4.1461	3.5679	3.1498	2.6760	2.4469	11.928	8.704	7.490	6.612	5.6177	5.1367
SOFC	8.6601	6.3102	5.4236	4.7817	4.0570	3.7039	18.180	13.247	11.386	10.038	8.5168	7.7755
	City 3 (*1e07) [m^3]											
AFC	2.9841	2.1816	1.8800	1.6623	1.4147	1.2960	6.264	4.5798	3.9467	3.4896	2.9697	2.7206
DMFC	2.2298	1.6313	1.4065	1.2443	1.0596	0.9714	4.681	3.4246	2.9527	2.6122	2.2244	2.0392
MCFC	3.9946	2.9181	2.5132	2.2207	1.8885	1.7287	8.386	6.1258	5.2759	4.6618	3.9645	3.6290
PAFC	4.5015	3.2872	2.8304	2.5002	2.1256	1.9450	9.450	6.9008	5.9418	5.2487	4.4622	4.0832
PEMFC	3.3838	2.4731	2.1307	1.8834	1.6023	1.4674	7.104	5.1916	4.4729	3.9538	3.3638	3.0805
SOFC	5.1548	3.7627	3.2388	2.8600	2.4305	2.2231	10.821	7.8990	6.7990	6.0038	5.1023	4.6669

Table 2.17: *Volumes of Freshwater [m^3] per each city considering all the FC technologies minimum efficiency and the two possible extreme values for the cavern - freshwater (needed for the construction) volume ratio*

	Max FC Efficiency											
	Min $V_{SaltCavern}/V_{Freshwater}$						Max $V_{SaltCavern}/V_{Freshwater}$					
	City 1 (*1.0e07) [m^3]											
Roof Depth [m]	457.24	609.6	762	914.4	1066.8	1219.2	457.24	609.6	762	914.4	1066.8	1219.2
AFC	1.9793	1.4484	1.2490	1.1052	0.9414	0.8632	4.1551	3.0406	2.6221	2.3202	1.9762	1.8122
DMFC	1.4796	1.0834	0.9346	0.8274	0.7051	0.6469	3.1061	2.2743	1.9621	1.7369	1.4802	1.3581
MCFC	2.5343	1.8536	1.5978	1.4132	1.2031	1.1026	5.3203	3.8911	3.3542	2.9667	2.5256	2.3147
PAFC	2.9841	2.1816	1.8800	1.6623	1.4147	1.2960	6.2644	4.5798	3.9467	3.4896	2.9697	2.7206
PEMFC	2.0483	1.4988	1.2925	1.1436	0.9740	0.8931	4.3000	3.1464	2.7132	2.4007	2.0447	1.8748
SOFC	2.7732	2.0278	1.7478	1.5456	1.3155	1.2054	5.8218	4.2570	3.6690	3.2446	2.7617	2.5304
	City 2 (*1e07) [m^3]											
AFC	5.0095	3.6570	3.1480	2.7800	2.3627	2.1613	10.516	7.677	6.6085	5.8360	4.9600	4.5372
DMFC	3.7415	2.7337	2.3547	2.0810	1.7700	1.6205	7.854	5.739	4.9433	4.3686	3.7158	3.4020
MCFC	6.4190	4.6821	4.0278	3.5546	3.0188	2.7592	13.475	9.829	8.4556	7.4620	6.3373	5.7923
PAFC	7.5615	5.5124	4.7398	4.1808	3.5488	3.2416	15.874	11.572	9.9502	8.7766	7.4499	6.8050
PEMFC	5.1849	3.7846	3.2575	2.8765	2.4445	2.2359	10.884	7.945	6.8385	6.0386	5.1317	4.6937
SOFC	7.0258	5.1232	4.4062	3.8874	3.3005	3.0157	14.749	10.755	9.2498	8.1607	6.9287	6.3307
	City 3 (*1e07) [m^3]											
AFC	2.9841	2.1816	1.8800	1.6623	1.4147	1.2960	6.2644	4.5798	3.9467	3.4896	2.9697	2.7206
DMFC	2.2298	1.6313	1.4065	1.2443	1.0596	0.9714	4.6811	3.4246	2.9527	2.6122	2.2244	2.0392
MCFC	3.8222	2.7925	2.4053	2.1256	1.8078	1.6551	8.0238	5.8622	5.0494	4.4621	3.7951	3.4744
PAFC	4.5015	3.2872	2.8304	2.5002	2.1256	1.9450	9.4499	6.9008	5.9418	5.2487	4.4622	4.0832
PEMFC	3.0883	2.2576	1.9454	1.7200	1.4636	1.3407	6.4833	4.7394	4.0840	3.6107	3.0726	2.8145
SOFC	4.1831	3.0554	2.6312	2.3247	1.9767	1.8092	8.7814	6.4140	5.5236	4.8802	4.1497	3.7980

Table 2.18: *Volumes of Freshwater [m^3] per each city considering all the FC technologies maximum efficiency and the two possible extreme values for the cavern - freshwater (needed for the construction) volume ratio*

As presented, the amount of freshwater needed in all cases (maximum and minimum efficiency for FC technologies, maximum and minimum volume ratio cavern - volume freshwater) is not negligible and has to be taken into account in terms of environmental impact and economic costs to treat and transport the brine.

Mass flow rates in pipelines and relative pressure drops

Analysing all the energy aspects, once calculated the dimensions of the underground storage it has been necessary to calculate the pressure drops in the pipelines feeding each storage site. To accomplish that, it has been necessary to evaluate the mass flow rates necessary to cover the demand when there's low wind production. It has been considered that there is request of H_2 from storage sites when the wind production is not covering the demand for energy. It has still been considered the same proportion of energy request between the three cities (50, 30 and 20 % respectively for city 2, 3 and 1). I have performed the calculations considering a modified demand curve, not continuous but stairs at

defined time intervals (for a 9-month period), using the script I have written and reported in Code 4.3 (in Code Appendix 4).

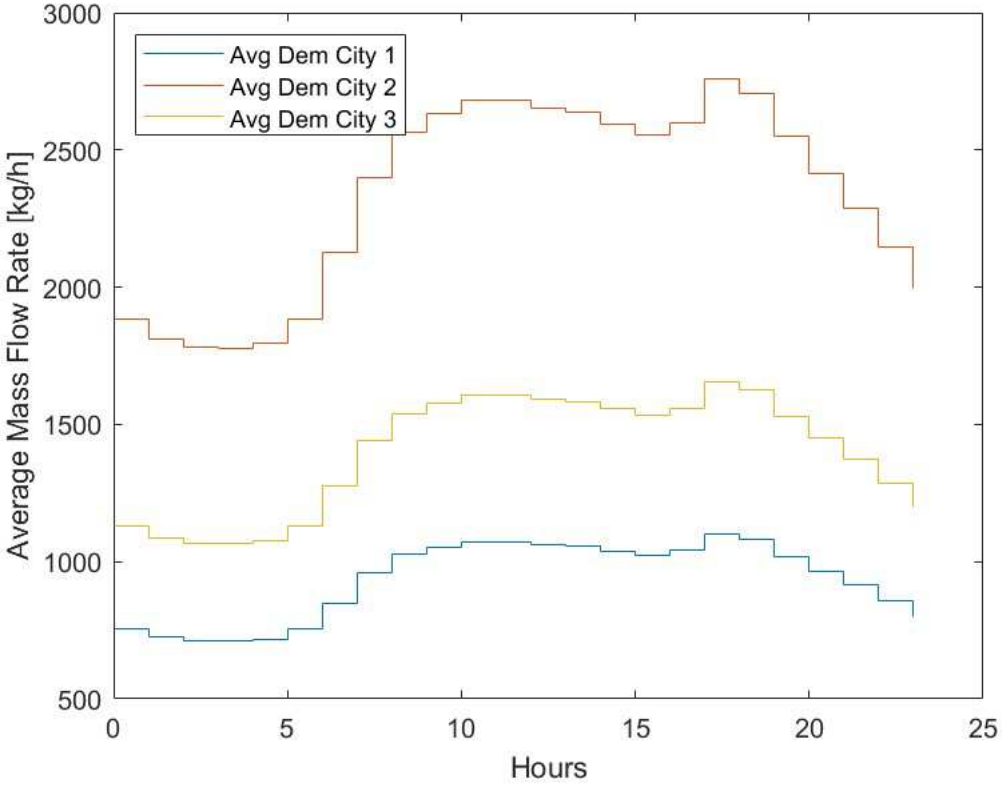

Figure 2.6: Average mass flow rate required for each city

$$\dot{m_{H_2,total}} = \frac{E_{trend,city1}+E_{trend,city2}+E_{trend,city3}-(P_{normalizedwindpowertrend}*P_{max,windfarm})}{\frac{\eta_{electrical,FC,\%}}{100}*\frac{LHV_{H_2}}{1000}} \quad (2.2)$$

The results (calculated through the Equation 2.2, with E the energy trend, P the power trend and the nominal wind farm power and $\eta_{electrical}$ the fuel cell electrical efficiency) are here plotted (Figure 2.6) and reported (Table 2.19). With a range of flow rates, considering always the hypothesis of having each storage site served by a dedicated pipeline, it has been possible to evaluate the pressure losses in the transmission process. From the calculations of the pressure losses has been possible to understand the necessity of intermediate compression sites

and the energy required for the compression of hydrogen. The pressure losses have been calculated with the following Script (Code 4.5, see Code Appendix 4), which is a modified version of an existing tool present in the community plugins of Matlab.

	Min $\eta_{FC}(*10^4)[kg/h]$			**Max** $\eta_{FC}(*10^4)[kg/h]$			**Min** $\eta_{FC}[kg/(person*day)]$	**Max** $\eta_{FC}[kg/(person*day)]$
AFC	1.32	3.31	1.98	1.32	3.31	1.98	0.25	0.25
DMFC	0.99	2.48	1.49	0.99	2.48	1.49	0.19	0.19
MCFC	1.76	4.41	2.64	1.69	4.22	2.53	0.34	0.32
PAFC	1.98	4.96	2.97	1.98	4.96	2.97	0.39	0.39
PEMFC	1.50	3.74	2.25	1.37	3.42	2.05	0.29	0.26
SOFC	2.27	5.67	3.40	1.84	4.61	2.77	0.43	0.35

Table 2.19: *Average flow rate* $[kg/h]$ *per each city (column) for the first two columns, third and fourth columns are the values expressed as* $\frac{kg_{H_2}}{person*day}$ *(considering the Danish population projections reported in [26]), considering all the FC technologies (rows) with their minimum and maximum values of effiencies*

For the analysis the following data and considerations have been assumed:

1. Average Danish Environmental Temperature $T_{avg,DK} = 281.45K$ [7]
2. Final Pressure considered $p_{final} = 20bar$ (it has been used for the calculation of the thermodynamic and transport properties)
3. Density used for pressure drop calculation $\rho_{pdrop} = 1.702kg/m^3$ (calculated with the average Danish environmental temperature and the final pressure)
4. Average viscosity (calculated with same temperature and pressure conditions as the density) $\mu_{pdrop} = 8.568e-06Pa*s$
5. Roughness considered for pressure drop $\epsilon_{pdrop} = 0.5*1e-03m$ (it has been considered the usage of steel pipes even though needs to be considered the corrosiveness of the hydrogen on steel)
6. Minimum diameter considered for the optimization script $D_{min} = 0.1m$
7. Maximum diameter considered for the optimization script $D_{max} = 2m$
8. Hydrogen velocity range considered inside pipelines $v_{pdrop} = [0.5, 20] * 3.5m/s$: it is roughly 3.5 times the natural gas one [9]
9. Lengths pipelines (from hydrogen island to relative onshore storage sites, see Figure 2.5):

(a) Length pipeline 1 (hydrogen island to storage 1 for city 3) $L_{pipeline1} = 709.3km$

(b) Length pipeline 2 (hydrogen island to storage 2 for city 2) $L_{pipeline2} = 1229.3km$

(c) Length pipeline 3 (hydrogen island to storage 3 for city 1) $L_{pipeline3} = 1309.3km$.

With these assumptions the following pressure drops (in [bar]) have been calculated (Table 2.20, each column shows the respective pipeline).

	Min η_{FC}			**Max** η_{FC}		
AFC	305.00	282.74	759.39	234.07	295.03	654.65
DMFC	375.93	442.55	903.41	361.74	381.08	890.32
MCFC	191.51	221.27	536.81	241.16	270.44	602.28
PAFC	156.04	245.86	549.90	156.04	233.57	445.16
PEMFC	255.35	282.74	680.83	198.60	295.03	615.37
SOFC	163.14	233.57	405.88	177.32	295.03	628.46

Table 2.20: *Pressure drops in* $[bar]$ *per each pipeline (column, first for city 1, second for city 2 and third for city 3), considering all the FC technologies (rows) with their minimum and maximum values of effiencies*

The values of the pressure drops make necessary the presence of intermediate pumping stations to increase the pressure and guarantee the arrival of the hydrogen to the storage sites.

Electrical Connection storage sites - cities

The analysis has been focused on the part of the system upstream the storage sites and the storage sites themselves so related on the system components between the wind farm and the storage sites. All the data in terms of energy required and efficiencies has been calculated and evaluated considering this approach. It is necessary though to add some considerations regarding the electrical connections between the storage sites and the single cities of the map. This aspect can't be neglected considering the distances between the storage sites and the cities which are estimated between 100 (storage 3 with city 1) to 350 km (storage 2 with city 2, see Figure 2.5).
The analysis of the efficiencies and the relative losses of power of transmission

lines and electrical intermediate elements are related to the type of transmission chosen: with transmission in alternate current (AC) it is necessary to consider the addition of inverters after the fuel cells since the latter produce electrical power in direct form (DC). Moreover, if the chosen approach is the AC one, it is required to consider the addition of transformers to enhance the value of voltage from the typical values of FC (can vary between 800-1000 V to few kV [10]) to the necessary values for the transmission lines (depending on the distance, usually 220 or 350 kV for HV transmission lines) and the step down transformers (necessary to reduce voltage) at arrival in the cities.
The second possibility is the usage of DC transmission: this permits to avoid energy losses in the transmission lines due to electrical effects typical of the AC lines (like skin effect [4]) and avoid the installation of inverters since FC already have DC current output. In this case though it is necessary to install DC-DC voltage step up converters (for transmission of power, example in Figure 2.7), DC-DC voltage step down converters (for user usable voltage levels) and DC-AC inverters (since users are AC based). All these conversion steps increase the losses and their efficiency therefore have to be considered. On average, considering a 1000 km 500 kV reference transmission line, it is possible to observe efficiencies with values of 88% for the AC line and of 94% for the DC line [24].
For the scenario 2.0.5 has to be considered if the technology for DC-DC conversion is sufficiently mature and can be used for conversion in an artificial offshore island, considering the rough conditions of the marine environment.

2.0.5 Scenario 2: Offshore storage and conversion of hydrogen with energy transmission to land through new electrical cables

The second possible solution is the transmission of energy through the usage of electrical lines and having the production of hydrogen directly on the storage sites. In this scenario there is not hydrogen transmission through pipelines: hydrogen is produced on the hydrogen island and stored offshore in a dedicated site. Moreover, hydrogen is also produced onshore with surplus of energy sent with electrical interconnection between the hydrogen island and the shore. The possible presence of offshore storage would permit to reduce the number of storage sites onshore and to increase the social acceptance of the hydrogen storage on the first place. As for the Scenario 2.0.4, the analysis has been carried

Figure 2.7: *Example of HVDC (high voltage direct current) conversion station, build by ABB for a 400 MW DC Denmark-Germany interconnection [1]*

out from the storage site while acknowledging that it is necessary to consider also the efficiency of electrical transmission from sites to cities.
The process for the calculation of the dimensions of the artificial caverns is the same as the previous scenario, the main difference is related to the addition of electrical components (with their efficiencies) between the hydrogen island and the onshore storage sites. Here the main components with their efficiencies are presented (part of these components are used also in the electrical connection from sites to cities, part which is in common between the two scenarios).

DC to AC Power Conversion: Inverter

Both the electrolyzers and the fuel cells work respectively using and generating DC current so it is necessary to consider the usage of inverters. In the case of the electrolyzer, it results necessary since most of the turbines from the main producers [34] have AC power output. Moreover, users generally require AC power so it is necessary to convert the Fuel Cell output. The commercially available fuel cell or electrolyzers units have generally integrated an inverter to solve this issue. If not, it can be considered an average value of efficiency around 98% (considering as reference the value from the industrial size centralized ABB inverters [1]). It is important to highlight how the efficiency of the inverters is not constant as the load changes and follows a curve similar to the one plotted in Figure 2.8. In the analysis though, for simplification purposes, it is considered

to be constant even at different load percentages compared to the nominal.

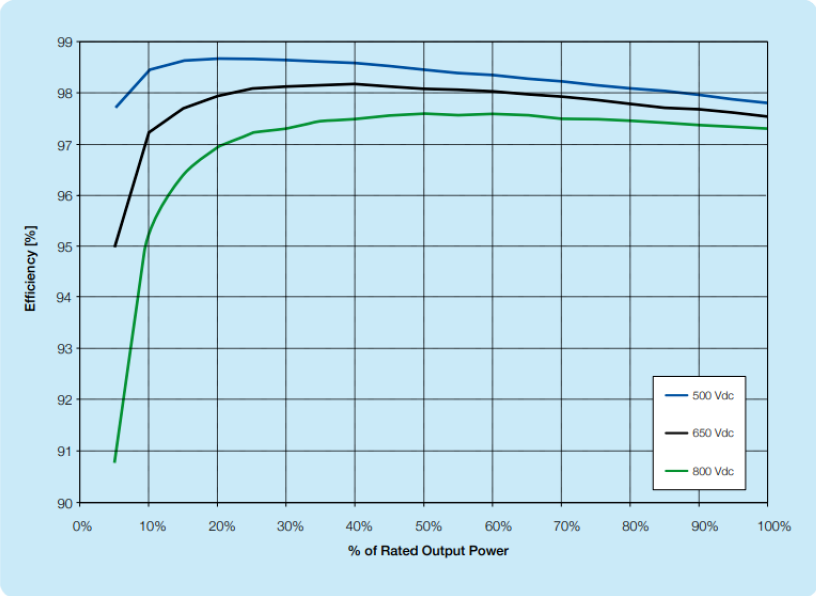

Figure 2.8: *Efficiency curves of an example of commercial industrial inverter (model ABB CORE-500.0/1000.0-TL) for different percentage values of the rated output power and voltage levels [1]*

Transmission Lines

The considerations regarding the transmission lines do not differ from what explained and presented in the subparagraph 2.0.4. The usage of DC transmission lines could permit to avoid some of the typical losses of AC lines but require the usage of DC-DC converters, high power electronic devices which are more complex and expensive compared to AC transformers. Avoiding these losses means that the lines register losses only for Joule effect and the actual limit on power transmission is related to thermal limits of the cable [16]. Taking into consideration the analysis for a 500 and 1000 MW wind farm carried out in [19], it has been possible to evaluate average values for the percentage losses in the transmission of power using different technologies.

As presented in Table 2.21 different configurations in terms of type of power transmitted (HVAC: High Voltage Alternate Current; HVDC LCC: High Voltage Direct Current Lince Commutated Converter; HVDC VSC: High Voltage Direct Current Voltage Source Converter; CS: Conversion Station) and distance of

	HVAC	HVDC LCC	HVDC VSC
Configuration	500 MW (400 kV)	600 MW CS	(350+220) MW CS
Number of cables	1	1	4
% Loss with Length: 50 km	1.13	1.75	4.05
% Loss with Length: 100 km	2.54	1.87	4.43
% Loss with Length: 150 km	4.98	1.99	4.82
Configuration	500 MW (400 kV)	600 MW CS	(350+220) MW CS
Number of cables	2	1	4
% Loss with Length: 200 km	7.76	2.11	5.20

Table 2.21: *Loss comparison for 500 MW wind farm at nominal wind speed (9 m/s for this plant) considering different transmission technologies [19]*

transmission determine different percentage losses. In this project analysis the distance from the wind farm and the coast is higher than 200 km (it is 300 km) so the transmission through the HVDC LCC technology would permit much lower transmission losses compared (considering 200 km, the losses would be about 2.11% as stated in the last line of the table) to HVAC. Sometimes combinations of HVAC and HVDC are considered for different aspects of the electrical grid like the reliability of the system and power stability. The border for the choice between AC and DC based on power transmitted and distance can be seen in the following graph (Figure): for distances greater than 70 km it is more convenient to switch to DC.

Transformer

In order to permit transmission with minimum losses it is necessary to step up the voltage (and step down at user level). In a AC system this is done through the usage of transformers. In the model it has been considered a constant value of the efficiency independently on the value of the load but, as it is possible to see in the plot of Figure 2.10, it is function of α (fraction of the load in respect to the nominal one) and $cos(\phi_e)$ (electrical phase angle). The efficiencies values still remain high, with values over 90% with loads from 25% of the nominal load. [2]

HVDC DC-DC Converters

Similarly to what has been described in the transformers subparagraph (2.0.5), also in case of DC power transmission it is necessary to step up the voltage to minimize the losses in electrical cables (and step down at user level

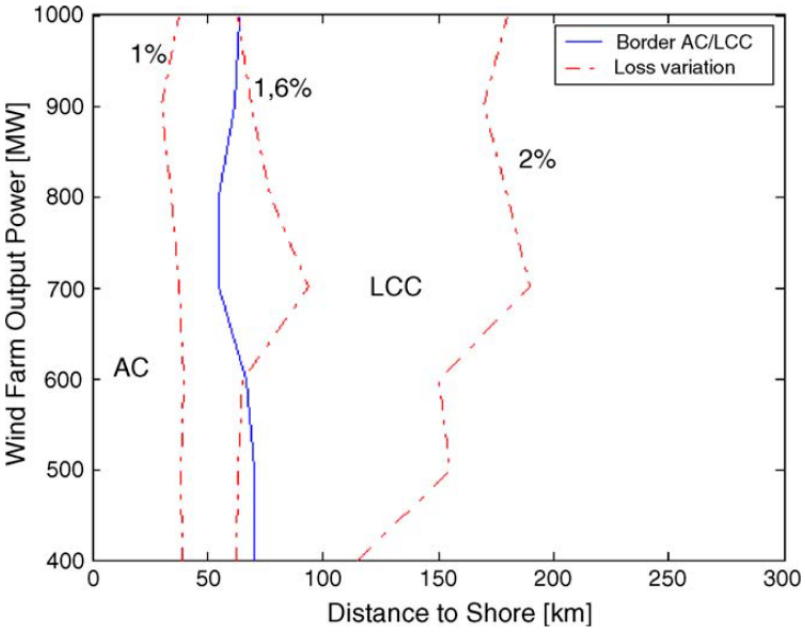

Figure 2.9: *MW-km plane for comparison HVAC-HVDC LCC as function of wind farm size at nominal speed (400-1000 MW) and different distances from shore [19]*

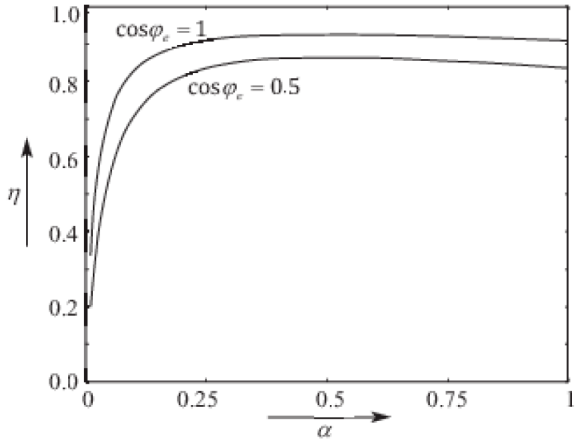

Figure 2.10: *Efficiency η of transformers based on fraction of nominal load α at different values of $cos(\phi_e)$ [2]*

to permit the usage of the power transmitted). In this case the process is done through the usage of HVDC DC-DC Converters: in Table 2.22 the evolution of the VSC HDVC technology is briefly presented with the relative percentage losses which permit to evaluate the efficiency of the power electronics device. In the analysis it has been supposed to use a constant value of the efficiency even though in reality the efficiency is function of the load and other electrical and

thermal parameters. [3]

Technology	Year first scheme commissioned	Converter Type	% Losses per converter	Swithching Frequency [Hz]	Example Project
HVDC Light 1st Gen	1997	Two-Level	3	1950	Gotland
HVDC Light 2nd Gen	2000	Three-level Diode NPC	2.2	1500	Eagle Pass
	2002	Three-level Active NPC	1.8	1350	Murraylink
HVDC Light 3rd Gen	2006	Two-Level with OPWM	1.4	1150	Estlink
HVDC Plus	2010	MMC	1	<150*	Trans Bay Cable
HVDC MaxSine	2014	MMC	1	<150*	SuperStation
HVDC Light 4th Gen	2015	CTL	1	=>150*	Dolwin 2

Table 2.22: *Evolution of VSC-HVDC Technology (*switching frequency is for a single module/cell) [3]*

As presented in Table 2.22, the percentage losses have limited values, lower than 3% so the DC-DC Conversion has high efficiency making the DC transmission a viable solution.

3

Dynamic Model

In the previous chapter (Chapter 2) the hydrogen storage requirements have been analyzed and calculated considering a static approach. This has meant to evaluate different aspects. Initially, the overall shortage of energy caused by the mismatch of the wind production and the user demand curves. Secondly the percentage of the surplus needed to cover that shortage through the production and storage of hydrogen.
The latter point has been carried out taking into account constant values of the efficiencies of the components of the system and ignoring the dynamic behaviour of the system. This behaviour is instead evaluated in this Chapter, taking into consideration the functioning and the consequences of the behaviour of the system components over time.
Now the assumptions considered and the composition of the analyzed system are presented before the evaluation of the results of the simulation.

3.1 Dynamic Model Assumptions

In order to proceed with the modelling and simulation, it has been necessary to simplify the system by making some assumptions. Those assumptions are here listed and explained:

a) The system is considered to be isolated thus no interconnections with other systems or grids are considered;

b) The system is entirely powered by offshore wind turbines and hydrogen storage, no other forms of energy production or storage have been considered for the analysis;

c) It has been considered a projection for the increase of the wind power installed and the increase of user demand with an expected enhance of 50% of the demand and a nominal wind power installed equal to 5 times the value of installed power in respect to the data considered (2017-2019);

d) The behaviour over time of electrolyzers and fuel cells is considered to be independent respectively from output and input pressure of hydrogen flow;

e) Dynamic behaviour for electrolyzers, fuel cells (start up and ramp up time) and compressors (time to reach defined pressure values) are considered;

f) Dynamic behaviour for hydraulic valves and electrical/electronic (inverters, converters, transformers and transmission lines) devices is neglected;

g) The model used for the description of the storage behaviour is 0-D (zero-dimensional or bulk model), thus considering no spacial variability withing the caverns; moreover, possible small leakages that may affect pressure have been neglected;

h) Due to the absence of spacial variability in the storage site (related to the bulk model) a constant average value of temperature is used for the calculation of hydrogen properties and for the simulation;

i) It is assumed that both input and output hydrogen mass flow rates to/from the storage site are stable and constant during a time period of one hour (temporal resolution of the model);

j) Input and output pipelines to/from storage sites are considered to be separated and with possibility of having different requirements in terms of pressure losses and diameters

k) Higher pressure losses are assumed to be acceptable for extraction pipelines since fuel cells functioning is considered independent from inlet hydrogen pressure (pressure losses have been calculated considering the available data for methane transmission);

l) Simulations have been carried out assuming values of the diameter of injection and extraction pipelines and with the definition of the maximum accepted pressure losses percentage (related to the instantaneous pressure value in the cavern; data of simulations has been taken from [30] and [14]);

m) Data used for the projection is 2017-2019 energy production and consumption from Energinet appropriately filtered and cleared of spikes and errors [8];

n) Values of initial percentage of filling of the storage site and the percentage of the surplus used are fixed for the calculations (different values have been considered for the analysis, e.g. we start the analysis with full storage).

Under these hypothesis a Matlab script and a Simulink model have been developed to calculate the impact of inertia of system components and the results of this in terms of required injected and extracted mass flow rates and volumes of storage sites.
The script and the model are now reported and explained in their different sections.

3.2 Simulink Model

Since a dynamic analysis is required to consider the variation over time a Simulink model has been developed (Figure 3.1).

Here the single components of the system and the whole system are described.

3.2.1 Power Shortage and Surplus

Power shortage and surplus (expressed in [MW]) have been calculated as difference between the wind power production (based on 2017-2019 wind data projected to 2050) and the user power demand (with data also based on 2017-2019 period projected to 2050) through the Code 4.4 (present in Code Appendix 4). The main equations used in this code are here reported (Equations 3.1, 3.2 and 3.3).

$$\Delta P_{production-load} = P_{production} - P_{load} \tag{3.1}$$

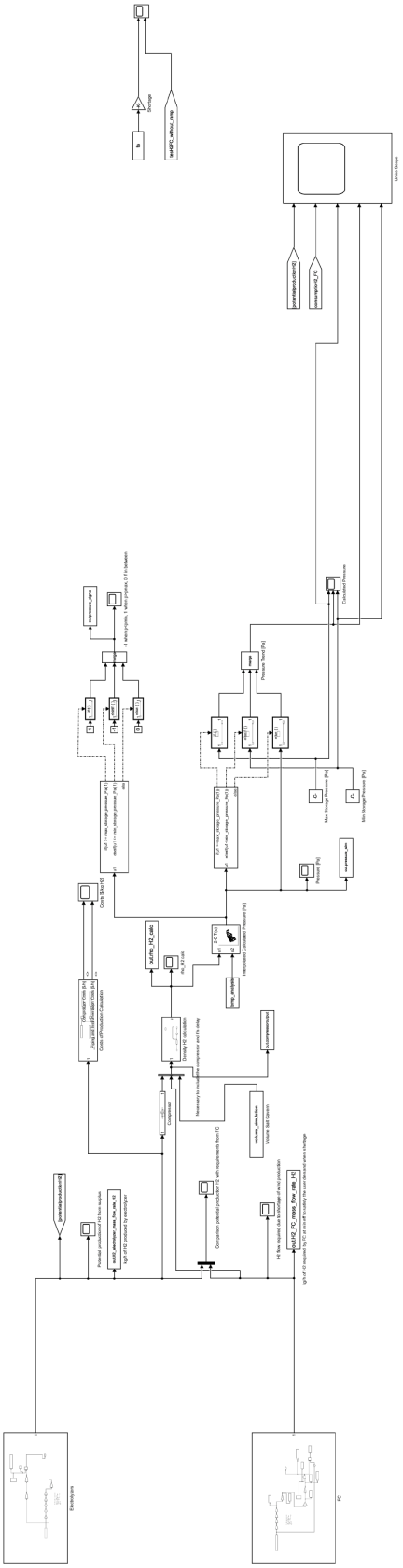

Figure 3.1: *Simulink Dynamic Model*

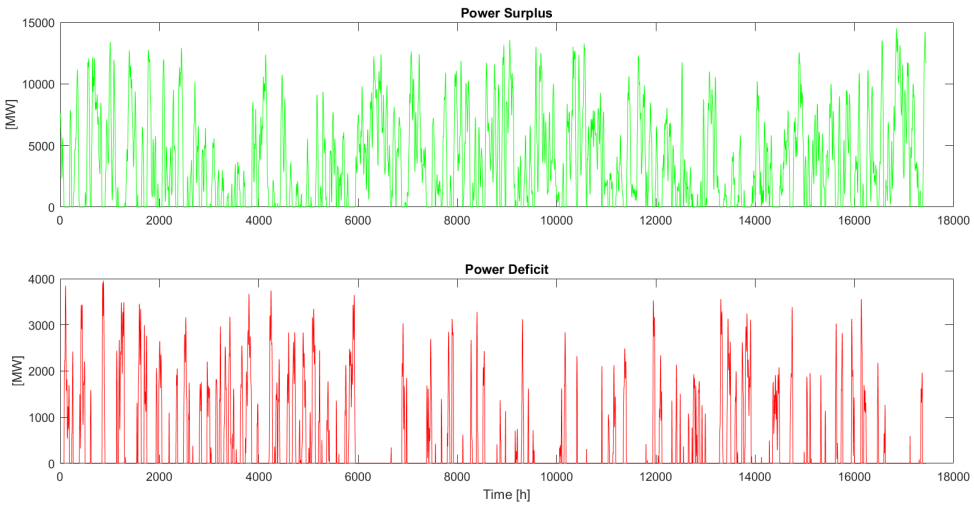

Figure 3.2: *Power surplus and deficit of the system (expressed in [MW])*

$$\Delta P_{surplus} = \Delta P_{production-load} (\Delta P_{production-load} > 0) \tag{3.2}$$

$$\Delta P_{deficit} = \Delta P_{production-load} (\Delta P_{production-load} < 0) \tag{3.3}$$

3.2.2 Control System

The data from 3.2.1 have been used in the model to define a simplified control system for the electrolyzers and fuel cells functioning. Defined the following parameters

- $\dot{W_{User}}[MW]$ as power requested by user
- $\dot{W_{Prod}}[MW]$ as wind power produced
- $p_{Storage}[Pa]$ as instant storage pressure value
- $p_{Storage,Max}[Pa]$ as maximum allowed storage pressure
- $p_{Storage,Min}[Pa]$ as minimum allowed storage pressure
- FC as fuel cell and El as electrolyzer

it has been possible to implement it based on these constraints:

- if $\dot{W_{User}} < \dot{W_{Prod}}$:
  - if $p_{Storage} < p_{Storage,Max} \Rightarrow$ FC off, El on
  - if $p_{Storage} = p_{Storage,Max} \Rightarrow$ FC off, El off
- if $\dot{W_{User}} > \dot{W_{Prod}}$:
  - if $p_{Storage} > p_{Storage,Min} \Rightarrow$ FC on, El off
  - if $p_{Storage} = p_{Storage,Min} \Rightarrow$ FC off, El off

This control system has been added in Simulink as it's possible to visualize in Figures 3.3 (for electrolyzers) and 3.4 (for fuel cells).

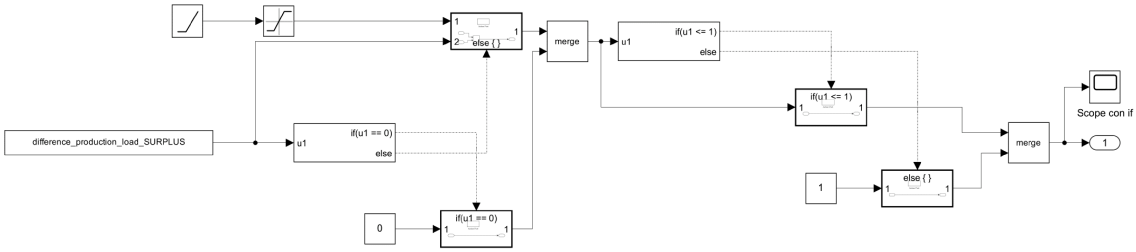

Figure 3.3: *Electrolyzer Control System*

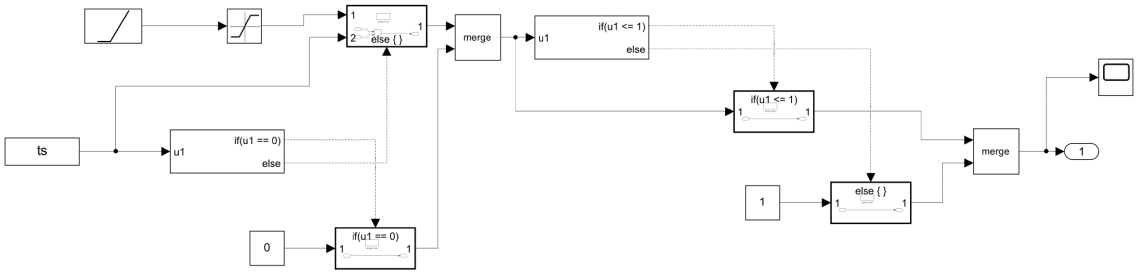

Figure 3.4: *Fuel Cell Control System*

3.2.3 Electrolyzers

Electrolyzers functioning (as molar flow rate of hydrogen produced [mol/s]) is related, following the Faraday's law (Equation 3.4), to the number of cells

n_{cells}, to the current flowing through I_{Ez}, Faraday's parameter F and Faraday's efficiency η_F (calculated with formula in Equation 3.5). [28]

$$\dot{n_{H_2}} = \frac{n_c I_{Ez}}{2F} \eta_F \tag{3.4}$$

$$\eta_F = 96.5 * e^{\frac{0.09}{I_{Ez}} - \frac{75.5}{I_{Ez}^2}} \tag{3.5}$$

In the analysis, though, a simplified version of its functioning based on a constant value of efficiency has been considered, independent from the parameters above cited and from the outlet pressure (as specified in Paragraph 3.1). It has been instead considered the behaviour over time of the electrolyzers in terms of start-up time (supposing a hot start-up) and ramp-up time, which are respectively defined as the time interval between the electrical connection and the hydrogen production start and the time interval necessary to reach the nominal power output from the end of start-up process.
These two parameters have been considered as part of the main simulation and have been obtained from data of products available on the market, like the electrolyzer Plug EX-425D [25]. They have been fixed at these values (even though they have been modified to see their impact on the simulation):

- $\Delta t_{Start-Up} = 10s$
- $\Delta t_{Ramp-Up} = 30s$

these parameters have been added to Simulink as presented in Figure 3.5. It has been considered a constant value of efficiency and then converted the value of energy "converted" by electrolyzers to the amount of hydrogen produced. From the product of this quantity and the block to consider the start-up and ramp-up times it has been obtained the trend over time of hydrogen mass flow rate produced (Figure 3.6). This mass flow rate has been then used in the zero-dimensional storage model to evaluate the amount of hydrogen stored and withdrawn over time. It is important to highlight that not the entire overproduction is converted into hydrogen to reduce the number of electrolyzers required. For this purpose a value of 30% of the surplus production has been considered and also varied to evaluate the impact of this parameter on the system.

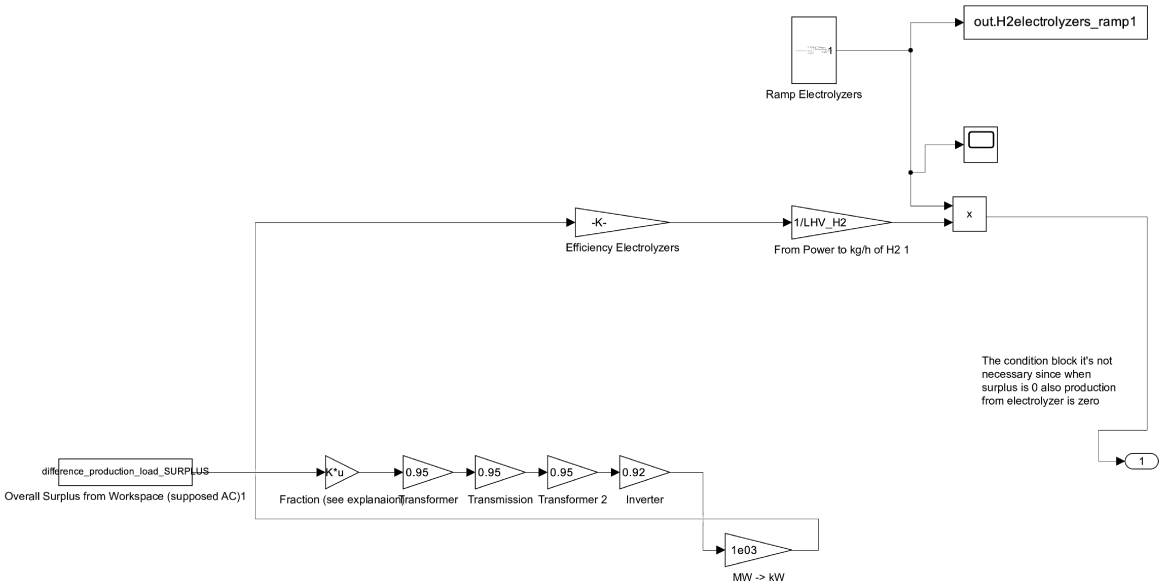

Figure 3.5: *Simulink electrolyzer simplified model*

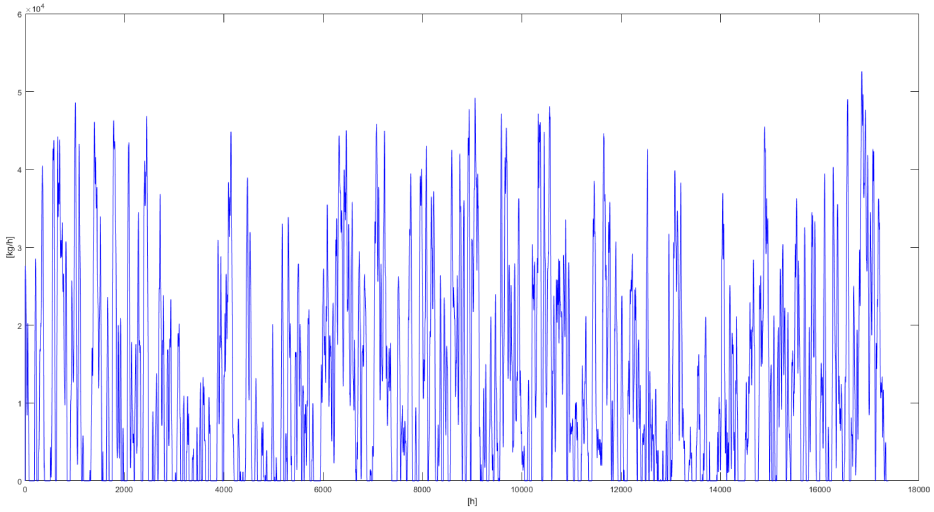

Figure 3.6: *Electrolyzers hydrogen mass flow production rate (reference conditions)*

3.2.4 Fuel Cells

Similarly to what has been considered in terms of model simplification with the electrolyzers, the behaviour of the fuel cells has been implemented (Figure 3.7) considering a constant value of efficiency and independent from the values of temperature and pressure of the hydrogen at inlet. The only parameters considered are the hydrogen mass flow rate at inlet and the time intervals of

start-up and ramp-up. The hydrogen mass flow rate trend required to cover the user requirements when wind production is not capable of directly covering it is reported in the plot of Figure 3.8.

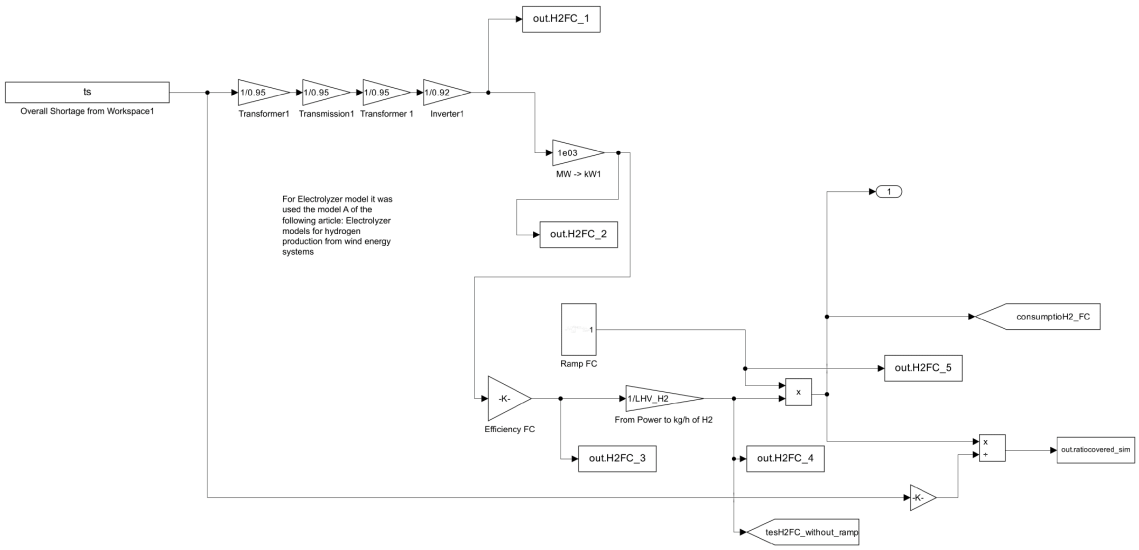

Figure 3.7: *Simulink FC simplified model*

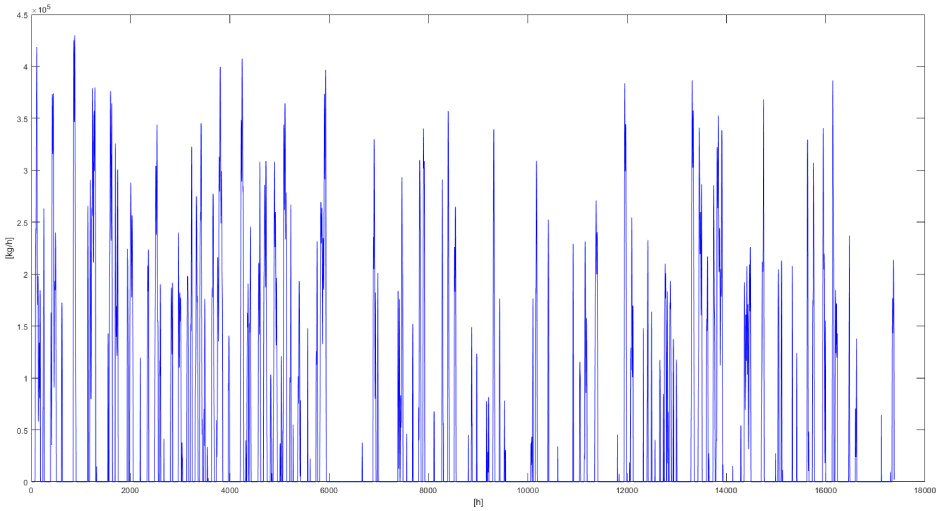

Figure 3.8: *Simulink scope of FC hydrogen mass flow rate required to cover wind production shortage and satisfy user demand*

The values of start-up and ramp-up time for the fuel cells have been evaluated from datasheets of models available on the market such as Gencell ([5]): based

on the technology chosen the values of start-up and ramp-up times change. In the analysis the following values have been considered:

- $\Delta t_{Start-Up} = 10s$
- $\Delta t_{Ramp-Up} = 15min = 900s$

These data have been implemented in the simplified Simulink model reported in Figure 3.4, in which the ramp block permits to consider the characteristic timing data previously described. As for electrolyzers' Simulink model (3.2.3), these two parameters have been modified to see the impact on the overall system.

3.2.5 Compressor

Another fundamental element of the system that has to be considered is the compressor, which increases pressure of the hydrogen produced by electrolyzers. Its inertia has to be considered in the analysis since it modifies the trend of the mass flow rate of hydrogen produced over time, which is a main parameter for the storage model. In order to consider this time dependant behaviour, in the modelling a time delay has been introduced from the starting up to the necessary pressure value to remain inside the storage site pressure limits. This is because we need to store hydrogen at a certain pressure and therefore till the compressor reaches that pressure value the flow rate is interrupted to avoid possible problems (like backflow) at storage site level. The pressure-time dependency for the compressor has been reported through the plot of Figure 3.9 [20].

This behaviour has been implemented in the simplified Simulink compressor model (Figure 3.10). The working principle has been based on this control system (reported in Figure 3.10), where the first input is the value of hydrogen mass flow rate in the previous time step while the second is for the current time step:

- if $\dot{m}_t = 0 \wedge \dot{m_{t-1}} = 0$ (both current and previous time step hydrogen mass flow rates are zero) the block transmits mass flow rate data without modifying it over time;
- if $\dot{m}_t > 0 \wedge \dot{m_{t-1}} = 0$ (previous time step had hydrogen mass flow rate equal to zero while current is positive) then the block transmits mass rate data considering the characteristic time step of the compressor;

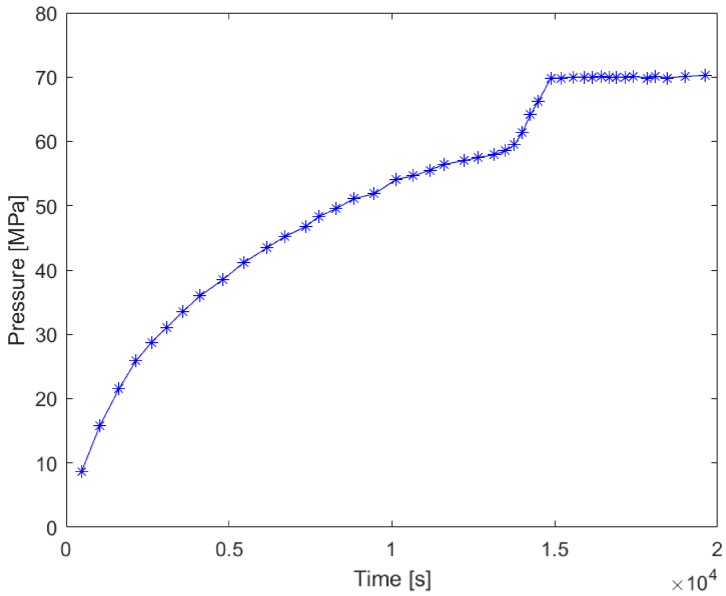

Figure 3.9: *Pressure-time dependency curve for a two stage adsorption-desorption compressor [20]*

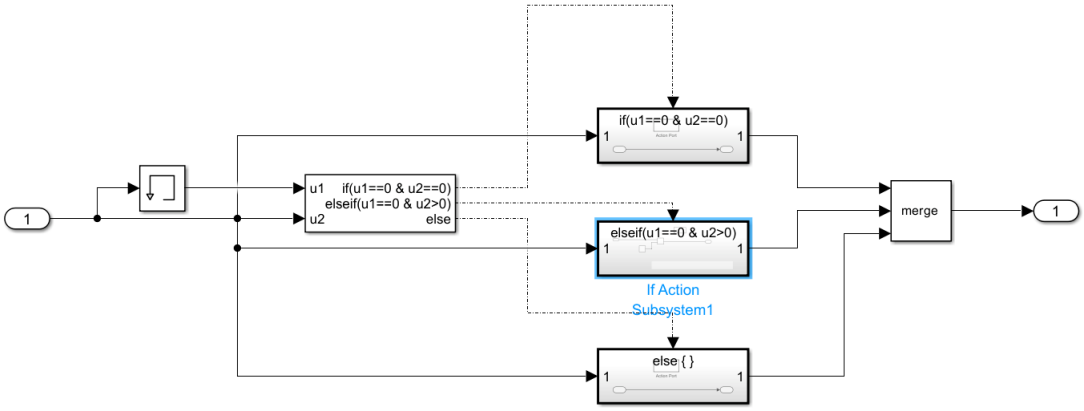

Figure 3.10: *Simulink compressor simplified model*

- else, similarly to the first one, there's not modifying over time of the mass flow rate data.

3.2.6 Storage system

As introduced in the assumptions of the Paragraph 3.1, the storage sites, which are subsurface artificial salt caverns, have been modelled considering a zero-dimensional or bulk model. This means that there's no spacial variability;

moreover, it has been considered a constant value of the temperature T in the site even though, due to geothermal gradient, the temperature varies with depth. So, based on these assumptions, it has been possible to write the following equation (3.6) that have been used for the Simulink model of the storage system:

$$\frac{d}{dt}(V_{Storage}\rho_{H_2}(p,T)) = \dot{m_{in}} - \dot{m_{out}} \tag{3.6}$$

With:

- $\rho_{H_2}(p,T) \Rightarrow$ density of stored hydrogen, function of pressure p and temperature T
- $\dot{m_{in}} \Rightarrow$ input mass flow rate of hydrogen
- $\dot{m_{out}} \Rightarrow$ output mass flow rate of hydrogen

Which can be simplified considering that the storage volume $V_{Storage}$ is constant and separating the derivatives (Equation 3.7):

$$V_{Storage}\frac{\partial\rho_{H_2}}{\partial p}\frac{\partial p}{\partial t} = \dot{m_{in}} - \dot{m_{out}} \tag{3.7}$$

This Equation 3.7 has been solved by Simulink evaluating firstly the density independently from its dependency on pressure and temperature. Once calculated (fixed the value of temperature and initial pressure to obtain the first value of density) the density trend over time (as presented in Figure 3.11) it has been possible through 2-D interpolation (based on CoolProp data, Figure 3.12) to obtain the trend over time of the pressure in the storage site. Known the value of pressure it has been possible to evaluate, comparing to minimum and maximum levels, the filling percentage of the salt caverns over time.
As previously stated (Paragraph 3.1), the pressure of hydrogen in the subsurface caverns must remain inside the pressure range stated: the minimum pressure guarantees the structural stability of the cavern and avoids the risk of collapsing; the maximum pressure is defined taking into account safety purposes and structural integrity of the storage site over time.

Based on the input values chosen in the running Matlab script, it has been possible to evaluate the trend of pressure over time and calculate the necessary values of the main parameters of the system to avoid loss of hydrogen when

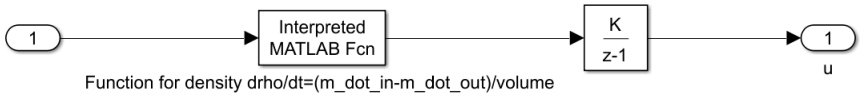

Figure 3.11: *Simulink storage model*

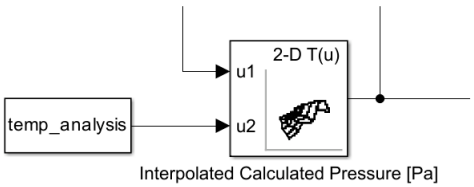

Figure 3.12: *2D interpolation to obtain hydrogen pressure trend in the storage site from the density pressure trend*

there's wind overproduction. In the following paragraph (3.4) these results will be presented and commented.

3.3 Matlab script for dynamic model simulation

The Matlab script has been developed considering three main objectives to reach:

1. Calculate the volume of the necessary subsurface artificial salt caverns necessary to cover the shortages while taking into account the dynamic nature of the analysis;
2. Therefore, the pressure trend of hydrogen in the storage site and the trends of mass flow rates injected and extracted;
3. Fixed a certain value for the maximum pressure losses allowed and the diameter of the injection/extraction pipelines, the calculation of the number of wells necessary to cover the mass flow rates required

The script (Code 3.3) is here reported and commented analysing how the modification of each single parameter can influence the result of the analysis.

```
1 fraction=0.3;
2 gridmesh_pressure;
```

```
3  percentage_filling_tank=                          0.8;
4  temp_analysis=300; % [K]
5  electrolyzer.startup_time=                        10;  % [s]
6  electrolyzer.rampup_time=                         30;  % [s]
7  FC.startup_time=                                  10;  % [s]
8  FC.rampup_time=                                60*15;  % [s]
9  volume_simulation=volumecavern_mineffFC(1,1,1)* 1000;  % [m3]
10 load('compressor_curve_seconds_MPa.mat');
11 out=sim("Test_compr.slx",length(surplus2050));
12
13 % find storage size considering range of pressure (with smooth data
       and
14 % delay of compressor we need larger storage to not lose hydrogen
       when wind overproduction)
15
16
17 idx23=1; volume_simulation_vector(1)=volume_simulation;
18 while height((find(out.pressure_signal.Data>0)))>0
19     idx23=idx23+1;
20     volume_simulation=volume_simulation+1e09;
21     volume_simulation_vector(idx23)=volume_simulation;
22     out=sim("Test_compr.slx",length(surplus2050));
23     clc
24     idx23
25     volume_simulation_vector(idx23)
26 end
```

Code 3.1: *Script for storage volume and pressure trend calculation*

Where Code 3.3 line 2 is a dedicated Matlab script for the calculation through interpolation of the pressure from temperature T (assumed to be fixed and constant) and density ρ_{H_2} (obtained from the storage model). This script (Code 4.6 in Code Appendix 4) has permitted the calculation of the actual storage volume necessary. This volume, which, as it'll be explained, is different from the static model one, has been calculated through a *while* cycle. This cycle had the objective of evaluating the storage volume in order to guarantee that the pressure in the site never overcomes the maximum allowed and, therefore, not losing H_2 produced during wind overproduction periods.
The second section of the script has been developed to calculate two aspects:

- The hydrogen mass flow rates required by FC and electrolyzers (respectively, extracted and injected to the storage system);

- The number of wells and FC/Electrolyzers - Storage site pipes necessary to guarantee those flow rates with fixed maximum values of pressure drops and defined pipes diameters.

```
Calculation of number of wells necessary for the mass flow rate required for FC
percentage_pressure_max_FC=10;                                    % [%]
diameter_FC=18/100;                                               % [m]
[solutionFC.lambda,solutionFC.v,solutionFC.reynolds,solutionFC.massflowratesinglepipe_kg_s,solutionFC.massflowratesinglepipe_kg_h,solutionFC.numberpipes]=numberwells(percentage_pressure_max_FC,out.pressure_sim,out.rho_H2_calc,out.H2_FC_mass_flow_rate_H2,double(cavern_roof_depth_m(1)),diameter_FC,temp_analysis);
% v should be lower than 60 m/s max
idxtest=1; v2=solutionFC.v; numberpipes=solutionFC.numberpipes;
if solutionFC.v>60
    while v2>60
    numberpipes=numberpipes+1
    idxtest=idxtest+1
    massflowrate_singlepipe_kg_s=(max(out.H2_FC_mass_flow_rate_H2.Data)/3600)/numberpipes;
    v2=vpa(massflowrate_singlepipe_kg_s/(solutionFC.wells_density*pi*diameter_FC^2/4))
    end
else
end
solutionFC.v=v2;
solutionFC.numberpipes=numberpipes;
volume_simulation
massflowrate_singlepipe_kg_s=round(vpa(massflowrate_singlepipe_kg_s),3)
solutionFC.massflowratesinglepipe_kg_s=massflowrate_singlepipe_kg_s;
massflowrate_singlepipe_kg_h=vpa(massflowrate_singlepipe_kg_s*3600)
solutionFC.massflowratesinglepipe_kg_h=massflowrate_singlepipe_kg_h;
Re=round(v2*diameter_FC/solutionFC.wells_viscosity_calculation)
solutionFC.reynolds=Re;
lambda=vpa(0.3164./(Re^0.25))
solutionFC.lambda=lambda;
solutionFC

% Calculation of number of pipes for injection (so from Electrolysers)
percentage_pressure_max_El=5;                                     % [%]
```

```
diameter_El=40/100;                                                    % [m]
[solutionEl.lambda,solutionEl.v,solutionEl.reynolds,solutionEl.
    massflowratesinglepipe_kg_s,solutionEl.massflowratesinglepipe_kg_h
    ,solutionEl.numberpipes]=numberwells(percentage_pressure_max_El,
    out.pressure_sim,out.rho_H2_calc,out.
    H2_electrolyzer_mass_flow_rate_H2,double(cavern_roof_depth_m(1)),
    diameter_El,temp_analysis);
% v should be lower than 60 m/s max
idxtest=1; v2=solutionEl.v; numberpipes=solutionEl.numberpipes;
if solutionEl.v>60
    while v2>60
    numberpipes=numberpipes+1
    idxtest=idxtest+1
    massflowrate_singlepipe_kg_s=(max(out.
    H2_electrolyzer_mass_flow_rate_H2.Data)/3600)/numberpipes;
    v2=vpa(massflowrate_singlepipe_kg_s/(solutionEl.wells_density*pi*
    diameter_FC^2/4))
    end
else
end
volume_simulation
solutionEl.v=v2; solutionEl.numberpipes=numberpipes;
massflowrate_singlepipe_kg_s=round(vpa(massflowrate_singlepipe_kg_s)
    ,3)
solutionEl.massflowratesinglepipe_kg_s=massflowrate_singlepipe_kg_s;
massflowrate_singlepipe_kg_h=round(vpa(massflowrate_singlepipe_kg_s
    *3600))
solutionEl.massflowratesinglepipe_kg_h=massflowrate_singlepipe_kg_h;
Re=round(v2*diameter_El/solutionEl.wells_viscosity_calculation)
solutionEl.reynolds=Re;
lambda=vpa(0.3164./(Re^0.25))
solutionEl.lambda=lambda;
solutionEl
```

Code 3.2: *Script for extracted/injected mass flow rates and number of necessary wells calculation*

These calculations have been executed through a dedicated function (Code 4.7) reported in Code Appendix 4.

This function (Code 4.7), which requires as input:

- The storage pressure as percentage in respect to the maximum pressure (to define the level of filling of the storage system);

- Actual pressure in the storage site p_{H_2};
- Hydrogen density in the site ρ_{H_2};
- Mass flow rate $\dot{m_{H_2}}$ (from previous calculations);
- Length l of the pipeline (corresponds to the roof depth);
- Diameter of the well d;
- Temperature assumed for the analysis T_{H_2}

permits the calculation of:

- $\lambda = \lambda\left(Re, \frac{\epsilon}{d}\right)$: with λ friction factor, function of Reynolds number Re and ratio of absolute pipe surface roughness ϵ and the pipe diameter d;
- Re: Reynolds number
- v: hydrogen speed inside the pipe;
- $\dot{m}_{H_2,singlepipe}$: mass flow rate of hydrogen per single pipe (both in $[kg/s]$ and $[kg/h]$);
- n_{pipes}: number of pipes required.

In the function, pressure p_{H_2} and density ρ_{H_2} (lines 2-17) have been calculated with interpolation procedures while the viscosity μ_{H_2} (lines 20-21) has been calculated through the Python package CoolProp with the pressure and temperature fixed values. Instead, the parameters λ, Re and v have been calculated (lines 22-29) solving the following system of equations (Equation 3.8) [29] (supposing Re in turbulent regime for the second equation of the system, hypothesis that will be confirmed by following calculations):

$$\begin{cases} \Delta p_{max} = \lambda \frac{l}{d} \rho_{H_2} v_{H_2}^2 \\ \lambda = 0.3164 \frac{1}{Re^{0.25}} \\ Re = v \frac{d}{\mu_{H_2}} \end{cases} \tag{3.8}$$

From the resolution of this system it has been possible to obtain, as said, λ, Re and especially the velocity v. With the value of the velocity it has been calculated the hydrogen mass flow rate that each tube is able to transmit respecting the

boundaries of pressure drops and fixed value of the pipe diameter. From this value, which has been evaluated for FC and Electrolyzers pipes separately, it has been possible to determine the number of pipes (and, therefore, wells) needed to inject/extract the hydrogen required. These values, though, are first attemp values since considering the NORSOK petroleum standard for methane and oil pipeline transmission ([21]), the limit in methane speed to avoid corrosion phenomena in the pipes should be $60 m/s$. Thus considered, and additional step in the calculation has been added, where with a $while$ cycle the number of wells has been iteratively increased till the limit for the velocity has been respected.

In the next paragraph the results of the simulation and how they're influenced by the elements reported in the Code 3.3.

3.4 Results and influence of parameters on simulation

In this paragraph the results of a reference set of values for the parameters is presented and then how the modification of each of those parameters influences the main results of the simulation.

3.4.1 Results with reference set values for parameters

Setting the following values for the parameters of the simulation (Codes 3.3 and 3.3):

- $fraction_{surplus} = 0.3 \Rightarrow$ fraction of the wind surplus power that is used to power the electrolyzers;
- $percentage_{fillingstorage} = 0.8 \Rightarrow$ initial percentage of storage filling;
- $T_{H_2} = 300K \Rightarrow$ fixed temperature for the analysis;
- $\Delta t_{Start-up,El} = 10s \Rightarrow$ start-up time for electrolyzers;
- $\Delta t_{Ramp-up,El} = 30s \Rightarrow$ ramp-up time for electrolyzers;
- $\Delta t_{Start-up,FC} = 10s \Rightarrow$ start-up time for FC;
- $\Delta t_{Ramp-up,FC} = 15min = 900s \Rightarrow$ ramp-up time for FC;

- $V_{simulation,firstattempt} = 6.49 * 10^8 m^3 \Rightarrow$ first attempt value for simulation storage volume (placed equal to the volume of storage in first case of minimum efficiency in the static model multiplied by 10^3);
- $\Delta p_{\%,Max,FC} = 10\% \Rightarrow$ maximum percentage pressure drop admitted for storage-FC pipelines;
- $d_{pipe,FC} = 18cm = 0.18m \Rightarrow$ diameter extraction well and storage-FC pipeline connection (considered a typical value for natural gas underground storage wells diameter [15])
- $\Delta p_{\%,Max,El} = 5\% \Rightarrow$ maximum percentage pressure drop admitted for electrolyzers-storage pipelines;

the simulation has returned the results presented in Table 3.1:

	FC	Electrolyzers
λ	0.01	0.01
$v_{H_2}\,[m/s]$	59.5	49.3
Re_{H_2}	$1.19 * 10^6$	$9.87 * 10^5$
$\dot{m}_{H_2,SinglePipe}\,[kg/s]$	6.64	4.87
$\dot{m}_{H_2,SinglePipe}\,[kg/h]$	$2.4 * 10^4$	$1.75 * 10^4$
n_{wells}	18	3
$V_{Storage}[m^3]$		$1 * 10^9$

Table 3.1: *Simulation results with reference values of simulation parameters*

The hydrogen flow is turbulent (as it's possible to see from the high values of Reynolds number), with high values, both for FC and electrolyzers, of speed and mass flow rates transported. An aspect that has been possible to notice is the number of wells (and, therefore, pipelines) required in both cases to satisfy the necessary mass flow rates respecting at the same time the restrictions in pressure drops and diameter. As it has been stated in the list at the beginning of Paragraph 3.4, the maximum admitted pressure drops fro the electrolyzers-storage connection has been considered lower than the maximum admitted for the storage-fuel cells pipelines since generally FC work at lower levels of pressure so it has been assumed less important the inlet value of pressure at the FC. Instead, a pressure loss in the electrolyzers-storage connection would cause a reduction of the pressure of the hydrogen injected in the storage site, reducing so the storage capability of the site itself, aspect that has to be taken

into account for its importance. With this set we have obtained a hydrogen storage pressure trend remaining between the minimum and maximum values allowed (taken as reference the values cited in [23], reported in Table 3.3) by the storage site, pressure trend based calculated from the trends of hydrogen potential mass flow rate production from surplus and H_2 mass flow rate required trend (all presented in Figure 3.13). At a higher value of hydrogen mass flow rate extracted to feed the fuel cells corresponds a reduction of the pressure, as it's possible to notice from the Plot 3.13.

	Minimum $p[Pa]$	**Maximum** $p[Pa]$
Pressure Limits (at model's roof depth)	$2.23 * 10^6$	$7.09 * 10^6$

Table 3.2: *Pressure limits used in the model [Pa] [23]*

In the following paragraphs it will be reported how single parameters from the set (of beginning of Paragraph 3.4) influence the results of the simulation.

3.4.2 Influence of fraction of surplus power considered

In the previous paragraph (3.4) it has been considered that 30% of the wind power surplus is used to be converted (with relative efficiencies of the system) into hydrogen through electrolyzers. The modification of this parameter influences the storage site and its pressure trend. It also affects, since modifies the mass flow rates of hydrogen produced,the number of wells necessary to satisfy the injection requirements. In the analysis it has been modified from 10% of the wind power surplus production to 100%. The changes generated by the different values of the surplus considered are here reported.

	10%	**20%**	**30%**	**40%**	**50%**	**60%**	**70%**	**80%**	**90%**	**100%**
$v_{H_2}\,[m/s]$	59.7	59.6	59.5	59.4	59.3	59.1	59	58.9	58.8	58.7
Re_{H_2}	1.20*10^6	1.19*10^6	1.19*10^6	1.19*10^6	1.19*10^6	1.18*10^6	1.18*10^6	1.18*10^6	1.18*10^6	1.17*10^6
$\dot{m}_{H_2,SinglePipe,Peak}\,[kg/h]$	2.39*10^4									
n_{wells}	18									

Table 3.3: *Simulation results for FC with reference values of simulation parameters except the percentage of surplus converted considered*

In Table 3.3 it is possible to visualize the effect of the power surplus converted on the FC system: with a higher value of the fraction of surplus wind power converted the values of λ, v_{H_2}, Re_{H_2}, $\dot{m}_{H_2,SinglePipe}$ and n_{wells} are essentially

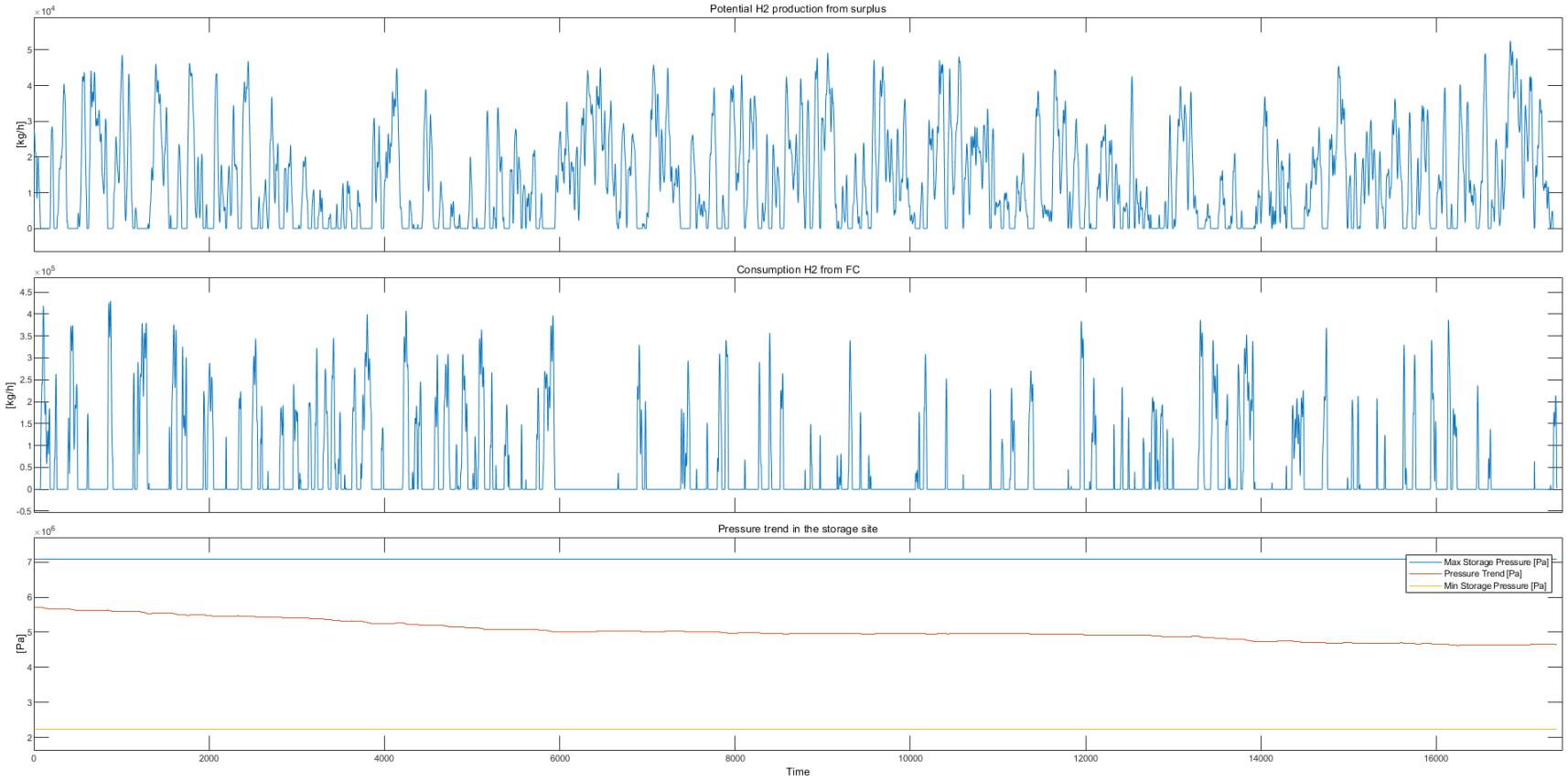

Figure 3.13: *From top to bottom: Potential mass flow rate production from surplus (before compression stage); H_2 mass flow rate required due to wind shortage and hydrogen pressure trend over time in the storage site (with minimum and maximum values allowed [Pa] [23])*

	10%	**20%**	**30%**	**40%**	**50%**	**60%**	**70%**	**80%**	**90%**	**100%**
$v_{H_2}\,[m/s]$	25.7	33.5	49.3	48.3	47.4	55.8	53.2	59.7	56.5	54
Re_{H_2}	5.15e+5	6.72e+5	9.88e+5	9.68e+5	9.49e+5	1.12e+6	1.07e+6	1.20e+6	1.13e+6	1.08e+6
$\dot{m}_{H_2,SinglePipe,Peak}\,[kg/h]$	8.76*10^3	11.7*10^4	17.5*10^4	17.5*10^4	17.5*10^4	21*10^4	20.4*10^4	23.4*10^4	22.5*10^4	21.9*10^4
n_{wells}	2	3	3	4	5	5	6	6	7	8

Table 3.4: *Simulation results for electrolyzers with reference values of simulation parameters except the percentage of surplus converted considered*

unchanged, with only a slight reduction on the velocity and Reynolds number. This effect is highlighted by the plot of Figure 3.14, referring to the mass flow rate required by FC in the system. The storage volume, important to avoid losses of produced hydrogen with surplus, has not changed through the iterations and results to be equal to the fixed reference volume (reported in Paragraph 3.4.1). The main noticeable changes have occurred instead in the electrolyzers system, as reported in Table 3.4: the mass flow rate peak for each well increased and overall there is an increase of the number of wells and the mass flow rate of hydrogen produced. This trend is visible also in the plot of Figure 3.15.

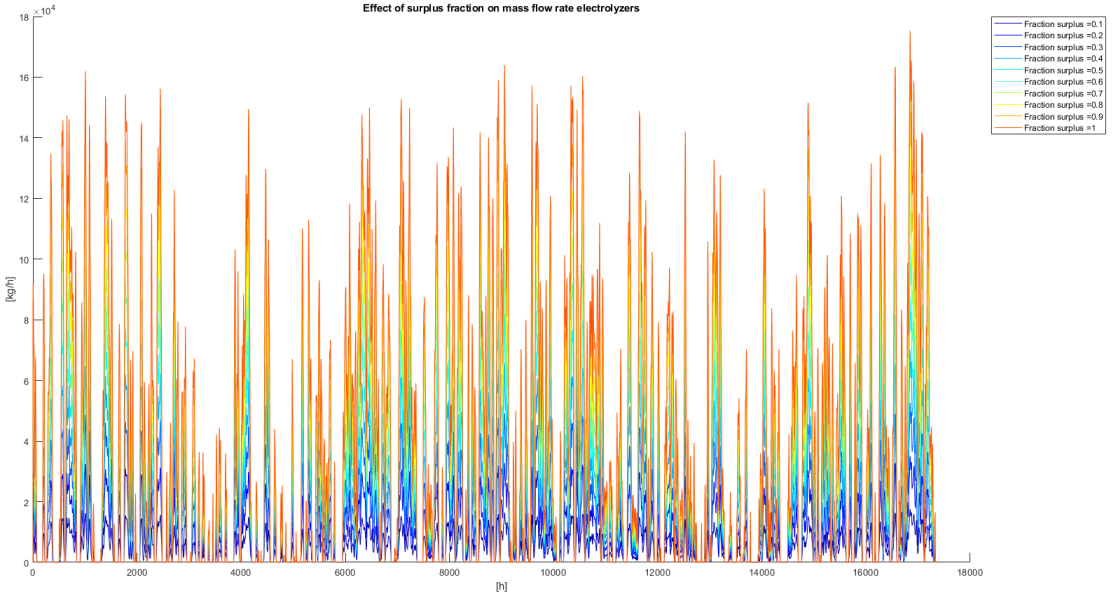

Figure 3.14: *Mass flow rate produced by electrolyzers system at different values of power surplus converted* $[kg/h]$

Concerning the pressure trend inside the storage system, since the FC mass flow rate is minimally influenced by the surplus fraction considered, with a higher hydrogen mass flow rate produced by the electrolyzers system the overall pressure of the system increases and maintains over time higher levels with small

variations (as presented in the plot of Figure 3.15). Higher values of the fraction of surplus used permit to maintain a more constant level of pressure in the storage site but this comes with additional investment costs for the infrastructure (since it results necessary to have more electrolyzers and drill a higher number of wells for the injection).

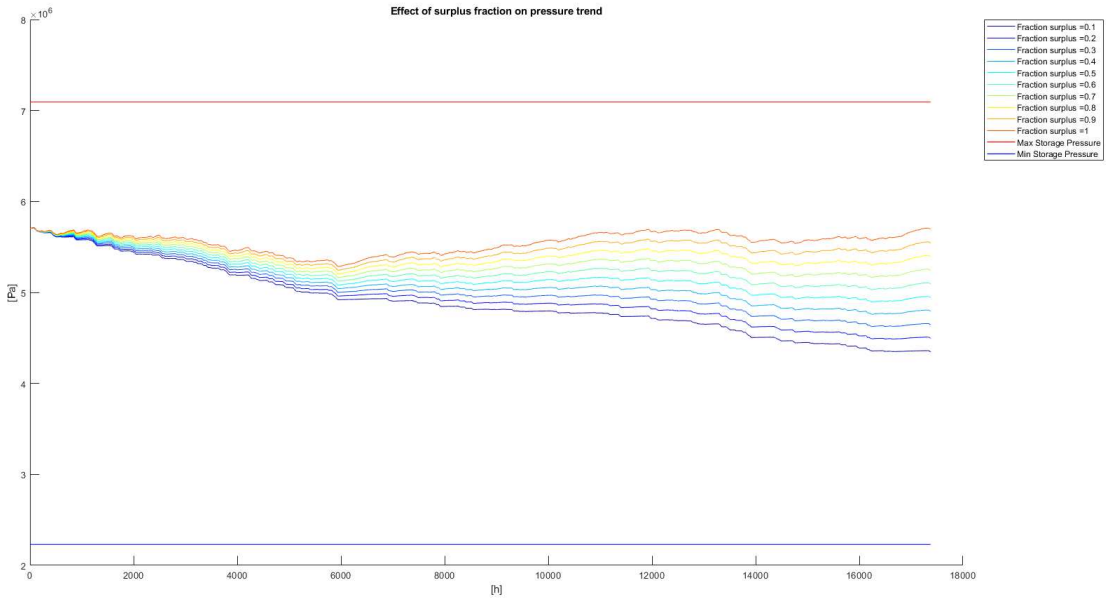

Figure 3.15: *Hydrogen pressure trend over time at different wind power surplus fractions converted* $[Pa]$

3.4.3 Influence of initial tank filling percentage

All the analysis in the reference value set simulation case has been carried out considering an initial value of the $percentage_{fillingstorage}$ = 80%. It is important though to evaluate the influence of this parameter in the results of the simulation. Considering percentage values between 10% and 100% the following results (Table 3.5 for FC, Table 3.6 for electrolyzers) have been obtained.

Analyzing the results for FC system (Table 3.5) with values obtained with reference data set (Table 3.1), it's possible to notice:

- v_{H_2} has slightly decreased;
- $\dot{m}_{H_2,SinglePipe}$ has increased as the filling percentage increased;

	10%	**20%**	**30%**	**40%**	**50%**	**60%**	**70%**	**80%**	**90%**	**100%**
$v_{H_2}\,[m/s]$	60	59.6	59.1	58.4	59.4	58.4	57.8	59.5	59.9	57.9
Re_{H_2}	1.21*10^6	1.2*10^6	1.19*10^6	1.17*10^6	1.19*10^6	1.17*10^6	1.16*10^6	1.19*10^6	1.19*10^6	1.15*10^6
$\dot{m}_{H_2,SinglePipe,Peak}\,[kg/h]$	3.8*10^3	6.71*10^3	9.56*10^3	1.23*10^4	1.54*10^4	1.79*10^4	2.05*10^4	2.39*10^4	2.69*10^4	2.87*10^4
n_{wells}	113	64	45	35	28	24	21	18	16	15

Table 3.5: *Simulation results for FC system with reference values of simulation parameters except the initial storage filling percentage*

	10%	**20%**	**30%**	**40%**	**50%**	**60%**	**70%**	**80%**	**90%**	**100%**
$v_{H_2}\,[m/s]$	59.1	56.3	56.8	53.3	49.5	50.4	42.6	49.3	43.5	39
Re_{H_2}	1.19*10^6	1.13*10^6	1.14*10^6	1.07*10^6	9.94*10^5	1.01*10^6	8.55*10^5	9.88*10^5	8.72*10^5	7.80*10^5
$\dot{m}_{H_2,SinglePipe,Peak}\,[kg/h]$	1*10^3	3.78*10^3	6.57*10^3	8.76*10^3	1.05*10^4	1.31*10^4	1.31*10^4	1.75*10^4	1.75*10^4	1.75*10^4
n_{wells}	51	14	8	6	5	4	4	3	3	3

Table 3.6: *Simulation results for electrolyzers system with reference values of simulation parameters except the initial storage filling percentage*

- n_{wells} has decreased as filling percentage increased: this effect, combined with the increase of $\dot{m}_{H_2,SinglePipe}$, has determined an overall mass flow rate which has remained stable (both trends are related to the respect of the 60 m/s H_2 speed limit in the pipelines; see Figure 3.16);
- $V_{Storage}$ is still the one considered in the reference case.

Similar considerations can be done for the results obtained in the electrolyzers system, reported in Table 3.6: also in for this subsystem the mass flow rate per single pipe has increased (as the filling percentage increased) while the number of wells decreased, resulting in an overall mass flow rate produced stable (see Figure 3.18). Concerning the trends over time, the trend of hydrogen pressure in the storage site has shift down since the starting pressure is lower than the reference case (see Figure 3.17). It is possible to highlight how it is fundamental the starting process of the system since placing the system electrolyzers-FC into operation with a low initial filling percentage value could cause an insufficient storage level to sustain the system (in Figure 3.17 with low levels of percentage filling the pressure values go below the lower allowed limit).

3.4.4 Influence of start-up time of Fuel Cells and Electrolyzers

In this paragraph it has been evaluated the effect of the start-up time of the Fuel cells and Electrolyzers comparing the results with the reference data set simulation results. It is defined as start-up time the time interval that is present between the instant of the beginning of production (hydrogen for electrolyzers,

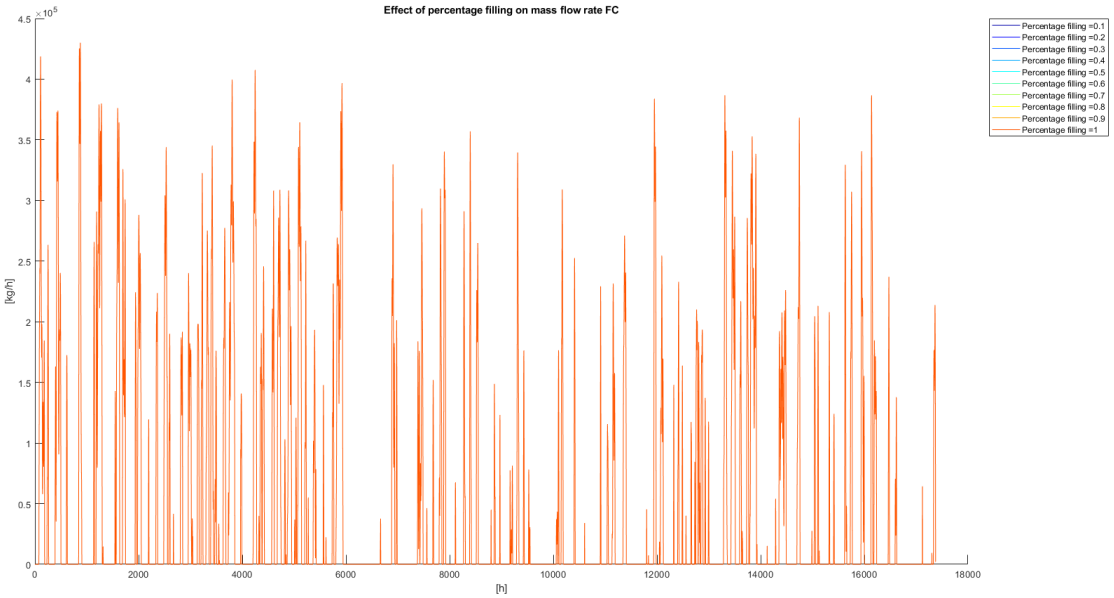

Figure 3.16: *Hydrogen mass flow rate FC system usage with reference data set except the initial storage filling percentage* $[kg/h]$*)*

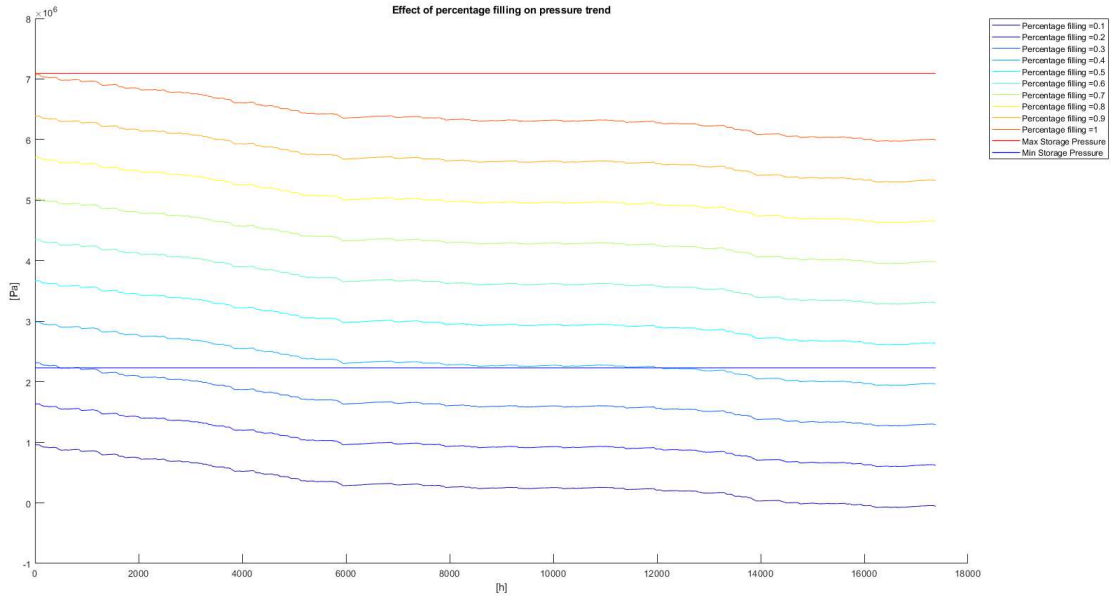

Figure 3.17: *Pressure of hydrogen in the storage site with reference data set except the initial storage filling percentage* $[Pa]$

electrical power for FC) and the instant of beginning of input in the system (electrical power for electrolyzers, hydrogen in the FC). In the analysis script I

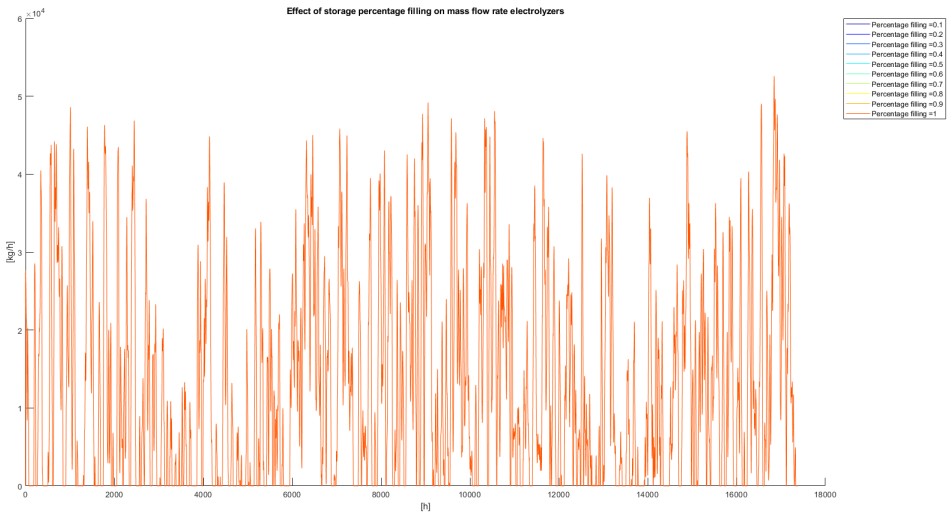

Figure 3.18: *Hydrogen mass flow rate electrolyzers system production with reference data set except the initial storage filling percentage* $[kg/h]$*)*

have considered different equally spaced start-up time intervals, both for the FC and for the electrolyzers, to evaluate the impact of this parameter. Even though the two subsystems (FC and electrolyzers) are separate and independent, considering that the first follow the user demand while the second follows the power surplus, it is possible to notice that the modification of the parameters of one subsystem influences the behaviour also of the other. It is important to notice that in both the simulations the value of the storage volume results to be equal to the value considered in the reference case (Paragraph 3.4.1). Here are separately presented the results for the modification of $\Delta t_{Start-up,Electrolyzers}$ and $\Delta t_{Start-up.FC}$.

Modification of $\Delta t_{Start-up,Electrolyzers}$

The increase of the start-up time of the electrolyzers has an impact for the mass flow rate of both FC and electrolyzers systems, concerning the value of the flow rate but also the time profile. Indeed, an increase of this parameter shifts forward the profile, enhancing the problem of the not perfect follow of the surplus curve profile. The mean values of production and consumption are not particularly influenced, with average values of:

- $\dot{m_{H_2,El}} = 1.007 * 10^4\, kg/h$, $n_{pipes} = 3$, $v_{H_2} = 49.3\, m/s$
- $\dot{m_{H_2,FC}} = 3.51 * 10^4\, kg/h$, $n_{pipes} = 18$, $v_{H_2} = 59.5\, m/s$

Considering the density of the data (the analysis spreads over a period of two years with a definition of 1 hour), in order to make the effect of the start-up time of electrolyzers in the mass flow rate plots (Figure 3.19 for electrolyzers, Figure 3.20 for FC) clearer it has been also added the plot of the difference of the mass flow rate profiles (Figure 3.21 for electrolyzers, Figure 3.22 for FC) compared to the first mass flow rate profile (with $\Delta t_{Start-up,Electrolyzers} = 10\,s$). The variation of the start-up time does not allow the electrolyzers to follow fast the overproduction trend, with a reduction of the capability of extracting energy from that surplus.
From the calculations it results that also the shape of the profile trend in the storage site is not much effected by the variation of the $\Delta t_{Start-up,Electrolyzers}$ (see Figure 3.23).

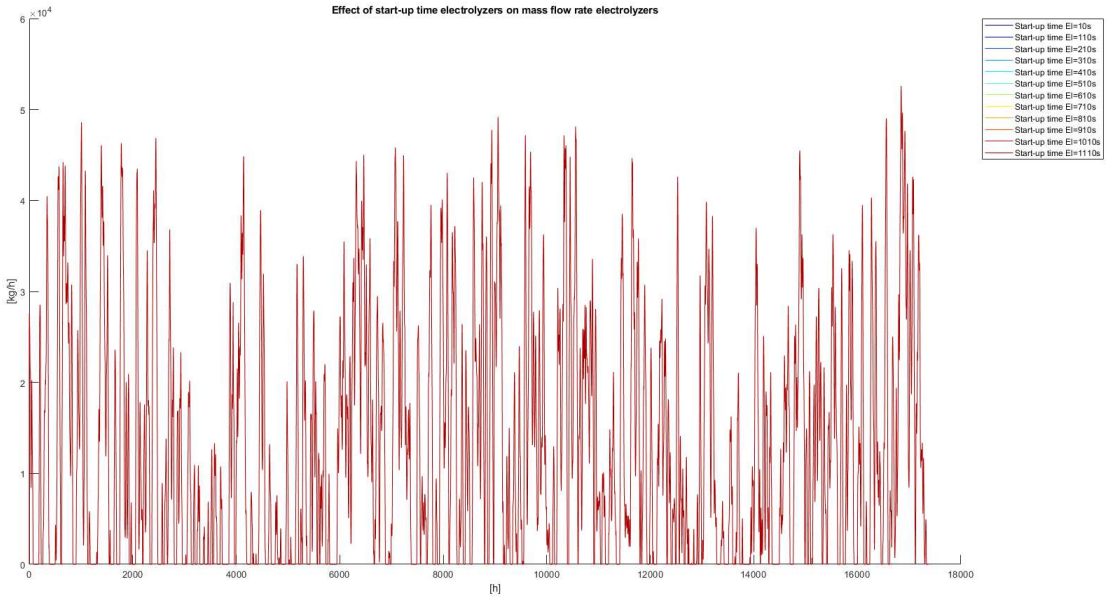

Figure 3.19: *Effect of $\Delta t_{Start-up,Electrolyzers}$ on hydrogen mass flow rate production from surplus (before compression stage)* $[kg/h]$

Modification of $\Delta t_{Start-up,FC}$

Similarly to the results of Paragraph 3.4.4, the average values of the hydrogen mass flow rate produced by electrolyzers and used by the FC (which are comparable to the ones reported in the previous paragraph 3.4.4) are not significantly

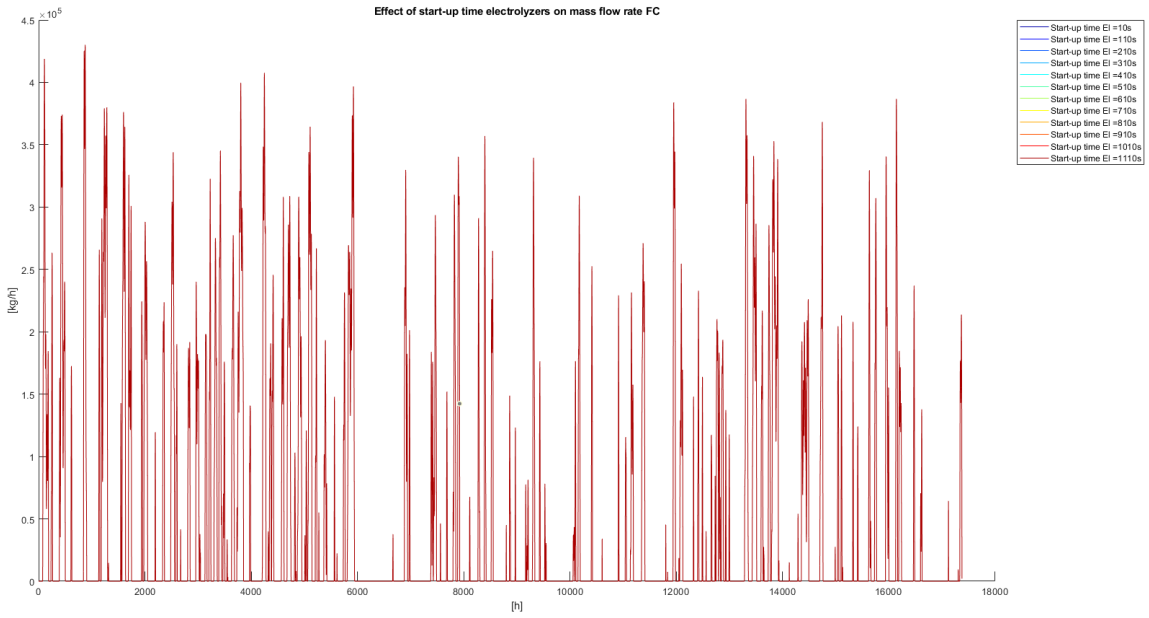

Figure 3.20: *Effect of $\Delta t_{Start-up,Electrolyzers}$ on hydrogen consumption FC system (all other values are set the reference ones)*

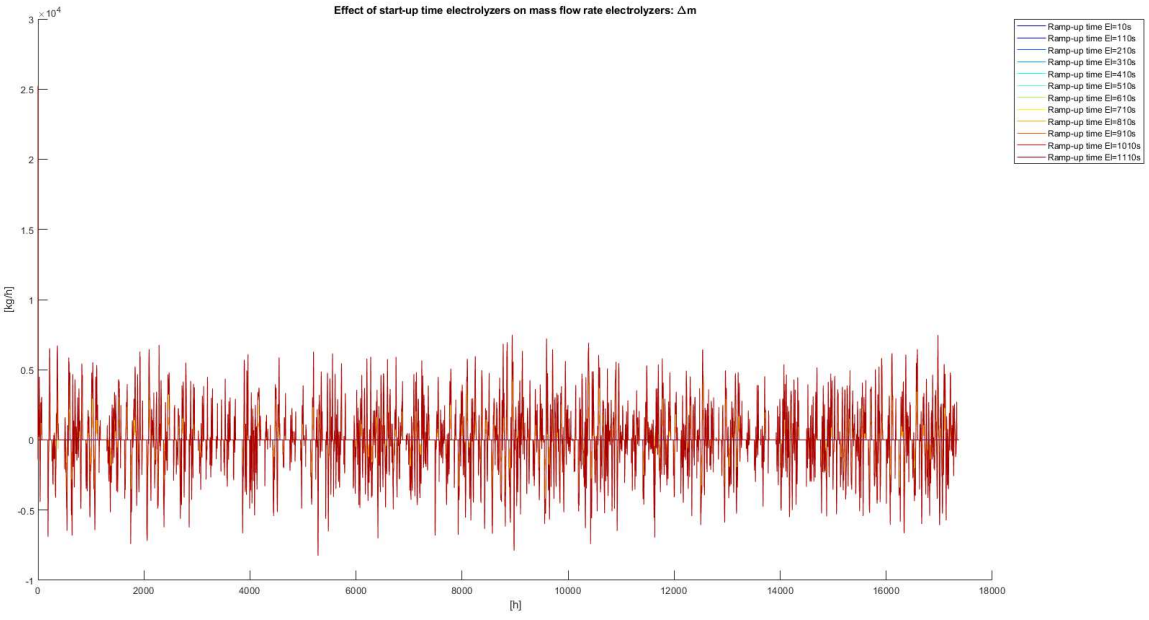

Figure 3.21: *$\Delta \dot{m}_{H_2,Electrolyzers}$ compared to the case with $\Delta t_{Start-up,Electrolyzers} = 10\,s$ $[kg/h]$*

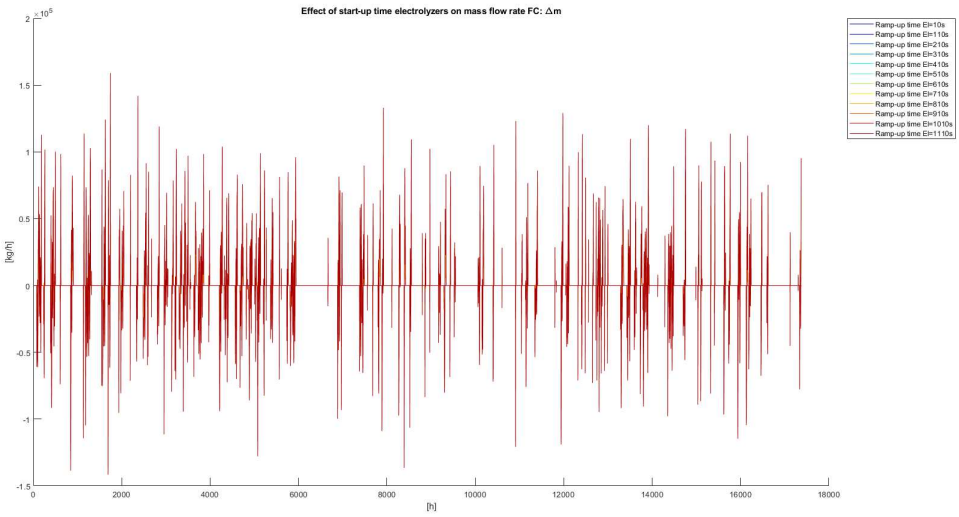

Figure 3.22: *$\Delta m_{H_2,FC}^{\cdot}$ compared to the case with $\Delta t_{Start-up,Electrolyzers} = 10\,s$ $[kg/h]$*

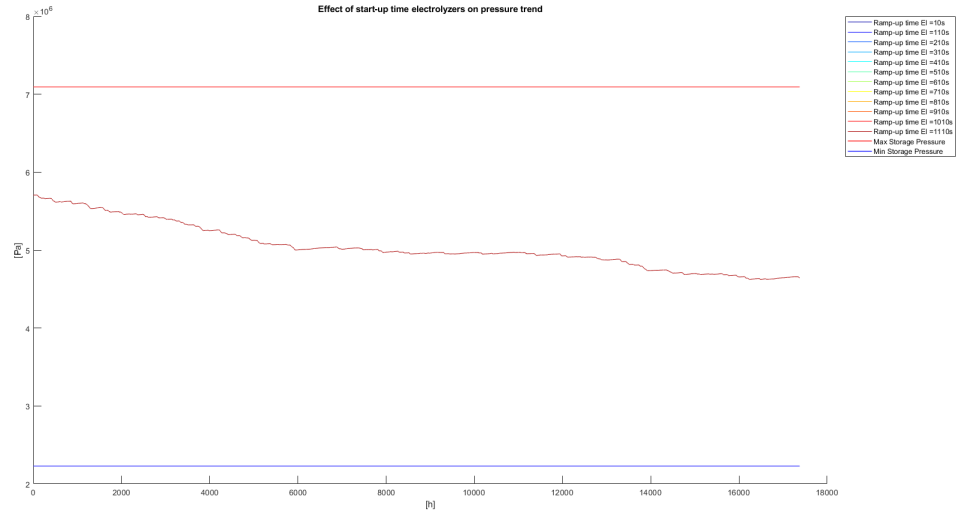

Figure 3.23: *Pressure trend in the storage site at different values of $\Delta t_{Start-up,Electrolyzers}$*

influenced by the variation of the $\Delta t_{Start-up,FC}$, as it is possible to see from the plots of Figures 3.24 and 3.25 (respectively for electrolyzers and FC). It is possible to notice though, as presented in plots of Figures 3.26 and 3.27 (respectively electrolyzers and FC), that the production and consumption mass flow rates are influenced by different $\Delta t_{Start-up,FC}$ values, determining a shift that does not allow a full match between the surplus production and user demand profiles. Also in this analysis, the profile of the pressure is not importantly modified by

the variation of $\Delta t_{Start-up,FC}$ (the profile is similar to the start-up electrolyzer case, Figure 3.23).

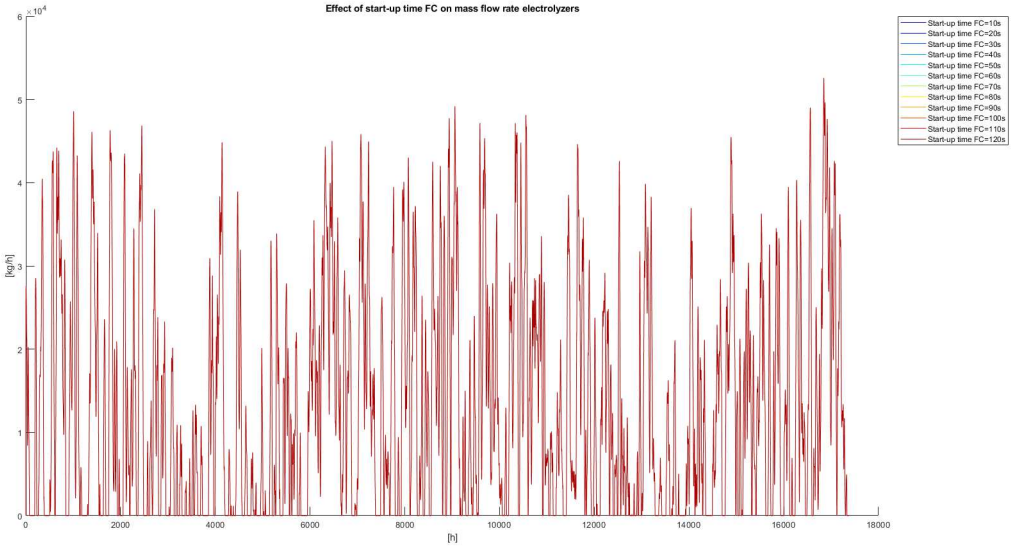

Figure 3.24: *Hydrogen mass flow rate electrolyzers' system production from surplus at different $\Delta t_{Start-up,FC}$ values (all other parameters are considered equal to reference set)*

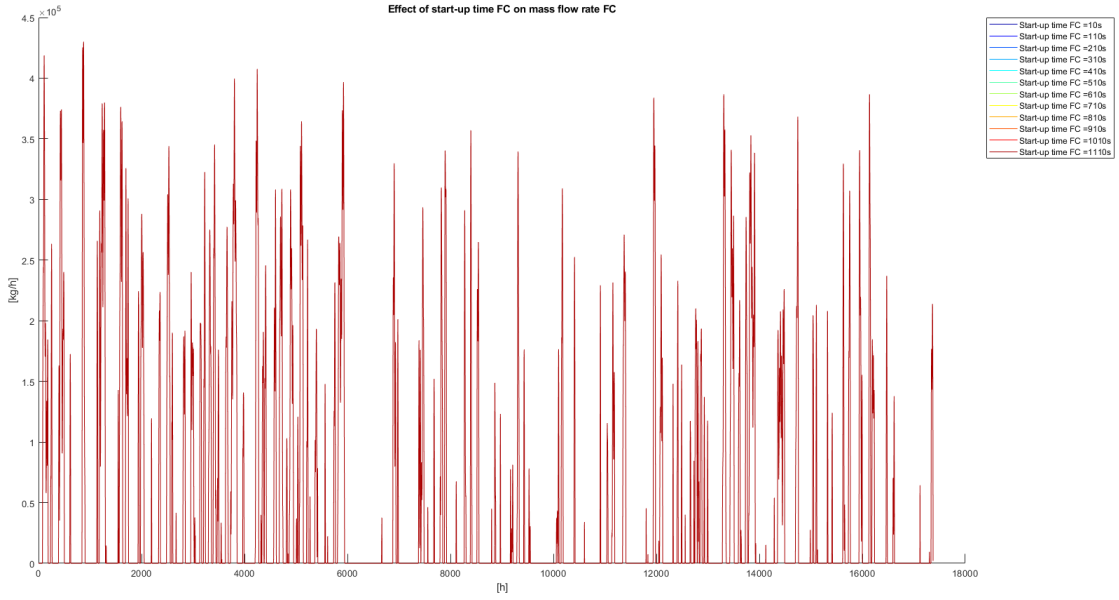

Figure 3.25: *H_2 mass flow rate required by FC system at different $\Delta t_{Start-up,FC}$ values (all other parameters are considered equal to reference set)*

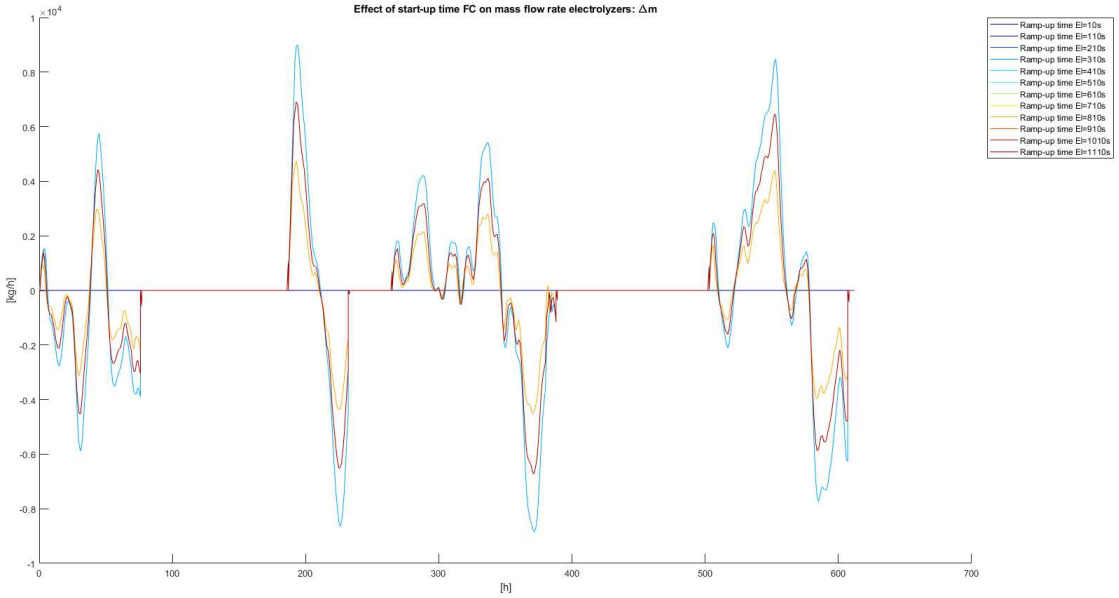

Figure 3.26: $\Delta m_{H_2,Electrolyzers}$ *compared to the case with* $\Delta t_{Start-up,FC} = 10\,s\ [kg/h]$

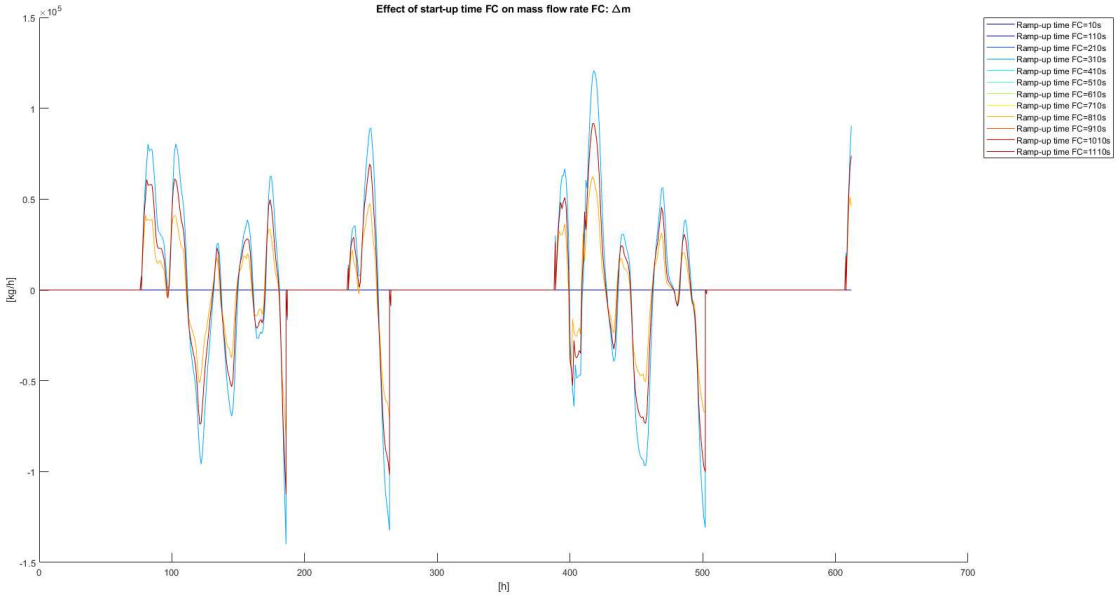

Figure 3.27: $\Delta m_{H_2,FC}$ *compared to the case with* $\Delta t_{Start-up,FC} = 10\,s\ [kg/h]$

3.4.5 Influence of ramp-up time of electrolyzers and fuel cells

In this subparagraph it is reported the influence of the parameter "ramp-up time", which is defined as the time difference between the instant when the system (electrolyzer or FC) reaches its nominal output (hydrogen mass flow rate production for electrolyzers, electrical power for the FC) and the instant when the system starts to produce (immediately after the start-up time interval). Also in this case, the average values (both for the electrolyzers ramp-up and fuel cells ramp-up cases) of hydrogen mass flow rates are not importantly influenced, and therefore the number of wells and the hydrogen velocity (always calculated taking into account the $60\,m/s$ limit). Here, for each ramp-up time considered, the main plots are reported.

Modification of $\Delta t_{Ramp-up,FC}$

From the plot of Figure 3.28 it is noticeable that the $\Delta t_{Ramp-up,FC}$ influences the hydrogen mass flow rate produced by electrolyzers:

- The production is shifted over time, causing a change of the shape since a change in the shape of the FC hydrogen mass flow rate consumption (plotted in Figure 3.29) also changes the time production of the electrolyzers
- This change of production is reflected on a reduction (visible in Figure 3.28) of the mass flow rate produced by electrolyzers.

Concerning then the effect of $\Delta t_{Ramp-up,FC}$ on the FC mass flow rate consumption, it is possible to highlight from plot of Figure 3.29:

- A variation of this parameter causes the shift of the profile of hydrogen consumption of the FC: this determines the inability of following in real time the user demand; an increase of $\Delta t_{Ramp-up,FC}$ does not necessarely cause a reduction of the production since it depends also on the interaction between the demand curve and the ability of the FC system to follow it
- Overall, though, the trend is a decreasing consumption as the $\Delta t_{Ramp-up,FC}$ increases.

It has been noticed also that even with this parameter the pressure trend is not modified, maintaining a trend similar to the one reported in Figure 3.23.

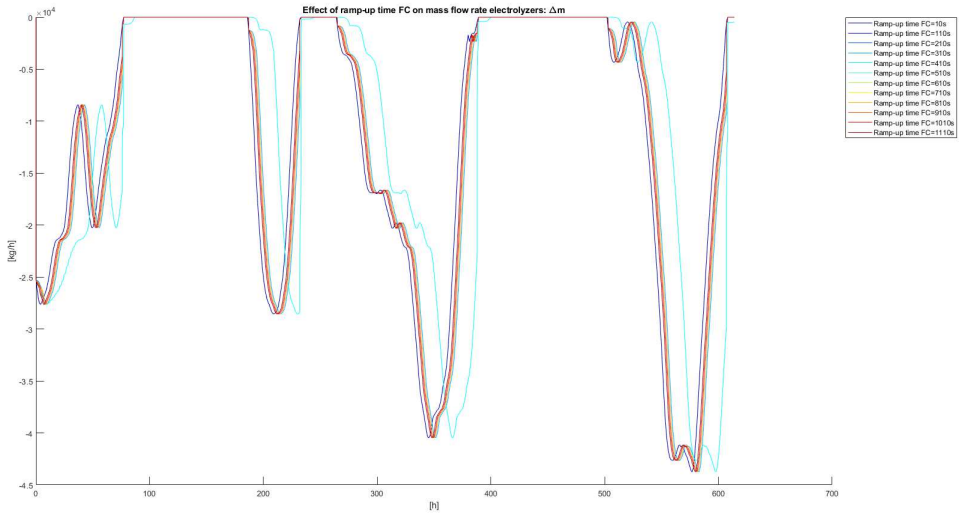

Figure 3.28: *$\Delta m_{H_2,\dot{Electrolyzers}}$ compared to the case with $\Delta t_{Ramp-up,FC} = 10\,s$ $[kg/h]$*

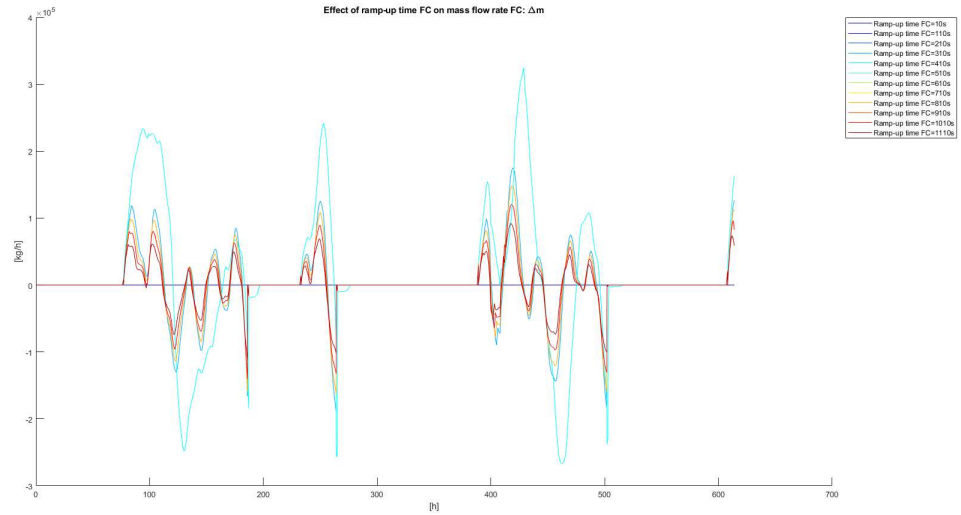

Figure 3.29: *$\Delta m_{\dot{H_2},FC}$ compared to the case with $\Delta t_{Ramp-up,FC} = 10\,s$ $[kg/h]$*

3.4.6 Influence of storage volume

Last parameter that has to be evaluated is the storage volume considered and its influence on the hydrogen mass flow rate (produced and consumed) and the pressure trend in the storage site. Concerning both the hydrogen mass flow rate produced (by electrolyzers) and consumed (by FC), it is visible respectively in Figures 3.30 and 3.31 how these are not modified by the value of the storage volume. The simulations has been carried out starting with a value of storage volume equal to 1000 $V_{Reference}$ and then increased with steps till reaching 2000 $V_{Reference}$. The major impact of this parameter is the pressure trend in the storage site: considering essentially similar values of the hydrogen mass flow rate injected and extracted, an increase of the storage volume determines a less pronounced pressure decrease trend, as it is visible in Figure 3.32, maintaining then a more stable pressure in the site.

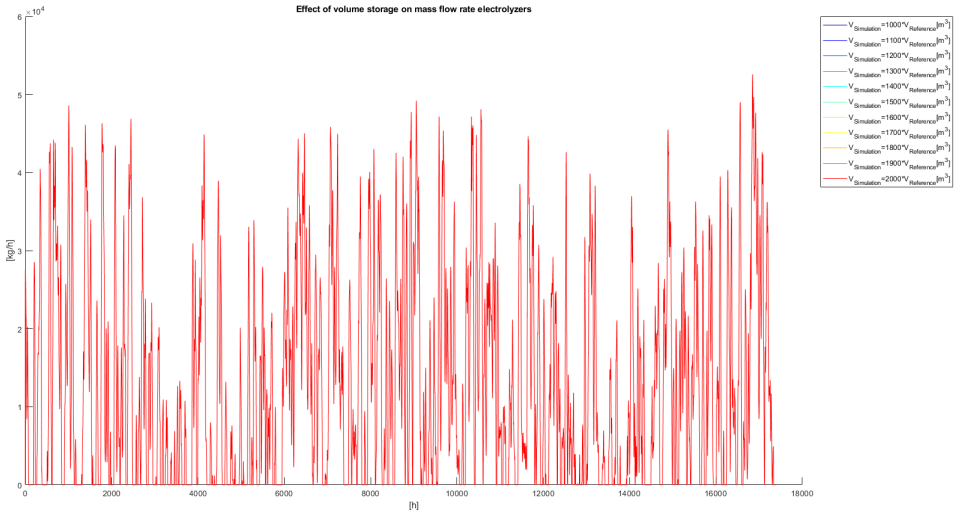

Figure 3.30: *Hydrogen mass flow rate required due to wind storage with different $V_{storage}$ values (rest of parameters has reference values)* $[kg/h]$

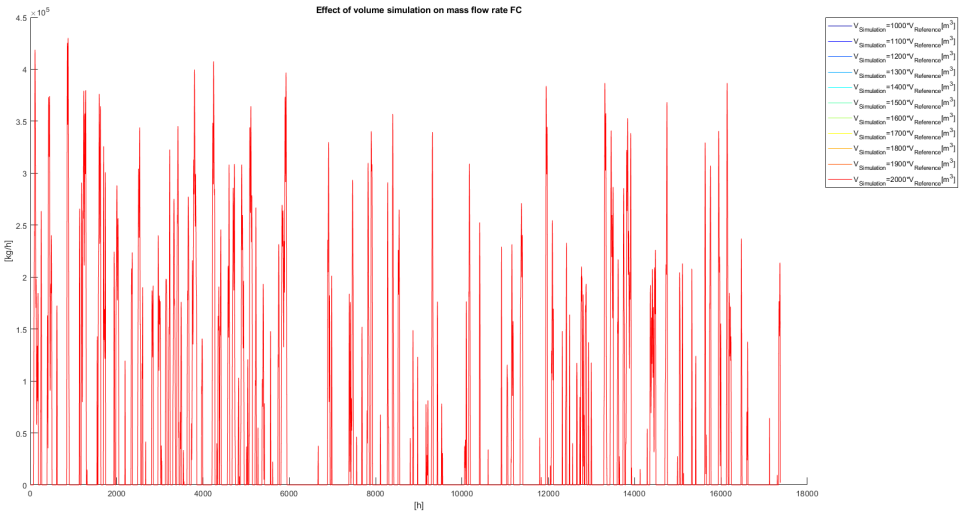

Figure 3.31: *Hydrogen mass flow rate consumed by FC system with different $V_{storage}$ values (rest of parameters has reference values)* $[kg/h]$

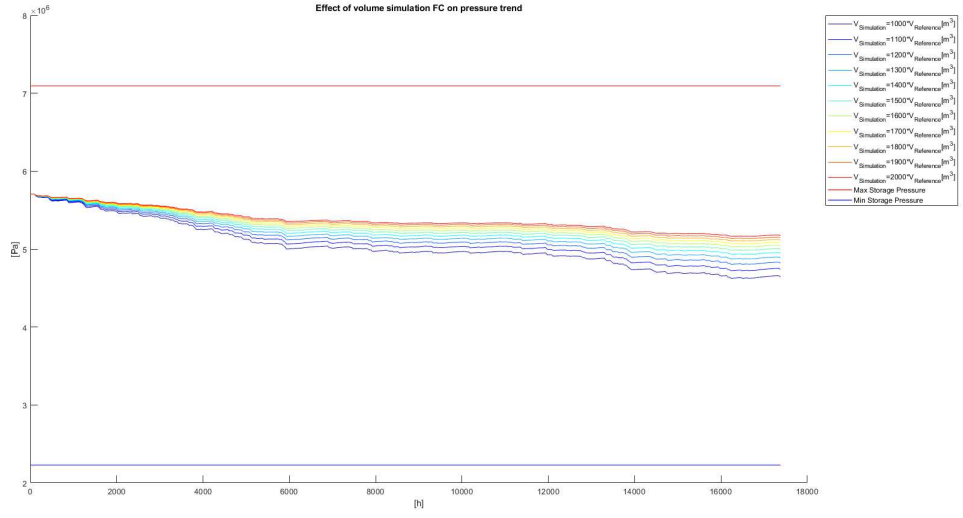

Figure 3.32: *Hydrogen pressure trend in the storage site with different $V_{storage}$ values (rest of parameters has reference values)* $[Pa]$

4

Conclusions

The main objective of this thesis project was the evaluation of the integration of hydrogen as an energy storage system in a 100% renewable energy scenario through the usage of the underground artificial salt cavern technology.

In order to do so, the study started with the Introduction Chapter (Chapter 1), in which all the most important energy storage technologies currently available have been presented, with an overall picture of their technology readiness, their advantages and disadvantages: **Electrochemical technologies**: covering the majority of the new energy solutions, they present fast response and high power delivered but generally low energy densities, considerable costs and high volume occupied; **CAES and hydro technologies**: the most used for long term storage, they allow the storage of important energy quantities but with lower flexibility compared to electrochemical solutions and the necessity of civil works (with the related environmental and economical impacts); **Thermal energy storage technologies**: mostly under development or present important drawbacks (such as the corrosive salts for the MSTES technology); **Electrical technologies**: fast response and high power density technologies but their low energy density make them not suitable for storage purposes.

In this panorama, the usage of hydrogen as a storage medium can have important implications: it is producible from a widely available resource (water) with a ***simple production principle***; can be stored in ***different solutions*** (tanks, aquifers, salt caverns for example) and could be used also for ***other purposes***

rather than electrical energy storage (such as heating or transportation).

Following these considerations, a simplified model of an energy system with the integration of underground salt caverns, based on the Danish current scenario projected to 2050 under specified assumptions, has been developed in the Chapter Simplified Model (Chapter 2). In this simplified model, where it has been considered the usage exclusively of wind power and hydrogen as energy storage in an isolated system, the characteristics of the system have been evaluated considering the energy aspect, not the power (evaluated instead in the Dynamic Model Chapter). The calculations have been started from the evaluation of the energy shortage (Paragraph 2.0.2) for each of the 3 cities of the simplified map. The results obtained allowed the calculations of the energy that needs to be extracted from the power surplus (defined as the positive difference for each time unit between the wind power production and the user power consumption) and the one that has to be stored through hydrogen considering all the different fuel cell and electrolyzers technologies with their respective minimum and maximum efficiencies (Paragraph 2.0.3). From these values of energies it has been possible to calculate, through a dedicated Matlab script that has taken into account the hydrogen density gradient caused by geothermal gradient, the dimensions of the necessary underground artificial salt caverns (Paragraph 2.0.4) and the fresh water volumes necessary to build them (Paragraph 2.0.4). In the system analysis it has also been considered two possible scenarios, considering the case with offshore storage and purely electrical energy transmission (Paragraph 2.0.4) and the case with energy transmission through hydrogen pipelines (Paragraph 2.0.5); these considerations have been carried out taking into account all the aspect that these two different cases determine.

From the results of the simplified model it has been possible to understand that the complexity and the extent of the system, even if simplified to a reduced map with 3 cities, makes essential the choice of the couple fuel cell - electrolyzers technologies considered. This choice directly affects, considering the range of efficiencies of the system, the amount of energy that has to be extracted (by electrolyzers) from the power surplus and the amount of energy that has to be actually stored in the site. This latter aspect is essential since influences the dimensioning process of the underground artificial storage site in height and diameter, modifying the amount of freshwater (and, therefore, the environmental

and economical impact) required for the construction process. Moreover, as it has been possible to highlight with the two scenarios (Scenario 2.0.4 and 2.0.5), design choices in terms of storage placement and energy transmission can affect the storage dimensioning and the system behaviour. System that can range from an offshore solution with main storage solution build under the seabed and electrical energy converted and transmitted from the hydrogen island to hydrogen production carried out in this dedicated artificial island, transmitted to land via pipelines and stored locally underground ready to be employed by the fuel cells system.

In the simplified model it has not been considered the inertia of the components of the system such as fuel cells, electrolyzers and compressors. This effect, through simulations carried out on a 2 years time frame (with 1 hour resolution), has been considered in the analysis of the Dynamic Model Chapter (Chapter 3). All these components have been implemented in a Simulink model, each one considering their fundamental working parameters and control systems. For the electrolyzers (Paragraph 3.2.3) it has been defined, taken into account and implemented the start-up and ramp-up time intervals in the model and its blocks. Similarly it has been done for the fuel cells (Paragraph 3.2.4), applying the same parameters and blocks in the model. Concerning the compressor, based on its pressure-time dependency curve (Figure 3.9), a simplified control system has been implemented. Lastly, for the overall system, different control systems (as explained in Paragraph 3.2.2) has been added. This Simulink model has been then exploited, as other functions that have been developed, inside a Matlab script with the aim of evaluating the storage volume, the number of electrolyzers and fuel cells wells and the mass flow rates through them respecting the pressure losses constraints (Paragraph 3.4.1) and constraints that has been placed in the assumptions of the model (Paragraph 3.1). This script (Paragraph 3.3) has been iteratively modified changing the value of the main parameters of the system elements to visualize their impact on the overall system.

From the results of the dynamic model it has been possible to visualize how certain parameters has an important influence on the system. Choosing a fuel cell or electrolyzer technology that has a high value of the start-up time has as consequence the inability of follow respectively the demand (in terms of shortage) and the production surplus curves. This issue may be solved developing or

choosing components with lower start-up time or with mathematical predictive approach, through which the components are activated earlier in time considering the predictions of production and demand made by the model. Components with high ramp-up times, instead, do not allow to fully exploit the potential of the power surplus (electrolyzers) or be able to supply the power needed by user in time: this problem may be solved with different approaches such as developing faster technologies, installing a higher number of these components to counterbalance the effect (but with additional investment costs and overdimensioning the system) or adding fast technologies (such as electrochemical storage) in parallel to mitigate this issue. The last two fundamental aspects considered were the fraction of surplus considered to be converted into hydrogen and the initial storage filling percentage. The first aspect is important since considering higher fractions allows to increase the production of hydrogen thus being a possible mitigating solution for electrolyzers with high start-up and ramp-up time intervals. Higher fraction though results in higher number of components, higher mass flow rates and therefore an increase of the size of the system with consequent increase of complexity and costs. Lastly, the initial storage filling percentage is significant in the starting of the system since low initial level do not allow to have a sufficient buffer to follow the user demand; for this reason it is necessary to consider the initial filling as part of the installation procedure.

From the considerations aforementioned in my analysis, that is available for further developments and improvements, it is possible to conclude that the hydrogen technology can be exploited for energy storage in large scale but presents some important issues that have to be solved. Firstly, the volume necessary to support even a simple 3-cities system is extremely high, making really difficult the process of construction of the caverns and to find sufficient available areas to be exploited (for what concerns the salt caverns technology). In addiction to this, the volume of freshwater necessary for the construction of these artificial subsurface salt caverns is relevant, considering that the resulting brine cannot be directly disposed in the sea but has to be treated because of the presence of polluting substances (such as heavy metals) that has been dissolved in it. Second, it is necessary, based on the technology considered, to make a considerable number of wells for injection and extraction, with important investments necessary. Third, it is a new system that has to be correctly designed, dimensioned and build, since the physical and chemical characteristics of hydrogen do not allow

its usage directly on existing natural gas grid network. Lastly, the actual technologies, especially fuel cells, considering the high values of critical parameters such as start-up and ramp-up times, make necessary the usage of additional systems (as, aforementioned, parallel electrochemical battery systems) or predictive models to deal with the not perfect following of the surplus and shortage curve by the components of the system. For these argumentations, it is reasonable to conclude that it is necessary to base a possible future energy system not only on one production (such as wind for Denmark) and storage (hydrogen) technology but it is needed to diversify the mix of technologies used.

References

[1] *ABB solar inverters - Explore the industrys broadest portfolio*. URL: https://web.archive.org/web/20221120144504/https://search-ext.abb.com/library/Download.aspx?DocumentID=BCB.00076&LanguageCode=en&DocumentPartId=&Action=Launch (visited on 11/20/2022).

[2] M. Andriollo et al. *I Trasformatori: Teoria ed Esercizi per i Corsi di Laurea di Ingegneria*. Settembre 2019. Italy: Esculapio, 2019. 178 pp. ISBN: 978-88-9385-154-1.

[3] Mike Barnes and Antony Beddard. "Voltage Source Converter HVDC Links The State of the Art and Issues Going Forward". In: *Energy Procedia*. Selected papers from Deep Sea Offshore Wind R&D Conference, Trondheim, Norway, 19-20 January 2012 24 (Jan. 1, 2012), pp. 108–122. ISSN: 1876-6102. DOI: 10.1016/j.egypro.2012.06.092. URL: https://www.sciencedirect.com/science/article/pii/S1876610212011320 (visited on 11/21/2022).

[4] Roberto Benato and Lorenzo Fellin. *Impianti elettrici*. OCLC: 898681646. Torino: UTET scienze tecniche, 2012. ISBN: 978-88-598-0618-9.

[5] *Comparing Fuel Cell Technologies*. GenCell - Fuel Cell Generators. URL: https://web.archive.org/web/20221202100950/https://www.gencellenergy.com/news/comparing-fuel-cell-technologies/ (visited on 12/02/2022).

[6] *Construction modeling and shape prediction of horizontal salt caverns for gas/oil storage in bedded salt | Elsevier Enhanced Reader*. DOI: 10.1016/j.petrol.2020.107058. URL: https://reader.elsevier.com/reader/sd/pii/S0920410520301510?token=7467C635CF9A7AF59FE156DBF8289181ED8B63800592506B2DE9originRegion=eu-west-1&originCreation=20221007124704 (visited on 10/07/2022).

[7] *Denmark - Climatology | Climate Change Knowledge Portal*. URL: https://web.archive.org/web/20221027122056/https://climateknowledgeportal.worldbank.org/country/denmark/climate-data-historical (visited on 10/27/2022).

[8] Energinet. *Home*. Energinet. URL: https://www.energidataservice.dk/tso-electricity/ConsumptionPerGridarea (visited on 11/30/2022).

[9] *H100_NIA_Hydrogen_Debris_Report.pdf*. URL: https://web.archive.org/web/20221027124902/https://sgn.co.uk/sites/default/files/media-entities/documents/2021-02/H100_NIA_Hydrogen_Debris_Report.pdf (visited on 10/27/2022).

[10] K. Hall. "4.14 - Future Perspective on Hydrogen and Fuel Cells". In: *Comprehensive Renewable Energy*. Ed. by Ali Sayigh. Oxford: Elsevier, Jan. 1, 2012, pp. 351–360. ISBN: 978-0-08-087873-7. DOI: 10.1016/B978-0-08-087872-0.00403-0. URL: https://www.sciencedirect.com/science/article/pii/B9780080878720004030 (visited on 10/18/2022).

[11] Fayaz Hussain et al. "Chapter 6 - Energy storage technologies". In: *Energy for Sustainable Development*. Ed. by MD. Hasanuzzaman and Nasrudin Abd Rahim. Academic Press, Jan. 1, 2020, pp. 125–165. ISBN: 978-0-12-814645-3. DOI: 10.1016/B978-0-12-814645-3.00006-7. URL: https://www.sciencedirect.com/science/article/pii/B9780128146453000067 (visited on 02/06/2023).

[12] Katinka Johansen. "Blowing in the wind: A brief history of wind energy and wind power technologies in Denmark". In: *Energy Policy* 152 (May 2021), p. 112139. ISSN: 03014215. DOI: 10.1016/j.enpol.2021.112139. URL: https://linkinghub.elsevier.com/retrieve/pii/S0301421521000082 (visited on 10/10/2022).

[13] Abraham Alem Kebede et al. "A comprehensive review of stationary energy storage devices for large scale renewable energy sources grid integration". In: *Renewable and Sustainable Energy Reviews* 159 (May 1, 2022), p. 112213. ISSN: 1364-0321. DOI: 10.1016/j.rser.2022.112213. URL: https://www.sciencedirect.com/science/article/pii/S1364032122001368 (visited on 10/11/2022).

[14] Szymon Kuczyski et al. "Thermodynamic and Technical Issues of Hydrogen and Methane-Hydrogen Mixtures Pipeline Transmission". In: *Energies* 12.3 (Feb. 12, 2019), p. 569. ISSN: 1996-1073. DOI: 10.3390/en12030569. URL: http://www.mdpi.com/1996-1073/12/3/569 (visited on 09/19/2022).

[15] Wenjing Li et al. "Study on thermodynamic behaviour of natural gas and thermo-mechanical response of salt caverns for underground gas storage". In: *Energy* 262 (Jan. 1, 2023), p. 125601. ISSN: 0360-5442. DOI: 10.1016/j.energy.2022.125601. URL: https://www.sciencedirect.com/science/article/pii/S0360544222024872 (visited on 12/05/2022).

[16] Zhenya Liu. "Chapter 3 - Characteristics of UHV DC Transmission System". In: *Ultra-High Voltage Ac/dc Grids*. Ed. by Zhenya Liu. Boston: Academic Press, Jan. 1, 2015, pp. 95–132. ISBN: 978-0-12-802161-3. DOI: 10.1016/B978-0-12-802161-3.00003-2. URL: https://www.sciencedirect.com/science/article/pii/B9780128021613000032 (visited on 11/20/2022).

[17] Xing Luo et al. "Overview of current development in electrical energy storage technologies and the application potential in power system operation". In: *Applied Energy* 137 (Jan. 2015), pp. 511–536. ISSN: 03062619. DOI: 10.1016/j.apenergy.2014.09.081. URL: https://linkinghub.elsevier.com/retrieve/pii/S0306261914010290 (visited on 02/06/2023).

[18] Ingelise Møller, Niels Balling, and Claus Ditlefsen. "Shallow subsurface thermal structure onshore Denmark: temperature, thermal conductivity and heat flow". In: *Bulletin of the Geological Society of Denmark* 67 (July 5, 2020), pp. 29–52. ISSN: 2245-7070. DOI: 10.37570/bgsd-2019-67-03. URL: https://2dgf.dk/publikationer/bulletin/bulletin-volume-67-2019/#3 (visited on 09/21/2022).

[19] N. Barberis Negra, J. Todorovic, and T. Ackermann. "Loss evaluation of HVAC and HVDC transmission solutions for large offshore wind farms". In: *Electric Power Systems Research* 76.11 (July 1, 2006), pp. 916–927. ISSN: 0378-7796. DOI: 10.1016/j.epsr.2005.11.004. URL: https://www.sciencedirect.com/science/article/pii/S0378779605002609 (visited on 11/20/2022).

[20] V. Nicolas et al. "Numerical simulation of a thermally driven hydrogen compressor as a performance optimization tool". In: *Applied Energy* 323 (Oct. 2022), p. 119628. ISSN: 03062619. DOI: 10.1016/j.apenergy.2022.

119628. URL: https://linkinghub.elsevier.com/retrieve/pii/S0306261922009308 (visited on 12/02/2022).

[21] *NORSOK STANDARD P-001*.

[22] *North Sea*. The European Maritime Spatial Planning Platform. June 17, 2016. URL: https://web.archive.org/web/20221018095906/https://maritime-spatial-planning.ec.europa.eu/sea-basins/north-sea-0 (visited on 10/18/2022).

[23] D. D. Papadias and R. K. Ahluwalia. "Bulk storage of hydrogen". In: *International Journal of Hydrogen Energy* 46.70 (Oct. 11, 2021), pp. 34527–34541. ISSN: 0360-3199. DOI: 10.1016/j.ijhydene.2021.08.028. URL: https://www.sciencedirect.com/science/article/pii/S0360319921030834 (visited on 08/30/2022).

[24] Caleb Jordache Pillay, Musasa Kabeya, and Innocent E Davidson. "Transmission Systems: HVAC vs HVDC". In: (2020).

[25] *Plug EX-425D Electrolyzer (English)*. URL: https://web.archive.org/web/20221201150032/https://resources.plugpower.com/electrolyzers/ex-425d-f041122 (visited on 12/01/2022).

[26] *Population projections - Statistics Denmark*. Feb. 2, 2023. URL: https://web.archive.org/web/20230202113648/https://www.dst.dk/en/Statistik/emner/borgere/befolkning/befolkningsfremskrivning (visited on 02/02/2023).

[27] Julia Rosen. "The Science of Climate Change Explained: Facts, Evidence and Proof". In: *The New York Times* (Nov. 6, 2021). ISSN: 0362-4331. URL: https://www.nytimes.com/article/climate-change-global-warming-faq.html (visited on 10/11/2022).

[28] Raúl Sarrias-Mena et al. "Electrolyzer models for hydrogen production from wind energy systems". In: *International Journal of Hydrogen Energy* 40.7 (Feb. 23, 2015), pp. 2927–2938. ISSN: 0360-3199. DOI: 10.1016/j.ijhydene.2014.12.125. URL: https://www.sciencedirect.com/science/article/pii/S0360319914035599 (visited on 11/08/2022).

[29] Vladimir Savi. "Determination of Pressure Losses in Hydraulic Pipeline Systems by Considering Temperature and Pressure". In: *Journal of Mechanical Engineering* (2009), p. 8.

[30] B. Sedaee et al. "Comprehensive modeling and developing a software for salt cavern underground gas storage". In: *Journal of Energy Storage* 25 (Oct. 1, 2019), p. 100876. ISSN: 2352-152X. DOI: 10.1016/j.est.2019.100876. URL: https://www.sciencedirect.com/science/article/pii/S2352152X19301161 (visited on 08/29/2022).

[31] Y. Tian and C. Y. Zhao. "A review of solar collectors and thermal energy storage in solar thermal applications". In: *Applied Energy* 104 (Apr. 1, 2013), pp. 538–553. ISSN: 0306-2619. DOI: 10.1016/j.apenergy.2012.11.051. URL: https://www.sciencedirect.com/science/article/pii/S0306261912008549 (visited on 02/06/2023).

[32] DEME RUG TNO NEC. *8a.-FINAL-NSE3_D3.8-Final-report-on-the-techno-economic-environmental-and-legal-assessment-of-offshore-energy-islands.pdf*. https://north-sea-energy.eu/static/0856dd12a36d1f321aaf757706bd5913/8a.-FINAL-NSE3_D3.8-Final-report-on-the-techno-economic-environmental-and-legal-assessment-of-offshore-energy-islands.pdf. URL: https://archive.org/download/8a.-final-nse-3-d-3.8-final-report-on-the-techno-economic-environmental-and-lega/8a.-FINAL-NSE3_D3.8-Final-report-on-the-techno-economic-environmental-and-legal-assessment-of-offshore-energy-islands.pdf (visited on 09/13/2022).

[33] *V164-10.0 MW*. URL: https://web.archive.org/web/20221013060704/https://www.vestas.com/en/products/offshore/V164-10-0-MW (visited on 10/18/2022).

[34] *Wind turbines | Vestas*. URL: https://www.vestas.com/en/products/overview (visited on 11/17/2022).

[35] Jose M. Yusta and Guillermo Matute. "Techno-Economic Analysis of Hydrogen Electrolysis Systems". In: *Comprehensive Renewable Energy*. Elsevier, 2022, pp. 505–532. ISBN: 978-0-12-819734-9. DOI: 10.1016/B978-0-12-819727-1.00007-8. URL: https://linkinghub.elsevier.com/retrieve/pii/B9780128197271000078 (visited on 10/18/2022).

Code Appendix

```
norm_windpower_trend=(d.OnshoreWindPower+d.OffshoreWindPower)/max(d.
    OnshoreWindPower+d.OffshoreWindPower) % normalized to max power
    production the wind power production trend
norm_demand_trend=d.TotalLoad/max(d.TotalLoad);
ratio_maxwind_maxpower_future=(max(4*(d.OnshoreWindPower+d.
    OffshoreWindPower)))/max(1.5*d.TotalLoad);
max_total_power_demand_3cities=max_power_wind_farm/
    ratio_maxwind_maxpower_future; % max total demand of power
    combined of the 3 cities [MW]
demandtrend_city1=percentage_demand_city1*
    max_total_power_demand_3cities*norm_demand_trend; % [MW]
demandtrend_city2=percentage_demand_city2*
    max_total_power_demand_3cities*norm_demand_trend; % [MW]
demandtrend_city3=percentage_demand_city3*
    max_total_power_demand_3cities*norm_demand_trend; % [MW]
overall_surplus=norm_windpower_trend*max_power_wind_farm-
    demandtrend_city1-demandtrend_city2-demandtrend_city3; % [MW]
    surplus of production from wind farm
overall_demand=demandtrend_city1+demandtrend_city2+demandtrend_city3;
     % [MW]
windfarm_production=norm_windpower_trend*max_power_wind_farm; % [MW]
    production trend of the wind farm
windfarm_production(windfarm_production>overall_demand)=
    overall_demand(windfarm_production>overall_demand);% Used to plot
    areas
overall_surplus(overall_surplus<0)=0;
overall_shortage=overall_demand-windfarm_production;
energy_shortage=trapz(date_num,overall_shortage);
energy_shortage_city1=energy_shortage*percentage_demand_city1
energy_shortage_city2=energy_shortage*percentage_demand_city2
energy_shortage_city3=energy_shortage*percentage_demand_city3
```

Code 4.1: *Energy shortage calculation per each city code snippet*

```
% F stands for Fuel Cell, E for electrolyzer

for i1=1:length(Electrolyzers_min_efficiency_percentage)
    for i2=1:length(FC_min_electrical_efficiency_percentage)
        data_energy_min(i1,i2)=energy_shortage/((
    FC_min_electrical_efficiency_percentage(i2)/100)*(
    Electrolyzers_min_efficiency_percentage(i1)/100));
        data_energy_max(i1,i2)=energy_shortage/((
    FC_max_electrical_efficiency_percentage(i2)/100)*(
    Electrolyzers_max_efficiency_percentage(i1)/100));
    end
end

energy_required_AMC   = [data_energy_min(:,1) data_energy_max(:,1)];
energy_required_DMFC  = [data_energy_min(:,2) data_energy_max(:,2)];
energy_required_MCFC  = [data_energy_min(:,3) data_energy_max(:,3)];
energy_required_PAFC  = [data_energy_min(:,4) data_energy_max(:,4)];
energy_required_PEMFC = [data_energy_min(:,5) data_energy_max(:,5)];
energy_required_SOFC  = [data_energy_min(:,6) data_energy_max(:,6)];

energy_required_AMC_city1   = [data_energy_min(:,1) data_energy_max
    (:,1)]*percentage_demand_city1;
energy_required_DMFC_city1  = [data_energy_min(:,2) data_energy_max
    (:,2)]*percentage_demand_city1;
energy_required_MCFC_city1  = [data_energy_min(:,3) data_energy_max
    (:,3)]*percentage_demand_city1;
energy_required_PAFC_city1  = [data_energy_min(:,4) data_energy_max
    (:,4)]*percentage_demand_city1;
energy_required_PEMFC_city1 = [data_energy_min(:,5) data_energy_max
    (:,5)]*percentage_demand_city1;
energy_required_SOFC_city1  = [data_energy_min(:,6) data_energy_max
    (:,6)]*percentage_demand_city1;

energy_required_AMC_city2   = [data_energy_min(:,1) data_energy_max
    (:,1)]*percentage_demand_city2;
energy_required_DMFC_city2  = [data_energy_min(:,2) data_energy_max
    (:,2)]*percentage_demand_city2;
energy_required_MCFC_city2  = [data_energy_min(:,3) data_energy_max
    (:,3)]*percentage_demand_city2;
energy_required_PAFC_city2  = [data_energy_min(:,4) data_energy_max
    (:,4)]*percentage_demand_city2;
energy_required_PEMFC_city2 = [data_energy_min(:,5) data_energy_max
    (:,5)]*percentage_demand_city2;
```

```
energy_required_SOFC_city2  = [data_energy_min(:,6) data_energy_max(:,6)]*percentage_demand_city2;

energy_required_AMC_city3   = [data_energy_min(:,1) data_energy_max(:,1)]*percentage_demand_city3;
energy_required_DMFC_city3  = [data_energy_min(:,2) data_energy_max(:,2)]*percentage_demand_city3;
energy_required_MCFC_city3  = [data_energy_min(:,3) data_energy_max(:,3)]*percentage_demand_city3;
energy_required_PAFC_city3  = [data_energy_min(:,4) data_energy_max(:,4)]*percentage_demand_city3;
energy_required_PEMFC_city3 = [data_energy_min(:,5) data_energy_max(:,5)]*percentage_demand_city3;
energy_required_SOFC_city3  = [data_energy_min(:,6) data_energy_max(:,6)]*percentage_demand_city3;

T_energy_required=table(energy_required_AMC,energy_required_DMFC,energy_required_MCFC,energy_required_PAFC,energy_required_PEMFC,energy_required_SOFC,'RowNames',Electrolyzers_tecnologies)

T_energy_required_city1=table(energy_required_AMC_city1,energy_required_DMFC_city1,energy_required_MCFC_city1,energy_required_PAFC_city1,energy_required_PEMFC_city1,energy_required_SOFC_city1,'RowNames',Electrolyzers_tecnologies)

T_energy_required_city2=table(energy_required_AMC_city2,energy_required_DMFC_city2,energy_required_MCFC_city2,energy_required_PAFC_city2,energy_required_PEMFC_city2,energy_required_SOFC_city2,'RowNames',Electrolyzers_tecnologies)

T_energy_required_city3=table(energy_required_AMC_city3,energy_required_DMFC_city3,energy_required_MCFC_city3,energy_required_PAFC_city3,energy_required_PEMFC_city3,energy_required_SOFC_city3,'RowNames',Electrolyzers_tecnologies)


% Hydrogen that has to be stored to take into account the efficiency of
% fuel cells and being able to cover the energy requirements of the cities

h2_storage_city1_MWh_minefficiency=energy_shortage_city1./(FC_min_electrical_efficiency_percentage/100);
```

```
h2_storage_city2_MWh_minefficiency=energy_shortage_city2./(
    FC_min_electrical_efficiency_percentage/100);
h2_storage_city3_MWh_minefficiency=energy_shortage_city3./(
    FC_min_electrical_efficiency_percentage/100);

h2_storage_city1_MWh_maxefficiency=energy_shortage_city1./(
    FC_max_electrical_efficiency_percentage/100);
h2_storage_city2_MWh_maxefficiency=energy_shortage_city2./(
    FC_max_electrical_efficiency_percentage/100);
h2_storage_city3_MWh_maxefficiency=energy_shortage_city3./(
    FC_max_electrical_efficiency_percentage/100);

h2_storage_city1_kg_minefficiency=h2_storage_city1_MWh_minefficiency
    /(LHV_H2/1000);
h2_storage_city2_kg_minefficiency=h2_storage_city2_MWh_minefficiency
    /(LHV_H2/1000);
h2_storage_city3_kg_minefficiency=h2_storage_city3_MWh_minefficiency
    /(LHV_H2/1000);

h2_storage_city1_kg_maxefficiency=h2_storage_city1_MWh_maxefficiency
    /(LHV_H2/1000);
h2_storage_city2_kg_maxefficiency=h2_storage_city2_MWh_maxefficiency
    /(LHV_H2/1000);
h2_storage_city3_kg_maxefficiency=h2_storage_city3_MWh_maxefficiency
    /(LHV_H2/1000);
```

Code 4.2: *Script for calculation of energy and hydrogen needed to cover shortages considering the efficiencies of Fuel Cells and Electrolyzers*

```
% Calculation mass flow rate hydrogen in pipeline based on the
    required
% flow rate by city
% NB 6 months data

for idx15=1:24 % 24h in a day
    numindex{idx15}=find(hour(d.HourDK)==(idx15-1));
    avgday_city1(idx15)=mean(demandtrend_city1(numindex{1,idx15}));
    avgday_city2(idx15)=mean(demandtrend_city2(numindex{1,idx15}));
    avgday_city3(idx15)=mean(demandtrend_city3(numindex{1,idx15}));
end

avgday_city1=avgday_city1'; avgday_city2=avgday_city2'; avgday_city3=
    avgday_city3';
figure(10)
```

```
stairs(linspace(0,23,24),avgday_city1)
hold on
stairs(linspace(0,23,24),avgday_city2)
stairs(linspace(0,23,24),avgday_city3)
legend('Avg Dem City 1','Avg Dem City 2','Avg Dem City 3','Location','northwest')
xlabel('Hours')
ylabel('Average Mass Flow Rate [kg/h]')
hold off

% Calculation of MWh per h so calculation of mass of hydrogen needed each
% hour

timeday=linspace(0,23,24);
for idx16=1:23
    avgday_city1_energy(idx16)=trapz(timeday(idx16:(idx16+1)),avgday_city1(idx16:(idx16+1))); % [MWh]
    avgday_city2_energy(idx16)=trapz(timeday(idx16:(idx16+1)),avgday_city2(idx16:(idx16+1))); % [MWh]
    avgday_city3_energy(idx16)=trapz(timeday(idx16:(idx16+1)),avgday_city3(idx16:(idx16+1))); % [MWh]
end


% Mass flow rate of H2 needed (considering min and max eff of different
% technologies of fuel cells)
for idx17=1:length(FC_min_electrical_efficiency_percentage) % columns are different FC technologies
    massflowrateH2_mineffFC_total(:,idx17)=(demandtrend_city1+demandtrend_city2+demandtrend_city3-(norm_windpower_trend*max_power_wind_farm))./((FC_min_electrical_efficiency_percentage(idx17)/100)*LHV_H2/1000); % [kg/h] of H2 that has to be sent to fuel cells to cover the shortage
    massflowrateH2_maxeffFC_total(:,idx17)=(demandtrend_city1+demandtrend_city2+demandtrend_city3-(norm_windpower_trend*max_power_wind_farm))./((FC_max_electrical_efficiency_percentage(idx17)/100)*LHV_H2/1000); % [kg/h]
    for idx18=1:length(massflowrateH2_maxeffFC_total)
        if massflowrateH2_mineffFC_total(idx18,idx17)<=0
           massflowrateH2_mineffFC_total(idx18,idx17)=0;
           massflowrateH2_maxeffFC_total(idx18,idx17)=0;
```

```
        else
        end
    end
    avgmassflowrateH2_mineffFC_total(:,idx17)=mean(
    massflowrateH2_mineffFC_total(:,idx17)); % average mass flow rate
    required with min eff FC
    avgmassflowrateH2_maxeffFC_total(:,idx17)=mean(
    massflowrateH2_maxeffFC_total(:,idx17)); % average mass flow rate
    required with max eff FC
end
```

Code 4.3: *Script for mass flow rates calculation*

```
dataEnerginet=readtable("dataDK.xlsx");
pricearea_remove=find(dataEnerginet.PriceArea=="DK2");
dataEnerginet(pricearea_remove,:)=[]; % usage only of area 1, not
    area 2
dataEnerginet=sortrows(dataEnerginet,2);
clear pricearea_remove
Calculation of wind production and load consumption with adapted data
     (4x wind production and 1.5x the consumption) for 2050
windproduction2050_MW=5*(dataEnerginet.OnshoreWindPower+dataEnerginet
    .OffshoreWindPower); % [MW]
loadconsumption2050_MW=1.5*dataEnerginet.TotalLoad; % [MW]
time_analysis=linspace(1,length(loadconsumption2050_MW),length(
    loadconsumption2050_MW)); % [h]

% remove spikes
loadconsumption2050_MW(windproduction2050_MW==max(
    windproduction2050_MW))=[];
windproduction2050_MW(windproduction2050_MW==max(
    windproduction2050_MW))=[];
windproduction2050_MW(loadconsumption2050_MW==max(
    loadconsumption2050_MW))=[];
loadconsumption2050_MW(loadconsumption2050_MW==max(
    loadconsumption2050_MW))=[];
loadconsumption2050_MW=smoothdata(loadconsumption2050_MW);
    windproduction2050_MW=smoothdata(windproduction2050_MW);


figure(2)
plot(linspace(1,length(loadconsumption2050_MW),length(
    loadconsumption2050_MW)),windproduction2050_MW,'g',linspace(1,
    length(loadconsumption2050_MW),length(loadconsumption2050_MW)),
```

```
    loadconsumption2050_MW,'r');
legend('Wind Production [MW]','Load Consumption [MW]')
difference_production_load=windproduction2050_MW-
    loadconsumption2050_MW;    % [MW]
surplus2050=difference_production_load(difference_production_load>=0)
    ;      % [MW]
surplus2050(difference_production_load<0)=0;
surplus2050_simulink(:,1)=linspace(1,length(surplus2050),length(
    surplus2050)); surplus2050_simulink(:,2)=surplus2050;
deficit2050=abs(difference_production_load(difference_production_load
    <0));  % [MW]
deficit2050(difference_production_load>=0)=0;
deficit2050_simulink(:,1)=linspace(1,length(deficit2050),length(
    deficit2050)); deficit2050_simulink(:,2)=deficit2050;

difference_production_load_SURPLUS=difference_production_load; % use
    for surplus
difference_production_load_DEFICIT=difference_production_load; % use
    for deficit

difference_production_load_SURPLUS(difference_production_load_SURPLUS
    <=0)=0;
difference_production_load_DEFICIT(difference_production_load_DEFICIT
    >=0)=0;
```

Code 4.4: *Script for data filtering, projection and calculation of power shortage and surplus*

```
% Input data
T_avg_DK=8.3+273.15; % [K] https://climateknowledgeportal.worldbank.
    org/country/denmark/climate-data-historical#:~:text=The%20Danish
    %20climate%20is%20temperate,(2006%2D2015%20level).
pbar_forpressuredrop=20;
density_forpressuredrop=py.CoolProp.CoolProp.PropsSI('DMASS','T',
    T_avg_DK,'P',pbar_forpressuredrop*100000,'H2');  % average density
     calculated considering average T in Denmark and pressure equal to
     20 bar [kg/m3]
mu_forpressuredrop=py.CoolProp.CoolProp.PropsSI('VISCOSITY','T',
    T_avg_DK,'P',pbar_forpressuredrop*100000,'H2');   % average
    viscosity calculated considering average T in Denmark and pressure
     equal to 20 bar [Pa*s]
roughness_forpressuredrop=0.5*1e-3; % [m] considering steel pipes
    even though needs to be considered the corrosivity of H2 on steel
Dmin_forpressuredrop=10/100; % [m] minimum diameter considered for
    the optimization process
```

```
Dmax_forpressuredrop=2;    % [m] maximum diameter considered for the optimization process
vel_forpressuredrop=[0.5,20]*3.5; % [m/s] https://www.cheresources.com/invision/topic/15547-natural-gas-pipe-line-sizing-calculations/#:~:text=A%3A%20gas%20velocities%20in%20transportation,s%20for%20intermittent%20operation...
% https://sgn.co.uk/sites/default/files/media-entities/documents/2021-02/H100_NIA_Hydrogen_Debris_Report.pdf
% H2 speed is roughly 3.5 times the natural gas one in pipelines
% pressure_drop_calc          necessary to run it only once

% load results and then use to calculate pressure drops
for idx20=1:3 % number of cities
    filename4=['pipelineresults_city',num2str(idx20),'_mineffFCtechnology_T_',num2str(T_avg_DK),'pbar_',num2str(pbar_forpressuredrop),'.mat'];
    load(filename4);
    m_dot_mineffFC(:,idx20)=all_results{:,1}; % columns are cities, rows are technologies  [kg/s]
    dp_mineffFC(:,idx20)=all_results{:,2};    % columns are pressure drops per city, row still technologies [Pa/m]
    diameterpipe_mineffFC(:,idx20)=all_results{:,4};  % columns are diameter for pipeline per city, row still technologies [mm]
    velocity_mineffFC(:,idx20)=all_results{:,5};  % columns are velocities of H2 in pipelines per city, row still technologies [m/s]
    reinolds_mineffFC(:,idx20)=all_results{:,6};  % columns are Reinolds numbers per city, row still technologies

    filename4=['pipelineresults_city',num2str(idx20),'_maxeffFCtechnology_T_',num2str(T_avg_DK),'pbar_',num2str(pbar_forpressuredrop),'.mat'];
    load(filename4);
    m_dot_maxeffFC(:,idx20)=all_results{:,1}; % columns are cities, rows are technologies  [kg/s]
    dp_maxeffFC(:,idx20)=all_results{:,2};    % columns are pressure drops per city, row still technologies [Pa/m]
    diameterpipe_maxeffFC(:,idx20)=all_results{:,4};  % columns are diameter for pipeline per city, row still technologies [mm]
    velocity_maxeffFC(:,idx20)=all_results{:,5};  % columns are velocities of H2 in pipelines per city, row still technologies [m/s]
    reinolds_maxeffFC(:,idx20)=all_results{:,6};  % columns are
```

```
    Reinolds numbers per city, row still technologies
31
32 end
33
34 % Calculation of pipeline lengths
35 % H2 island to storage 1 (for city 3)
36 pipeline1=distance2points(start_point_H2island_coordinates(1),
    base_x_sm(1),start_point_H2island_coordinates(2),
    y_onshore_connection)+distance2points(base_x_sm(1),textplot(
    base_x_storage1_sm),y_onshore_connection,y_onshore_connection)+
    distance2points(textplot(base_x_storage1_sm),textplot(
    base_x_storage1_sm),y_onshore_connection,textplot(
    base_y_storage1_sm)) % [km]
37 % H2 island to storage 2 (for city 2)
38 pipeline2=distance2points(start_point_H2island_coordinates(1),
    base_x_sm(1),start_point_H2island_coordinates(2),
    y_onshore_connection)+distance2points(base_x_sm(1),textplot(
    base_x_storage2_sm),y_onshore_connection,y_onshore_connection)+
    distance2points(textplot(base_x_storage2_sm),textplot(
    base_x_storage2_sm),y_onshore_connection,textplot(
    base_y_storage2_sm)) % [km]
39 % H2 island to storage 3 (for city 1)
40 pipeline3=distance2points(start_point_H2island_coordinates(1),
    base_x_sm(1),start_point_H2island_coordinates(2),
    y_onshore_connection)+distance2points(base_x_sm(1),textplot(
    base_x_storage1_sm),y_onshore_connection,y_onshore_connection)+
    distance2points(textplot(base_x_storage1_sm),textplot(
    base_x_storage1_sm),y_onshore_connection,textplot(
    base_y_storage3_sm))+distance2points(textplot(base_x_storage1_sm),
    textplot(base_x_storage3_sm),textplot(base_y_storage3_sm),textplot
    (base_y_storage3_sm)) % [km]
41
42 % Calculation of pressure drops
43 % Pipeline 1 (city 3)
44 % Min eff
45 dp_pipeline1_mineffFC_Pa=dp_mineffFC(:,3)*pipeline1*1000;  % [Pa]
    rows are different FC technologies
46 dp_pipeline1_mineffFC_bar=dp_pipeline1_mineffFC_Pa/(10^5)  % [bar]
    rows are different FC technologies
47 % Max eff
48 dp_pipeline1_maxeffFC_Pa=dp_maxeffFC(:,3)*pipeline1*1000;  % [Pa]
    rows are different FC technologies
49 dp_pipeline1_maxeffFC_bar=dp_pipeline1_maxeffFC_Pa/(10^5)  % [bar]
```

```
    rows are different FC technologies
% Pipeline 2 (city 2)
% Min eff
dp_pipeline2_mineffFC_Pa=dp_mineffFC(:,2)*pipeline2*1000;  % [Pa]
    rows are different FC technologies
dp_pipeline2_mineffFC_bar=dp_pipeline2_mineffFC_Pa/(10^5)  % [bar]
    rows are different FC technologies
% Max eff
dp_pipeline2_maxeffFC_Pa=dp_maxeffFC(:,2)*pipeline2*1000;  % [Pa]
    rows are different FC technologies
dp_pipeline2_maxeffFC_bar=dp_pipeline2_maxeffFC_Pa/(10^5)  % [bar]
    rows are different FC technologies
% Pipeline 3 (city 1)
% Min eff
dp_pipeline3_mineffFC_Pa=dp_mineffFC(:,1)*pipeline3*1000;  % [Pa]
    rows are different FC technologies
dp_pipeline3_mineffFC_bar=dp_pipeline3_mineffFC_Pa/(10^5)  % [bar]
    rows are different FC technologies
% Max eff
dp_pipeline3_maxeffFC_Pa=dp_maxeffFC(:,1)*pipeline3*1000;  % [Pa]
    rows are different FC technologies
dp_pipeline3_maxeffFC_bar=dp_pipeline3_maxeffFC_Pa/(10^5)  % [bar]
    rows are different FC technologies
```

Code 4.5: *Script for pressure losses calculation*

```
% Similarly to density a grid mesh is created also for pressure in
    order to
% be able to evaluate the value of pressure based on temperature and
% density of H2

% Temperature (from 300 to 600 K)
Tmesh=linspace(300,600,50);          % 50 points

% Density (from 1 to 10 kg/m3)
densitymesh=linspace(1,10,50);       % 50 points

% Calculation of pressure through CoolProp

for idx21=1:length(Tmesh)            % T on columns
    for idx22=1:length(densitymesh) % rho on rows
        pressuremesh(idx22,idx21)=py.CoolProp.CoolProp.PropsSI('P','T
    ',Tmesh(1,idx21),'DMASS',densitymesh(1,idx22),'H2');
    end
```

```
end

% Data preparation and fitting
[xData1,yData1,zData1]=prepareSurfaceData(Tmesh,densitymesh,
    pressuremesh);
cf2=fit([xData1,yData1],zData1,'poly23','Normalize','on');
```

Code 4.6: *Script for grid mesh calculation*

```
function [solution_lambda,solution_v,solution_reynolds,
    massflowrate_singlepipe_kg_s,massflowrate_singlepipe_kg_h,
    numberofpipes]=numberwells(percentage_pressure_max,pressure,
    density,massflowrate,length,diameter,temp_analysis)
%% Preliminary part
% Interpolation pressure
polynomial_coeff_pressure=fit(pressure.Time,pressure.Data,'
    smoothingspline','Normalize','on');
interpolation_pressure=feval(polynomial_coeff_pressure,1:massflowrate
    .Time(end));
[M, index_maxH2flowrate]=max(massflowrate.Data);

% Pressure
wells_pressure=interpolation_pressure(index_maxH2flowrate);
                            % [Pa]
wells_deltap_max=wells_pressure*percentage_pressure_max/100;
                            % [Pa]

% Interpolation density
polynomial_coeff_density=fit(density.Time,density.Data,'
    smoothingspline','Normalize','on');
interpolation_density=feval(polynomial_coeff_density,1:massflowrate.
    Time(end));

% Density
wells_density=interpolation_density(index_maxH2flowrate);
                            % [kg/m3]

% Viscosity
wells_viscosity_calculation=py.CoolProp.CoolProp.PropsSI('VISCOSITY',
    'P',wells_pressure,'T',temp_analysis,'H2');

%% System solving
% Equations
syms lambda v Re
```

```
25 equation_deltap= wells_deltap_max==lambda*(length/diameter)*
       wells_density*(v^2)/2;
26 equation_lambda= lambda==0.3164./(Re^0.25);
27 equation_reynolds=v*diameter/wells_viscosity_calculation==Re;
28 [solution_lambda,solution_v,solution_reynolds]=(solve([
       equation_deltap,equation_lambda,equation_reynolds],[lambda,v,Re]))
       ;
29 solution_lambda=round(vpa(solution_lambda),3); solution_v=round(vpa(
       solution_v),3); solution_reynolds=round(vpa(solution_reynolds),3);
30
31
32 %% Number of pipes part
33 % Calculation of mass flow rate for each pipe
34 massflowrate_singlepipe_kg_s=round(wells_density*solution_v*pi*
       diameter^2/4,3);
35 massflowrate_singlepipe_kg_h=round(massflowrate_singlepipe_kg_s
       *3600,3);
36
37 % Number of pipes
38 numberofpipes=ceil(max(massflowrate)/massflowrate_singlepipe_kg_h);
39
40 end
```

Code 4.7: *Function for mass flow rate and number of wells calculation (called* $numberwells$*)*